②

PORTS

Fourth Quarter
1992

AD-A261 569

93-03781

Defense
Armed Forces Rad   *Institu*
Bethesda,

REPORT DOCUMENTATION PAGE

Public reporting burden for this collection of information is estimated to average 1 hour per response including the time for reviewing instructions searching existing data sources gathering and maintaining the data needed, and completing and reviewing the collection of information. Send comments regarding this burden estimate or any other aspect of this collection of information including suggestions for reducing this burden to Washington Headquarters Services Directorate for Information Operations and Reports 1215 Jefferson Davis Highway Suite 1204 Arlington VA 22202 4302 and to the Office of Management and Budget Paperwork Reduction Project (0704-0188) Washington DC 20503

1 AGENCY USE ONLY (Leave blank)	2 REPORT DATE	3 REPORT TYPE AND DATES COVERED
	January 1993	Reprints/Technical

4 TITLE AND SUBTITLE

AFRRI Reports, Fourth Quarter 1992

5 FUNDING NUMBERS

PE: NWED QAXM

6 AUTHOR(S)

7 PERFORMING ORGANIZATION NAME(S) AND ADDRESS(ES)

Armed Forces Radiobiology Research Institute
8901 Wisconsin Avenue
Bethesda, MD 20889-5603

8 PERFORMING ORGANIZATION REPORT NUMBER

SR92-39 - SR92-48

9 SPONSORING/MONITORING AGENCY NAME(S) AND ADDRESS(ES)

Defense Nuclear Agency
6801 Telegraph Road
Alexandria, VA 22310-3398

10 SPONSORING/MONITORING AGENCY REPORT NUMBER

11 SUPPLEMENTARY NOTES

12a. DISTRIBUTION/AVAILABILITY STATEMENT

Approved for public release; distribution unlimited.

12b DISTRIBUTION CODE

13 ABSTRACT (Maximum 200 words)

This volume contains AFRRI Scientific Reports SR92-39 through SR92-48 for October-December 1992.

14 SUBJECT TERMS

15 NUMBER OF PAGES

107

16 PRICE CODE

17 SECURITY CLASSIFICATION OF REPORT	18 SECURITY CLASSIFICATION OF THIS PAGE	19 SECURITY CLASSIFICATION OF ABSTRACT	20 LIMITATION OF ABSTRACT
UNCLASSIFIED	UNCLASSIFIED	UNCLASSIFIED	UL

CLASSIFIED BY:

DECLASSIFY ON:

CONTENTS

Scientific Reports

SR92-39: Baker WH, Nold JB, Patchen ML, Jackson WE. Histopathologic effects of soluble glucan and WR-2721, independently and combined in C3H/HeN mice.

SR92-40: Colden-Stanfield M, Cramer EB, Gallin EK. Comparison of apical and basal surfaces of confluent endothelial cells: Patch-clamp and viral studies.

SR92-41: Kalinich JF, McClain DE. An *in vitro* method for radiolabeling proteins with ^{35}S.

SR92-42: King GL, Weatherspoon JK. Possible potentiation of the emetic response to oral S(-) zacopride by various receptor ligands in the ferret.

SR92-43: Ledney GD, Madonna GS, Moore MM, Elliott TB, Brook I. Synthetic trehalose dicorynomycolate and antimicrobials increase survival from sepsis in mice immunocompromised by radiation and trauma.

SR92-44: Mickley GA, Ferguson JL, Nemeth TJ. Serial injections of MK 801 (Dizocilpine) in neonatal rats reduce behavioral deficits associated with x-ray-induced hippocampal granule cell hypoplasia.

SR92-45: Neta R, Oppenheim JJ. Anti-cytokine antibodies reveal the interdependence of pro-inflammatory cytokines in protection from lethal irradiation.

SR92-46: Rabin BM, Hunt WA. Relationship between vomiting and taste aversion learning in the ferret: Studies with ionizing radiation, lithium chloride, and amphetamine.

SR92-47: Schmauder-Chock EA, Chock SP. Prostaglandin E_2 localization in the rat ileum.

SR92-48: Yang GL, Swenberg CE. Estimation of open dwell time and problems of identifiability in channel experiments.

Histopathologic Effects of Soluble Glucan and WR-2721, Independently and Combined in C3H/HeN Mice (43497)

WILLIAM H. BAKER,*.¹ JAMES B. NOLD,¹ MYRA L. PATCHEN,* AND WILLIAM E. JACKSON*

Armed Forces Radiobiology Research Institute,* Bethesda, Maryland 20889-5145 and Hazelton Laboratory,' Department of Pathology, Madison, Wisconsin 53707

Abstract. Soluble glucan, an immunomodulator, and Walter Reed (WR)-2721, a radioprotectant, increase postirradiation survival when administered before and after exposure, respectively. Combined, these agents act synergistically through WR-2721's ability to spare hematopoietic stem/progenitor cells from radiation injury and glucan's ability to subsequently stimulate spared cells to proliferate. In this study, the histopathologic effects of WR-2721 (200 mg/kg, ip) and glucan (250 mg/kg, iv), at doses capable of increasing survival in lethally irradiated mice, were evaluated in unirradiated and irradiated female C3H/HeN mice. After treatment, whole body weights and wet organ weights of liver, spleen, and kidney, as well as gross and histologic changes in these and other tissues, were monitored on Days 1, 4, 7, 11, 15, 21, and 28. Morphometric studies of splenic white and red pulps were also performed. Soluble glucan, with or without WR-2721, in unirradiated groups, was associated with splenomegaly, transient morphometrically determined perturbations of white and red pulp areas, and histologic alterations of white pulp. In irradiated mice, splenic weight loss was initially dampened in glucan groups and accompanied by morphologic and histologic changes similar to those seen in unirradiated counterparts. The subsequent rebound of splenic parameters in irradiated mice was limited to WR-2721-treated mice and was associated with hematopoietic reconstitution. Glucan, with or without WR-2721, in unirradiated groups was associated with transient hepatomegaly and associated histologic changes. Similar changes in irradiated animals were seen only in the combined treatment group.
[P.S.E.B.M. 1992. Vol 201]

Survival following lethal exposure to γ-radiation in mice can be enhanced by both immunomodulators and aminothiol radioprotectants (1–4). Glucan, a β-1,3-polyglucosepolymer isolated from the inner wall of the yeast *Saccharomyces cervisiae*, is one such survival-enhancing immunomodulator (3, 5). Glucan-mediated survival enhancement is correlated with enhanced and/or prolonged macrophage function, as well as with accelerated hematopoietic regeneration (5–9). Walter Reed (WR)-2721 (ethiofos, S-2(3-aminopropylamino)ethylphosphorothioic acid), on the other

hand, is a traditional sulfhydryl radioprotectant (10, 11). The mechanisms by which WR-2721 protects cells from radiation-induced lethality include free radical scavenging, hydrogen atom donation, and induction of hypoxia (1). In addition to the ability of glucan and WR-2721 to individually enhance survival, synergistic survival enhancement can be obtained with the agents used in combination. Specifically, glucan and WR-2721 used individually and in combination have resulted in dose-reduction factors (radiation dose lethal for 50% of treated animals divided by radiation dose lethal for 50% of control animals) of 1.08, 1.37, and 1.52, respectively (1).

Although beneficial in enhancing survival, these agents are not without side effects. Particulate forms of glucan have been reported to induce hepatosplenomegaly, granuloma formation, enhanced susceptibility to endotoxin, and microembolization (12–16). Severe granuloma formation, enhanced susceptibility to endotoxin, and microemboli have not been reported after

administration of more recently produced soluble glucan preparations. However, a recent preclinical safety evaluation demonstrated splenomegaly and mononuclear infiltrates in the liver after intravenous injection of 1000 mg/kg of soluble glucan over an extended period (16). Such an extremely high dose of glucan, however, is well above the levels needed to enhance survival in irradiated mice. High doses of WR-2721, as well as inducing performance decrements (17), have produced renal tubular epithelial degeneration and necrosis in lymphoid tissues (spleen, lymph nodes, and thymus) (18). The doses of WR-2721 used for radioprotection are below the levels that produce such lesions. Histologic evaluation of combined WR-2721 and glucan has not been reported.

The present study investigates the histopathologic effects of soluble glucan and WR-2721 alone and combined. This study was done in unirradiated and irradiated female C3H/HeN mice using drug doses previously shown effective at promoting hematopoietic recovery and enhancing survival following exposure to lethal doses of ^{60}Co radiation.

Materials and Methods

Mice. C3H/HeN female mice (approximately 20 g) were purchased from Charles River Laboratories (Raleigh, NC). Mice were maintained in an accredited American Association for Accreditation of Laboratory Animal Care (AAALAC) facility in Micro-Isolator cages on hardwood-chip contact bedding and were provided commercial rodent chow and acidified water (pH 2.5) ad libitum. Animal rooms were maintained on a 12:12-hr light:dark cycle at 70°F ± 2°F, 50% ± 10% relative humidity, and at least 10 air changes per hour of 100% conditioned fresh air. Upon arrival, all mice were tested for Pseudomonas and quarantined until test results were obtained. Only healthy mice were released for experimentation. All animal experiments were approved by the Institute of Animal Care and Use Committee before performance.

WR-2721 and Glucan. Stock WR-2721 was obtained from Dr. David Davidson (Walter Reed Army Institute of Research, Washington, DC) and kept frozen at −20°C until use. Immediately before each use, the appropriate amount of WR-2721 was weighed out and dissolved in sterile pyrogen-free saline. Exposure of the material to light was minimized. Mice were injected intraperitoneally with 200 mg/kg of WR-2721 in a volume of 0.5 ml. This dose of WR-2721 has been shown to have minimal side effects in mice (18). Glucan used in these studies was a soluble endotoxin-free preparation purchased from Tulane University School of Medicine, New Orleans, LA. Preparation of this glucan (which has sometimes been referred to as glucan-F) has been described previously by DiLuzio et al. (19). Mice were injected intravenously in the lateral tail vein with

250 mg/kg of glucan in a volume of 0.5 ml. In combined treatments, mice were administered WR-2721 30 min before irradiation and glucan 60 min after irradiation. Unirradiated mice were injected with glucan approximately 90 min after WR-2721, thereby simulating protocols used in irradiated mice. Control mice were injected intraperitoneally or intravenously with 0.5 ml of normal saline.

Irradiation. Mice were placed in plastic containers and exposed bilaterally to 9.0 Gy total body gamma rays at a dose rate of 0.4 Gy per min in a "Co source. Dosimetry was determined by ionization chambers as described previously (20).

Experimental Design. Mice were randomly assigned to the following treatment groups: control (CON), glucan (GLU), WR-2721 (WR), combined WR-2721 and glucan (WR/GLU), radiation control (RC), radiation + glucan (RG), WR-2721 + radiation (WR/R) and combined WR-2721 and glucan with interposed radiation exposure (WR/R/GLU). On Days 1, 4, 7, 11, 15, 21, and 28 after treatment, six CON mice and five mice from each treatment group were sacrificed by cervical dislocation, and total body weights and wet organ weights for the liver, left kidney, and spleen were recorded. Samples of the following tissues were then collected and immersed in 10% neutral buffered formalin: brain, bone marrow (left femur), lung, thymus, heart, liver, left kidney, spleen, adrenal glands, stomach, small intestine, urinary bladder, mesenteric lymph node, and pancreas. After adequate fixation, tissues were trimmed, dehydrated in graded alcohols, cleared, embedded in paraffin, cut at 6 μm, and stained with hematoxylin and eosin for qualitative and morphometric microscopic examination. Slides were labeled and coded, and morphometric and qualitative evaluations were performed by a boarded pathologist without knowledge of which treatment group was being examined.

Morphometry. Area measurements of the spleen and splenic substructures were obtained by planimetry, using a computer-assisted semiautomated image analysis program (Bioquant IV; R & M Biometrics, Nashville, TN) in conjunction with a digitizing tablet and microscope equipped with a fixed-arm reflector tube. The digitizing tablet was calibrated in the metric system, and corrective factors for each microscope objective lens were entered into the computer program. The splenic areas measured included the total splenic area and white pulp area. The red pulp area was calculated by subtracting the white pulp area from the total splenic area. Percentages of the white and red pulp areas were calculated using planimetric area measurements (21). These percentages were subsequently used to determine the component weights of the white and red pulps.

Qualitative Evaluation. Grading of hematopoietic cellularity in splenic red pulp sinusoids and bone mar-

row was done by scoring cellularity numerically: 0 (severe hypocellularity), no foci of hematopoiesis to occasional hematopoietic clusters over several high power fields ([HPF], ×400 magnification); 1 (mild), 1-2 clusters of hematopoietic cells/HPF; 2 (moderate), 3-5 hematopoietic clusters/HPF; and 3 (confluent), >5 hematopoietic clusters/HPF. Megakaryocytes in 2 HPF of bone marrow and splenic red pulp were counted and averaged/HPF. Lymphoid cellularity in the white pulp was scored as: 0, severe lymphoid depletion; 1, moderate lymphoid depletion; 2, mild lymphoid depletion; and 3, normal lymphoid cellularity. Additionally, white pulp foci of single cell necrosis were counted in 3 HPF/spleen and averaged/HPF. Liver lesions were scored 0 (no lesions), no cellular foci within the section; 1 (minimal), 1-10 foci/10× field; 2 (mild), 11-20 foci/10× field; and 3 (moderate), >20 foci/10× field.

Statistics. Before statistical analysis was done, a log transformation was made on body and organ weights, and an arcsine transformation was used on percentages. The t test was then used to compare these data. Comparisons of scored data were made using the Mann-Whitney U test. P-values of <0.05 were considered significant.

Results

Effects of WR-2721, Glucan, and Combined Treatment in Unirradiated Mice. *Effects on body weights and splenic weights.* No significant differences in body weight were observed. All groups displayed total body weight gain patterns similar to CON mice, with net weight gain recorded for each group (Table I). Splenic weights of CON and WR mice were similar, with the exception of Days 4 and 28, when WR values were significantly less (Fig. 1A). Elevated splenic weights observed in GLU and WR/GLU mice throughout the study were significantly greater than weights of CON and WR mice.

Quantitation of splenic white and red pulp areas and weights. Significant differences in white and red pulp areas between groups were limited to the first 11 days. As demonstrated in white pulp to red pulp ratios (W:R ratios) (Table II), GLU and WR/GLU white pulp areas were significantly elevated above CON on Day 1 and decreased to levels significantly less than CON by Day 4. Subsequently, W:R ratios of all groups remained near or slightly below unity, excluding Day 11, when the WR/GLU white pulp area approached a level significantly greater than CON. WR, and GLU. Distinctive microscopic changes noted in GLU and WR GLU white pulps on Day 1 are described below.

The white pulp weights of the WR group remained below CON weights throughout the study; however, differences were not significant (Fig. 2A). WR GLU and GLU white pulp weights were significantly greater than COn within the first 24 hr, but decreased by Days 7 and 11, respectively, to values not significantly different from CON or WR. Subsequently, white pulp weights in WR/GLU and GLU increased on Days 11 and 15, respectively, to levels significantly above CON and WR weights and remained elevated thereafter.

CON and WR red pulp weights remained at a consistent level, with a significant difference noted only on Day 28, when WR red pulp weight was reduced. GLU and WR/GLU red pulp weights on Day 1 were not significantly different from CON or WR; however, by Day 4, they were markedly increased and remained significantly elevated above CON and WR weights throughout the study (Fig. 3A).

Gross and microscopic changes in the spleen. On gross examination, GLU and WR/GLU spleens were enlarged throughout the study. Microscopic qualitative changes associated with increased proportions of white pulp in GLU and WR/GLU spleens consisted of accumulations of a large cell population at white pulp peripheries, and an admixture of a remnant population

Table I. Body Weights in Grams of Unirradiated and Irradiated Mice

Treatment Group	Days after treatment						
	1	4	7	11	15	21	28
Unirradiated groups							
CON	22.8 ± 0.8	22.9 ± 1.40	24.3 ± 0.7	23.5 ± 0.7	22.0 ± 0.8	24.1 ± 0.7	25.5 ± 0.7
GLU	21.5 ± 0.7	21.7 ± 0.80	22.5 ± 0.6	23.3 ± 0.4	23.3 ± 0.4	24.1 ± 0.7	25.3 ± 1.2
WR	21.3 ± 1.0	21.9 ± 0.40	22.5 ± 0.6	23.7 ± 0.6	23.0 ± 0.8	24.5 ± 0.9	24.1 ± 0.4
WR/GLU	20.9 ± 0.6	20.7 ± 0.03	21.7 ± 1.4	22.3 ± 0.7	23.8 ± 1.0	22.9 ± 1.2	24.6 ± 0.9
Irradiated groups							
RC	22.1 ± 0.5	22.3 ± 0.5	22.2 ± 0.6	19.8 ± 0.3	17.1 ± 0.5	NS'	NS
RG	20.3 ± 1.2ᵇ	21.4 ± 0.3	20.2 ± 0.4ᵇ	17.0 ± 0.5	15.8 ± 0.4	NS	NS
WR/R	23.5 ± 0.5	21.9 ± 0.7	22.1 ± 0.5	22.3 ± 0.9	22.9 ± 0.7	22.9 ± 0.9	24.4 ± 0.9
WR/R/GLU	21.1 ± 0.7ᵇ	20.9 ± 0.5	19.9 ± 1.0	21.8 ± 1.0	23.5 ± 0.5	23.0 ± 1.2	23.7 ± 0.5

ᵃ NS, no survivors.
ᵇ Significantly different from WR/R.
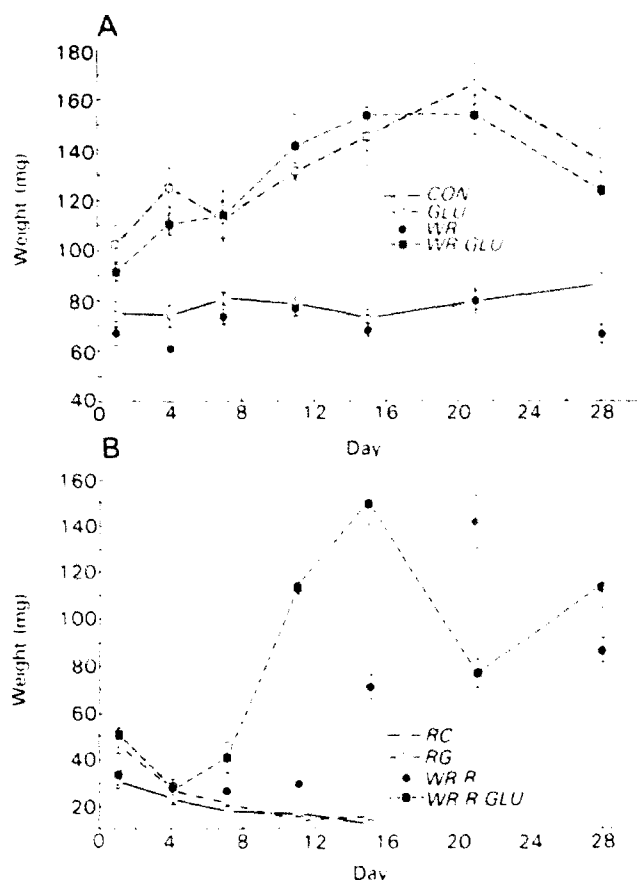ᶜ Significantly different from RC.
ᵈ Significantly different from RG.

Figure 1. Effects of GLU and WR individually and in combination on splenic weight of (A) unirradiated and (B) irradiated mice.

areas. Beyond Days 7 and 11, respectively, WR/GLU and GLU white pulps were essentially normal, with only occasional large cell aggregates observed on Days 7 and 11. Regardless of these changes, WR/GLU and GLU white pulp cellularities were judged abundant (3.0).

Single cell necrosis within the white pulp consisted of karyorrhectic and pyknotic debris within the interstitium or within macrophages (tingible body macrophages) (Fig. 4). GLU and WR/GLU spleens displayed significantly greater numbers of foci of necrosis than CON or WR spleens on Day 1, with foci in WR/GLU spleens being more numerous than in GLU spleens. After Day 1, there was a marked decrease of necrosis in both glucan-treated groups to levels lower than that of the CON group.

Splenic red pulp cellularity, assessed by judging relative quantities of erythropoietic aggregates, megakaryocytes, and granulopoietic foci, was abundant (3.0) for all groups on all sample days, excluding GLU spleens on Days 1 and 4 and WR/GLU spleens on Day 1 (all moderate). In general, decreased cellularity in GLU and WR/GLU spleens was attributed primarily to decreased hematopoietic tissue characterized by individual clusters of erythrocytic and myelocytic cells. This contrasted with the coalescing to confluent aggregates of hematopoietic cells noted in CON and WR spleens. Additionally, sinusoids adjacent to these islands of hematopoiesis were engorged with numerous red blood cells (congestion). On subsequent sample days, all groups displayed comparable cellularities, and congestion was resolved. There was no significant difference in the numbers of megakaryocytes/HPF among treatment groups or between treatment groups and CON. Prominent foci of granulopoiesis, occasionally noted subjacent to the splenic capsule and along trabeculae, were not associated with a particular treatment group or time frame.

Effects on liver. Liver weights in all groups in-

of small lymphocytes and foci of single cell necrosis in inner periarteriolar sheath regions. Accumulations (Fig. 4A) consisted of coalescing aggregates of numerous cells 15–20 μm in diameter interpreted light microscopically as large lymphocytes and macrophages. By Day 4, cellular accumulations in GLU and WR/GLU groups decreased, and the proportion of small lymphocytes increased, coincident with the decrease in white pulp

Table II. White to Red Pulp Ratios of Unirradiated and Irradiated Mice

Treatment group	Days after treatment						
	1	4	7	11	15	21	28
Unirradiated groups							
CON	0.67	0.93	1.02	0.64	0.72	0.81	0.75
GLU	1.30	0.59	0.61	0.44	0.85	0.87	0.87
WR	0.43	0.63	0.87	0.62	0.70	0.74	0.90
WR/GLU	1.20	0.50	0.54	1.06	0.94	0.88	1.03
Irradiated groups							
RC	0.31	0.26	0.34	0.24	0.10	NS[a]	NS
RG	0.59	0.26	0.31	0.27	0.14	NS	NS
WR/R	0.37	0.27	0.36	0.38	0.27	0.21	0.33
WR/R/GLU	0.64[b]	0.22	0.30	0.22	0.16	0.41	0.32

[a] NS, no survivors.
[b] Significantly different from RC and WR/R

A

80
70
60
50
40
30
20
10

Weight (mg)

— — CON
- - - GLU
● WR
- - ■ - WR GLU

0 4 8 12 16 20 24 28
Day

B

28
24
20
16
12
8
4
0

Weight (mg)

— - RC
- - - RG
● WR R
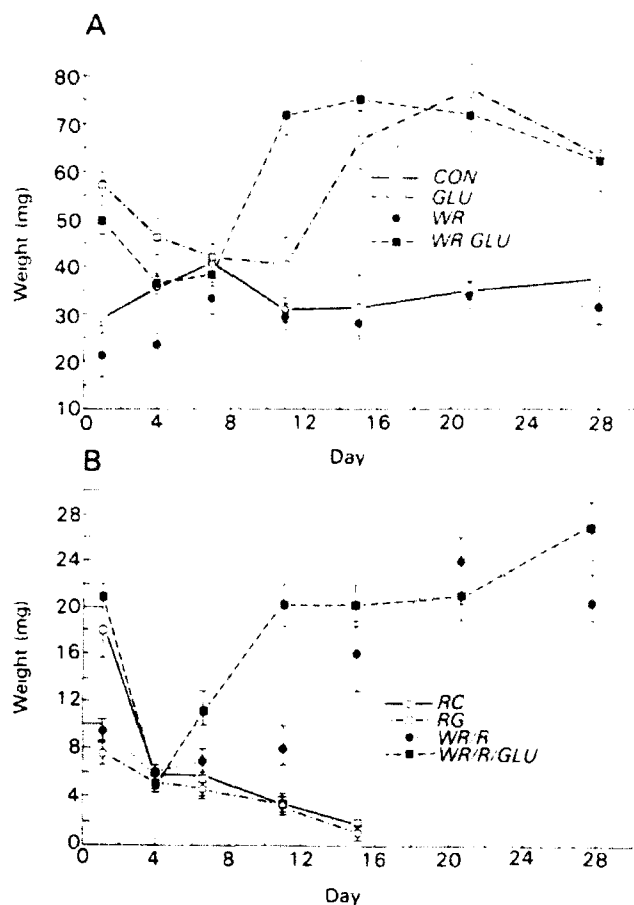- - ■ - - WR/R/GLU

0 4 8 12 16 20 24 28
Day

Figure 2. Effects of GLU and WR individually and in combination on splenic white pulp weight of (A) unirradiated and (B) irradiated mice. Each point represents the mean product of individual splenic weights and percentage of white pulp area, derived morphometrically from histologic sections.

A

100
80
60
40
20

Weight (mg)

— — CON
- - - GLU
● WR
■ WR GLU

0 4 8 12 16 20 24 28
Day

B

140
120
100
80
60
40
20

Weight (mg)

— — RC
- - - RG
● WR R
■ - WR R GLU

4 8 12 16 20 24 28
Day

Figure 3. Effects of GLU and WR individually and in combination on splenic red pulp weight of (A) unirradiated and (B) irradiated mice. Each point represents the mean product of individual splenic weight and percentage of red pulp area, derived morphometrically from histologic sections.

creased over the first 21 days, with a slight decrease in treatment groups by Day 28 (Fig. 5A). Throughout the study, WR and WR/GLU liver weights were comparable to CON and GLU, respectively. GLU weights were significantly greater than CON and WR weights on Days 7, 11, 15, and 21 and Days 11, 15, and 21, respectively; WR/GLU weights were significantly greater than CON and WR weights on Day 15 and on Days 4 and 15, respectively.

On gross examination, livers from both groups of glucan-treated mice displayed occasional, ≤1 mm in diameter, light tan foci subjacent to the organ capsule. These foci were most prominent on sample Days 11–21. Microscopic changes within the liver of WR, GLU, and WR/GLU groups were inflammatory in nature, with lesions in WR mice limited to normal background lesions noted in CON animals. Histologic changes in GLU and WR/GLU groups were comparable with initial minimal acute to subacute hepatitis, building to mild-to-moderate granulomatous hepatitis by Day 21 and initiating regression by Day 28 (Fig. 6A). Day 1 lesions consisted predominantly of randomly scattered
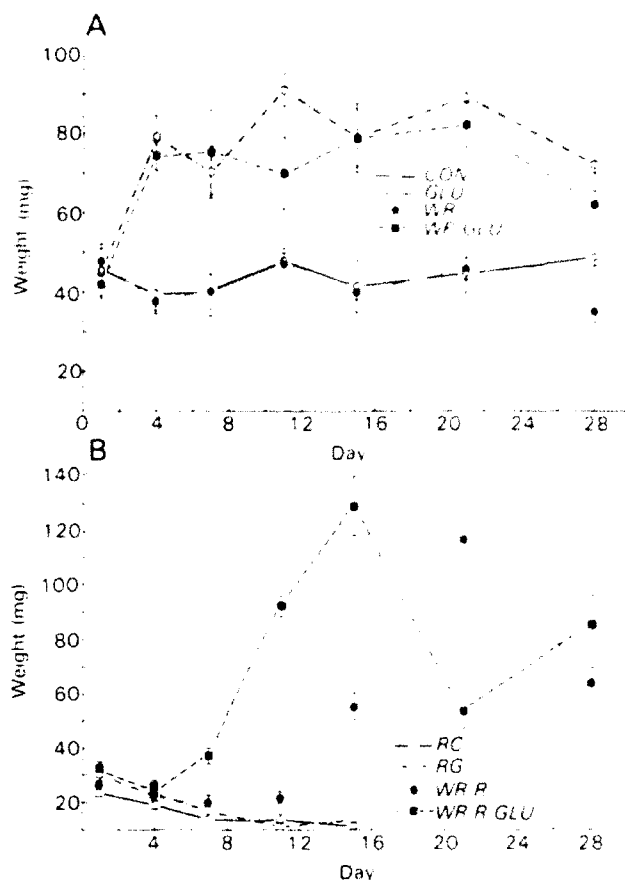
40–60-μm diameter foci of neutrophils with an occasional macrophage. By Day 4, macrophages were the principal cell type admixed with neutrophils, lymphocytes, cellular debris, and infrequent degenerating hepatocytes (Fig. 7, inset). Infrequently, cellular debris was also evident in sinusoids and central veins. By Day 7, involvement was still minimal, but a slight increase in the number and size of foci was evident. There were also noticeable accumulations of mononuclear cells, macrophages, and lymphocytes, directly subjacent to the endothelium of larger efferent vessels (Fig. 7). Portal regions, for the most part, were spared, except in several sections in which there was occasional minimal subacute pericholangitis. By Day 11 and continuing to Day 15, foci were larger (100–200 μm at greatest dimension) and consisted of macrophages, lymphocytes, and increased numbers of degenerating and necrotic hepatocytes. The number and severity of subendothelial foci increased, and additional foci were present beneath the liver capsule (Fig. 7). On Day 21, inflammatory changes were at a maximum, based on number and cumulative area of foci; however, there was a minimal decrease in
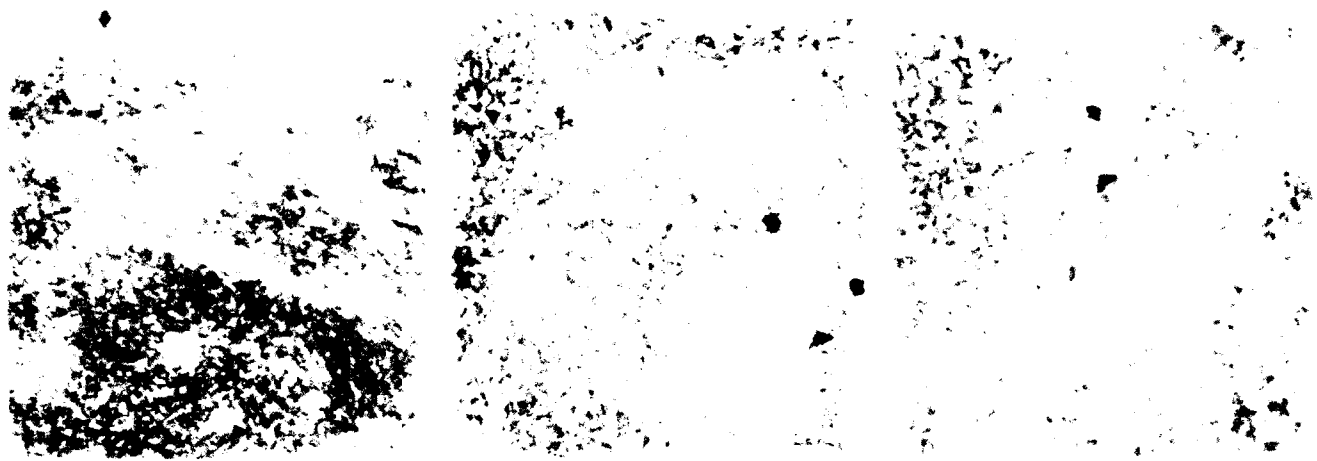
Figure 4. (A) Normal splenic white (W) and red (R) pulp, capsule (arrow), and central artery (arrowhead). (B and C) White and red pulp surface (white arrows) with peripheral mononuclear cells and central necrosis (black arrows) on Day 1 after glucan treatment in (B) unirradiated and (C) irradiated animals. The white pulp central artery is at the arrowhead (bars, 100 μM)
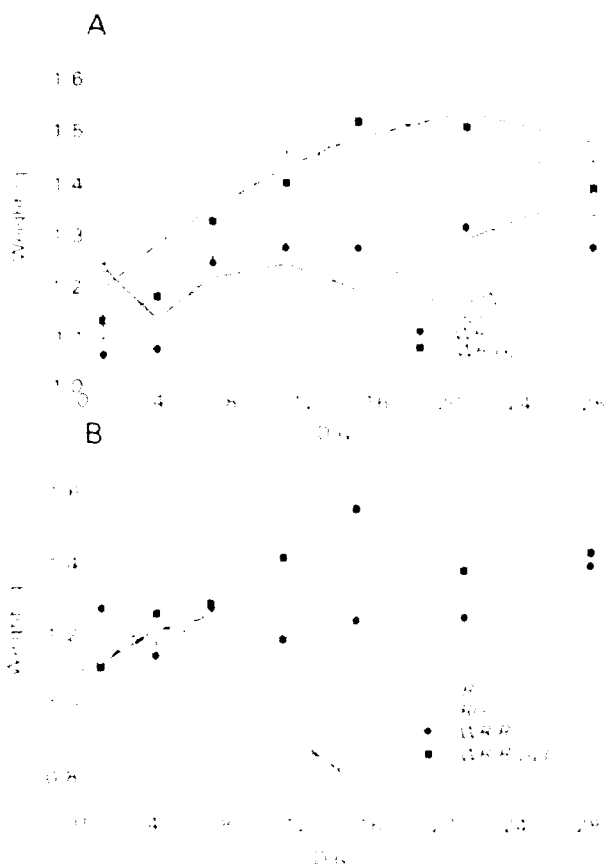

Figure 5. Effects of GLU and WR individually and in combination on hepatic weight of (A) unirradiated and (B) irradiated mice

Figure 6. Hepatic inflammation in treated mice. The horizontal dashed line in (A) represents the average background observed in controls (mean 0.64). The lesions were graded as follows: 1, minimal; 2, mild; 3, moderate; and 4, severe.

the cellularity of foci with a preponderance of macrophages, fewer neutrophils and lymphocytes, and occasional normal hepatocytes. By Day 28, marked involution of lesions was noted by a decrease in size and number of foci and reestablishment of normal hepatic architecture.
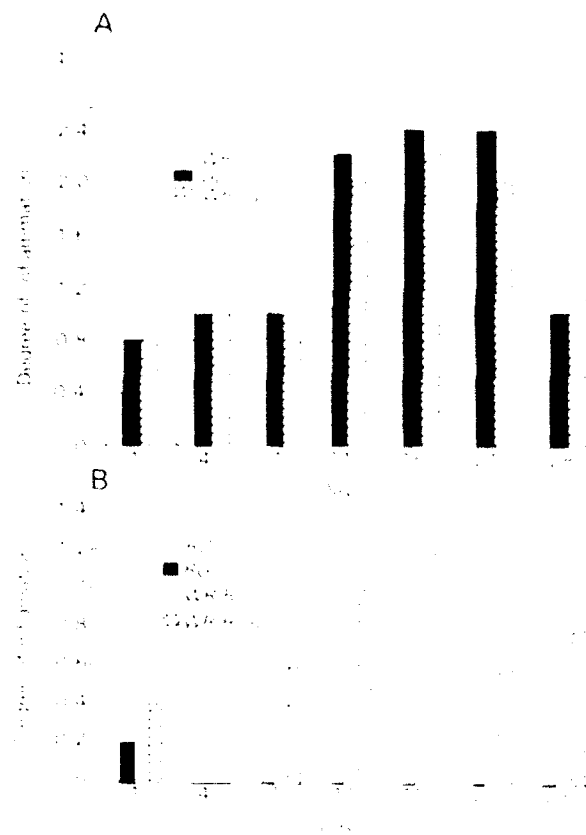
Effects on kidney. Significant differences in kidney weight were not observed. Microscopic findings were limited to normal background lesions.

Other tissues examined. Other tissues examined included bone marrow, mediastinal lymph node, the
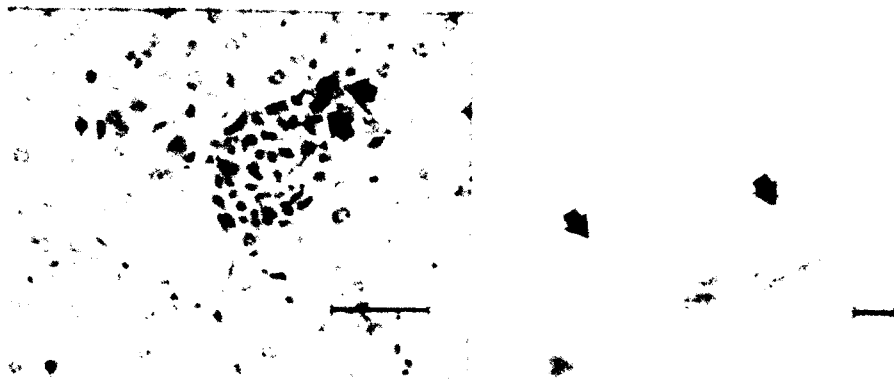
Figure 7. Liver from a WR/GLU-treated mouse 11 days after treatment. Subcapsular (arrowhead) and subendothelial (arrows) lesions consist primarily of admixtures of macrophages, lymphocytes, and neutrophils (bar, 150 μM). Inset: Subendothelial centrolobular lesion at Day 4, consisting of macrophages, lymphocytes, and two degenerating hepatocytes (arrows) (bar, 50 μM).

mus, and lung. Cellularity of bone marrow for all treatment groups was judged abundant (3.0) on all sample days except for Day 1 of the WR/GLU group, in which cellularity was moderate (2.0) with mild congestion. Lymph node and thymic morphologies and cellularities were normal. Lung fields were within normal limits.

Effects of WR-2721, Glucan, and Combined Treatment in Irradiated Groups. *Effects on body and splenic weights.* RG and WR/R/GLU body weights were less than WR/R and RC weights for the first 7 days, with sporadic significant differences noted on Days 1 and 7 (Table I). Subsequently, WR/R and WR/R/GLU body weights increased minimally during the balance of the study, whereas RC and RG weights decreased significantly by Day 15. There were no survivors in the RC and RG groups beyond Day 15. Splenic weights in RG and WR/R/GLU groups on Day 1 were comparable and both were significantly greater than those of RC and WR/R groups (Fig. 1B). By Day 4, splenic weights in all groups were equal. Subsequently, RC and RG splenic weights decreased by Day 15, whereas WR/R/GLU and WR/R splenic weights increased significantly above RC and RG groups by Days 11 and 15, respectively. Rebound and recovery patterns of WR/R/GLU and WR/R splenic weights were similar, but approximately 4 to 5 days out of synchronization, apparently due to a 4- to 5-day ad-

vanced recovery in WR/R/GLU mice. Intergroup comparison of WR/R/GLU and WR/R splenic weights of Day 15 with Day 21, respectively, and likewise of Day 21 with Day 28, did not reveal significant differences.

Quantitation of splenic white and red pulp areas and weights. Red pulp predominated in all groups throughout the experiment. Significant differences in splenic compartments were noted on Day 1, with the WR/R/GLU white pulp area significantly greater than the WR/R and RC areas (Table II). Although not statistically significant, there was a similar increase on Day 1 in RG white pulp. Microscopic changes seen in RG and WR/R/GLU white pulps are described below. After Day 1 perturbations, W:R ratios of all groups remained relatively static, with slight decreases noted in the RG and RC groups on Day 15.

RG and WR/R/GLU white pulp weights on Day 1 were comparable, and weights of both were significantly greater than those of the RC and WR/R groups (Fig. 2B). By Day 4, RG and WR/R/GLU weights decreased to levels similar to RC and WR/R groups. Subsequently, WR/R and WR/R/GLU white pulp weights increased from their Day 4 nadir to levels significantly greater than RC and RG weights by Day 15 and remained at levels comparable to their respective Day 15 weights for the remainder of the study. Red pulp weights in RC and RG groups decreased to Day 15 (Fig. 3B). Initial decreases in WR/R and WR/R/

GLU red pulp weights with nadirs at Days 7 and 4, respectively, were followed by increases to levels significantly greater than RC and RG weights by Days 11 and 7, respectively.

Gross and microscopic changes in spleens. By Day 4, all spleens were smaller than normal. WR/R and WR/R/GLU spleens displayed one to several approximately 1-mm diameter colonies that were directly subjacent to and that slightly elevated the splenic capsules. On microscopic examination, these colonies consisted of clusters of erythrocytic and myelocytic elements. Beyond Day 4, RC and RG spleens remained small, whereas WR/R and WR/R/GLU spleens continued to grow to approximately twice normal size as colonies increased in size and number and eventually reached confluency. Confluency was noted by Days 15 and 11 for WR/R and WR/R/GLU spleens, respectively.

Light microscopic changes were as follows: RC and WR/R groups on Day 1 displayed hypocellularity of white (1.0 and 1.8, respectively) and red pulps (0.0 and 1.0, respectively), characterized by a decrease in density of small lymphocytes with mildly scattered single cell necrosis in the white pulp and loss of the bulk of the usual dense hematopoietic elements within the red pulp.

On Day 1, RG and WR/R/GLU groups displayed hypocellularity of red pulp (0.0 and 2.2, respectively) similar to that of RC and WR/R groups. RG and WR/R/GLU white pulps, with cellularities of 1.8 and 2.0, respectively, displayed reactive and degenerative changes as described earlier in GLU and WR/GLU spleens. Necrosis in RG and WR/R/GLU white pulps was sufficiently intense to lower cellularity indexes of the white pulp, even in the face of peripheral expansion (Fig. 4B). Megakaryocyte counts on Day 1 for all groups (RC, 8.3; RG, 8.2; WR/R, 10.1; and WR/R/GLU, 6.3) were comparable.

On Day 4, white pulps of all groups were hypocellular and resembled RC and WR/R white pulps of Day 1 (RC, 1.2; RG, 1.0; WR/R, 1.0; and WR/R/GLU, 1.0). Large cell populations noted in the RG and WR/R/GLU groups on Day 1 were no longer present. Red pulps in all four groups were hypocellular (RC, 0.2; RG, 1.0; WR/R, 2.0; and WR/R/GLU, 1.2); one WR/R spleen was hypercellular with diffuse hematopoiesis. RC and RG red pulp cellularity was concentrated in occasional foci of hematopoiesis, whereas WR/R and WR/R/GLU cellularity was judged slightly higher due to more numerous and larger foci. Megakaryocyte counts on Day 4 in all groups (RC, 1.9; RG, 1.5; WR/R, 2.7; and WR/R/GLU, 1.9) were significantly lower than Day 1 levels.

RC and RG groups on Days 7, 11, and 15, with exceptions noted below, displayed hypocellular white (RC, 1.0, 1.6, and 0.3, respectively; RG, 1.0, 1.0, and

1.5, respectively) and red (RC, 0.0, 0.0, and 0.3, respectively; RG, 0.2, 0.4, and 1.5, respectively) pulps, with reduced numbers of lymphocytes in the white pulp and fewer hematopoietic colonies and no megakaryocytes in the red pulp. One RC spleen on Day 15 displayed a microscopically detectable focus of hematopoiesis in the red pulp. In the RG group on Days 7, 11, and 15, there were one, two, and two spleens, respectively, that displayed several prominent colonies.

WR/R and WR/R/GLU white pulps demonstrated partial re-establishment of small lymphocyte populations by Day 15. From Days 7 to 15, red pulp displayed enlargement of hematopoietic colonies with confluency in three of five WR/R/GLU spleens by Day 11 and in all five WR/R spleens by Day 15. Megakaryocyte counts were at their nadirs in both groups by Day 7 (0.0 and 0.1, respectively), with slight increases noted by Day 15 (0.1 and 0.3, respectively).

On Days 21 and 28, WR/R and WR/R/GLU white pulps displayed a normal complement of small lymphocytes, and red pulps in all spleens were confluent. WR/R/GLU and WR/R megakaryocyte counts rebounded by Day 21 (2.2 and 0.7, respectively) and reached near normal levels by Day 28 (5.6 and 5.9, respectively).

Effects on liver. Liver weights of all groups on Days 1, 4, and 7 were similar with the exception of the WR/R group, with mean weights significantly heavier than WR/R/GLU on Day 1 and lighter by Day 4 (Fig. 5B). By Day 11, RC and RG liver weights decreased significantly below WR/R and WR/R/GLU weights. From Days 7 to 28, WR/R and WR/R/GLU weights displayed slight increases with significant differences between WR/R and WR/R/GLU noted only on Day 15.

On gross examination, no remarkable changes were noted in any of the four groups. Histologic changes in RC and RG livers on Day 1 consisted of occasional minimally dilated pericentrilobular sinusoids (congestion), with and without minimal vacuolar changes in neighboring hepatocytes. Additionally, in RG livers, there were normal background changes as noted in normal, unirradiated control mice (Fig. 6B). Inflammatory changes were not observed in the RC group or in the RG group beyond Day 1. From Day 4 to Day 11, dilation of sinusoids was progressively aggravated to severe and moderate proportions in RC and RG groups, respectively. By Day 11 vacuolar change of hepatocytes within these regions was mild and moderate in RG and RC, respectively. Additionally, RG livers at this time displayed marked necrosis of centrilobular hepatocytes and dissociation of hepatic plates, with occasional single cells or rafts of hepatocytes in sinusoids. These latter changes were not observed in RC mice until Day 15.

Histologic changes in WR/R and WR/R/GLU livers on Day 1 consisted of minimal congestion, with

minimal vacuolar change in WR/R hepatocytes adjacent to congested areas. By Day 4, congestion was not present in the WR/R group, but was still minimal in WR/R/GLU livers and remained so through Day 15. On Days 4 through 15, there were remarkable mitotic figures within hepatocytes in both groups. Such a change was noted in RC and RG groups only on Days 4 and 7. Excluding occasional clusters (3–10 cells) of mononuclear cells within sinusoids on Days 15 and 21, no other hepatic lesions beyond background (degree of inflammation ≤ 0.65) (1) were noted in the WR/R group. These clusters were interpreted as foci of extramedullary hematopoiesis. In WR/R/GLU livers, inflammatory change was the key feature from Days 7 through 28. By Day 7, there was minimal to mild, subacute hepatitis with multifocal, random to centrilobular (10–50 cells) admixtures of lymphocytes, macrophages, and occasional neutrophils within focally expanded sinusoidal spaces. In several foci, there were adjacent degenerating or necrotic hepatocytes. By Day 15, the inflammatory process had developed maximally, presenting primarily a mild to moderate granulomatous hepatitis with increased numbers of multifocal and coalescing aggregates of macrophages, lymphocytes, and neutrophils. Occasional degenerating or necrotic hepatocytes, as well as prominent multinucleated giant cells, were present in some foci. By Days 21 through 28, the inflammatory process was in regression, and aggregates were less cellular. Reduced cellularity in these foci was at the expense of lymphocytes and neutrophils, with remaining cells often consisting exclusively of macrophages.

Effects on kidney. Kidney weights for the WR/R and WR/R/GLU groups did not significantly differ during the study, and on Days 1, 4, and 7, there were no significant differences in kidney weights for all groups. By Day 11, RG kidney weights were significantly below weights of the other groups, and by Day 15, kidney weights of both RC and RG groups decreased to equivalent levels, significantly different from the WR/R and WR/R/GLU groups.

Microscopically, RC kidneys appeared essentially normal for Days 1 through 11. By Day 15, there was occasional minimal, focal, single cell necrosis of cortical tubular epithelium in all samples. RG kidneys were essentially normal, with the exception of incidental focal changes in one Day 7 (minimal, focal, cortical tubular epithelial necrosis) and in one Day 15 (minimal, focal, interstitial fibrosis with glomerular atrophy) preparation. The WR/R kidneys, as in the groups above, displayed focal, cortical, tubular epithelial necrosis; however, in WR/R kidneys, there was also mild epithelial regeneration. On Day 15, one of five WR/R kidneys displayed a focal wedge-shaped lesion whose base abutted a depressed renal capsule and whose apex extended to the pelvis. The lesion consisted of multiple mildly

dilated tubules lined by regenerating, plump, basophilic epithelial cells and surrounded by minimal fibrous connective tissue admixed with accumulations of lymphocytes. This lesion is characteristic of a repairing infarct. The remaining renal tissues of this group were essentially normal. The WR/R/GLU kidneys did not differ in presentation of incidental lesions. However, on Day 15, two of five WR/R/GLU kidneys displayed focal, infarctive lesions undergoing repair (Fig. 8). Differing from the infarctive lesions noted in the WR/R kidney, numerous tubules in these two kidneys contained basophilic hyalin material, interpreted as hyaline casts. Other than these changes, the WR/R/GLU kidneys were essentially normal.

Other tissues examined. Bone marrow cellularity of all groups by Day 1 was severely decreased. The cellularity present consisted of stroma, numerous polymorphonuclear cells, and red blood cells (hemorrhage). The bone marrow of RC and RG groups remained moderately to severely hypocellular through Day 15, even though occasional foci of blast cells were observed on Days 4 and 11, respectively. Hemorrhaging subsided by Day 15 and Day 11 in RC and RG groups, respectively. By Day 7, the WR/R and WR/R/GLU marrow cavities were normocellular and consisted predominantly of polymorphonuclear cells with scattered foci of blast cells.

Thymic responses after irradiation consisted of severe necrosis of cortical thymocytic populations, with maintenance of a population of small thymocytes in the medulla within the first 24 hr. Full repopulation of the thymic cortex was noted in sections of the RC, WR/R, and WR/R/GLU groups by Day 11. Cortical thymocyte recovery in the RG group was not observed.

Lymph nodes from all groups displayed severe lymphocytolysis on Day 1, with clearance of necrotic debris by Day 4. WR/R and WR/R/GLU nodes gradually regained normocellularity around Day 15, whereas RC and RG nodes remained hypocellular.

Discussion

Dosage levels and combinations of WR-2721 and soluble glucan used in our study have been demonstrated capable of affecting survival in C3H/HeN female mice exposed to otherwise lethal doses (9–15 Gy) of ^{60}Co radiation (1). At these doses, toxic effects of the two agents, as measured by any overt physiologic signs, were reportedly minimized. Histopathologic effects of WR-2721 and glucan administered individually have been reported previously (12, 15, 18, 19, 22, 23), but their effects when given in combination at doses producing the previously noted dose-reduction factors, have not been described in irradiated or unirradiated animals.

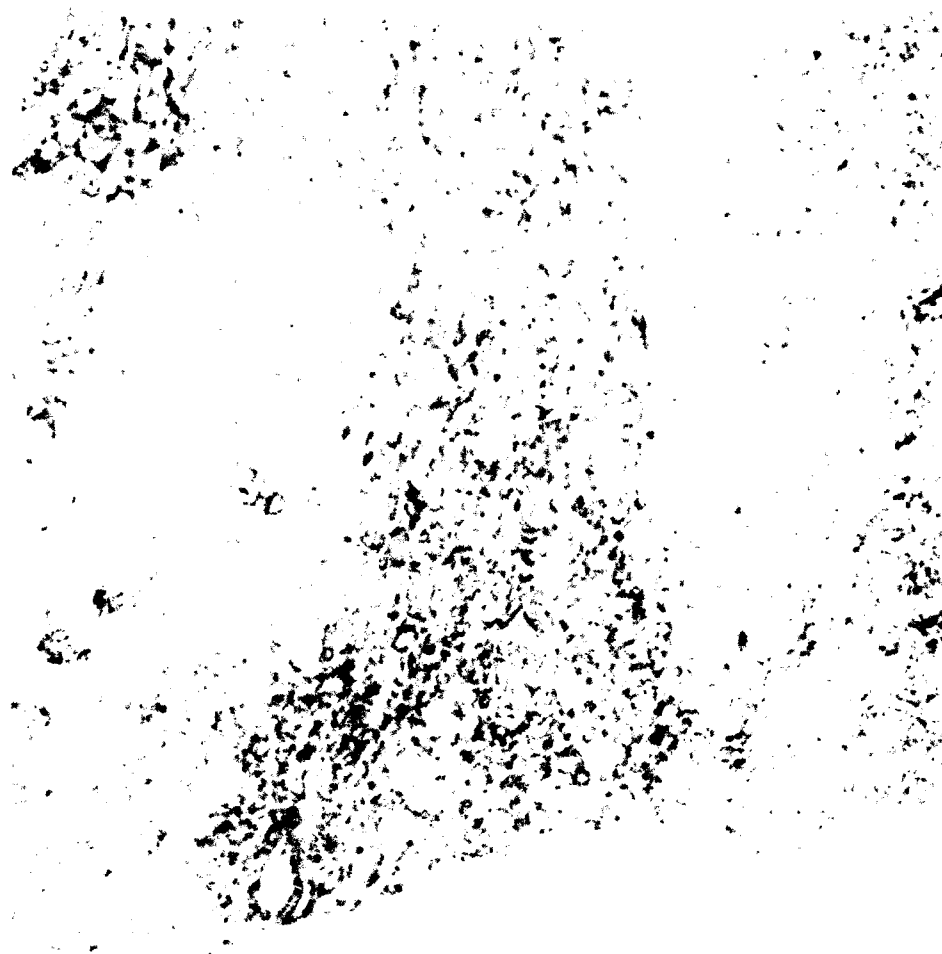In our study, survival responses in irradiated groups were comparable with those of a previous study (1),

Figure 8. Renal lesion in a WR/R/GLU-treated mouse (Day 15) displaying a resolving infarct consisting of mildly dilated cortical tubules lined with regenerating epithelium and variably filled with hyaline casts and surrounded by minimal accumulations of lymphocytes.

The dose of WR-2721 used in this experiment (200 mg/kg ip) is substantially below reported doses at which lethality, transient decreased body weights, and histologic changes have been observed (9, 18). Our mice did display slightly decreased locomotor activity several hours after treatment, a change reported previously (17).

The glucan used (250 mg/kg iv) was a soluble preparation. Unlike particulate glucan preparations, soluble glucan administration generally has not been associated with hepatosplenomegaly or granuloma formation (19), although prolonged treatment with 1000 mg/kv iv has produced hepatomegaly and liver lesions (16). Splenomegaly was also reported at this high dose, as well as at a low dose of 40 mg/kg, but splenic lesions were absent in both instances.

In our study, body weights of irradiated and unirradiated groups were similar for the first 7 days. Subsequently, WR/R and WR/R/GLU body weights remained comparable to unirradiated groups, whereas

RC and RG groups displayed significant weight losses. Of note here is the sparing effect of WR-2721 in irradiated groups.

Soluble glucan alone has produced mixed splenic responses in unirradiated mice ranging from no increases in weights to significant increases of 44% (16). Attendant histologic lesions were either not observed or not described in previous studies (12, 16, 19). In our study, multiple parameters in irradiated and unirradiated spleens changed significantly after treatment with glucan alone or combined with WR-2721. Twenty-four hours after treatments, splenic weights in unirradiated WR/GLU and GLU mice were significantly greater than in WR and CON mice (37%), and although splenic weights of all irradiated groups were significantly less than CON at this time, a similar relationship was noted in irradiated counterparts WR/R/GLU and RG when compared with WR/R and RC (51% and 53%, respectively). Also common to all glucan-treated groups on Day 1 were significantly greater white pulp

areas and white pulp weights, relative to their non-glucan-treated controls. Finally, microscopic changes within splenic white pulp on Day 1 consisted of marked accumulations of a population of large cells at follicular peripheries and central single cell necrosis (lymphocytolysis). Lymphocytolysis in irradiated groups was more prominent, a characteristic attributed to the additive effects of irradiation and glucan treatments, both independently associated with lymphocytolysis and observed in independent control groups RC and GLU. Early histologic changes in spleens of our mice suggest a transient change within the first 24–72 hr following a single dose of soluble glucan. Similar histologic changes have been noted in C3H/He mice 24 hr after a single intravenous injection of lipopolysaccharide (24). Having assessed only light microscopic changes, we speculate that the cellular accumulations represent admixtures of lymphocytes, macrophages, and, perhaps, dendritic cells (25, 26) activated directly by exposure to glucan and/or activated indirectly by cytokine release from other primary activated cells (25).

Beyond Day 1, continued elevation in unirradiated WR/GLU and GLU splenic weights to Days 7 and 11, respectively, was associated with increased red pulp areas. This glucan-stimulated expansion of red pulp coincides with significant increases in splenic cellularity in general and specifically in splenic red pulp hematopoietic stem and progenitor cells reported previously in soluble, glucan-treated C3H/HeN female mice (6). Subsequently, elevated WR/GLU and GLU splenic weights were accompanied by comparable increases in white pulp areas to proportions approximately equal to red pulp, with recovery in WR/GLU spleens four days in advance of GLU spleens. Ultimate recovery of WR/R/GLU and WR/R splenic weights to levels comparable to or greater than CON spleens was attributed to radioprotective effects of WR-2721 and accompanied by reconstitution of white and red pulps. An estimated 4-day advanced recovery of WR/R/GLU splenic weights was ascribed to glucan and supported by previously documented advanced increases of splenic cellularity and splenic granulocyte-macrophage colony-forming cells in similarly treated C3H/HeN female mice (1). Advanced changes noted in combined treatment groups (WR/GLU and WR/R/GLU) are apparently due to a synergy between WR-2721 and glucan.

Hepatomegaly, as assessed by increased liver weight, was associated with glucan treatment. Previously reported increases in rats and mice (0–13% of control) given soluble glucan were not significant (12, 16), but increases in hepatic weights in our unirradiated (GLU and WR/GLU) and irradiated (WR/R/GLU) groups (15–31% of control) were significant. Increasing and decreasing liver weights within GLU, WR/GLU, and WR/R/GLU groups were directly associated with the onset of and the increase and decrease in severity

of microscopic hepatic lesions. We attribute maintenance of normal liver weights in WR/R mice to the radioprotectant effects of WR-2721, the greater weights in GLU and WR/GLU mice to the phlogistic effects of glucan, and greater weights in WR/R/GLU to glucan's phlogistic effects potentiated by WR-2721.

Microscopic liver lesions were not observed in rats (12) or mice (16, 19) given 10 mg/kg and 200 mg/kg of soluble glucan intravenously, respectively. Hepatic lesions were reported, however, in mice receiving 1000 mg/kg iv (16). In our study, lesions apparent as early as Day 4 were at times difficult to distinguish from normal background changes. Not until around Day 11 were they readily identifiable. This may explain in part the absence of liver lesions 4–5 days after single or multiple doses, as reported in earlier studies (12, 19). Further explanation may be found in the use of lower dosages and different animal species/strains in the studies (12, 16, 19).

The nature of glucan-induced infiltrates and proliferations within our preparations is consistent with previous observations independent of the form of glucan used (16, 23, 27). This was not the case with distribution of our lesions, the majority of which were either random or centrilobular. Similarly, lesions in mice treated with extremely high doses of soluble glucan, 1000 mg/kg, were represented photographically as random (16). However, several studies using particulate glucan in rats or mice reported a predominance of periportal lesions (27, 28). The difference in distribution may be due to physical properties of particulate versus soluble glucan.

Significant renal changes were limited to irradiated groups. Specifically, decreases in kidney weights were noted in RG and RC groups by Days 11 and 15, respectively, and attributed to radiation. Although WR/R and WR/R/GLU kidneys did not display weight losses, they did demonstrate significant microscopic changes in the form of infarcts. These lesions are, in part, compatible with previously reported toxic responses to WR-2721 (18). In addition to the reversible changes of tubular epithelial necrosis and proteinaceous cases reported in that study (CDF₁ female mice given 540 mg/kg of WR-2721 iv), our mice displayed chronic, irreversible renal lesions. These lesions were apparently potentiated by the added stress of lethal irradiation in that our mice received only 200 mg/kg ip, a dose judged nontoxic to CON and WR/GLU mice. This observation supports the caveat extended by authors of the above-cited study warning of potential toxicologic changes at low doses of WR-2721 in debilitated patients.

In conclusion, treatment with soluble glucan (250 mg/kg), whether combined with WR-2721 (200 mg/kg) or not, was associated with transient hepatosplenomegaly with accompanying histologic changes in unir-

radiated mice. In lethally irradiated mice. radiation-induced splenic weight loss was dampened in glucan groups on Day 1 and accompanied by morphometric and histologic changes similar to those seen in unirradiated counterparts. Subsequent rebounds of irradiated splenic weights were associated with hematopoietic reconstitution in WR-2721-treated groups, a change that occurred 4 days earlier in the combined treatment group. Hepatic lesions, similar to those noted in unirradiated groups, were observed only in the combined treatment group (WR/R/GLU), in which glucan-induced phlogistic changes were potentiated by the radioprotective effects of WR-2721. Additionally, in the WR/R and WR/R/GLU groups, limited observations suggest that irreversible renal lesions, not present in unirradiated WR-2721 recipients, may be induced with WR-2721 when followed by lethal radiation exposure. Further study is needed to verify the combined effects of WR-2721 and irradiation on renal tissues.

1. Patchen ML, MacVittie TJ, Jackson WE. Postirradiation glucan administration enhances the radioprotective effects of WR-2721. Radiat Res 117:59-69, 1989.

2. Patchen ML, MacVittie TJ. Stimulated hemopoiesis and enhanced survival following glucan treatment in sublethally and lethally irradiated mice. Int J Immunopharmacol 7:923-932, 1985.

3. Patchen ML, MacVittie TJ. Comparative effects of soluble and particulate glucans on survival in irradiated mice. J Biol Response Mod 5:45-60, 1986.

4. Patchen ML, MacVittie TJ, Solberg BD, D'Alesandro MM, Brook I. Radioprotection by polysaccharides alone and in combination with aminothiols. Adv Space Res 12(2-3):(2)233-(2)248, 1992.

5. Patchen ML, MacVittie TJ. Use of glucan to enhance hemopoietic recovery after exposure to cobalt-60 irradiation. Adv Exp Med Biol 155:267-272, 1982.

6. Patchen ML, MacVittie TJ, Wathen LM. Effects of pre- and postirradiation glucan treatment on pluripotent stem cells, granulocyte, macrophage and erythroid progenitor cells and on hematopoietic stromal cells. Experientia 40:1240-1244, 1984.

7. Patchen ML, MavVittie TJ. Hemopoietic effects of intravenous soluble glucan administration. J Immunopharmacol 8:407-425, 1986.

8. Patchen ML, DiLuzio NR, Jacques P, MacVittie TJ. Soluble polyglycans enhance recovery from cobalt-60 induced hemopoietic injury. J Biol Response Mod 3:627-633, 1984.

9. Patchen ML, D'Alesandro MM, Brook I, Blakely WF, MacVittie TJ. Glucan: Mechanisms involved in its "radioprotective" effect. J Leukocyte Biol 42:95-105, 1987.

10. Yuhas JM. Biological factors affecting the radioprotective efficiency of S-2[3-aminopropylamino]ethylphosphorothioic acid (WR-2721). LD₅₀ doses. Radiat Res 44:621-628, 1970.

11. Sigdestad CP, Grdina DJ, Connor AM, Hanson WR. A comparison of radioprotection from three neutron sources and ⁶⁰Co by WR-2721 and WR-151327. Radiat Res 106:224-233, 1986.

12. Bowers GJ, Patchen ML, MacVittie TJ, Hirsch FF, Fink MP. A comparative evaluation of particulate and soluble glucan in an endotoxin model. Int J Immunopharmacol 8:313-321, 1986.

13. Way CF, Dougherty WJ, Cook JA. Effects of essential fatty acid deficiency and indomethacin on histologic, ultrastructural and phagocytic responses of hepatic macrophages to glucan. J Leukocyte Biol 37:137-150, 1985.

14. Riggi SJ, DiLuzio NR. Hepatic function during reticuloendothelial hyperfunction and hyperplasia. Nature 193:1292-1294, 1962.

15. Deimann W, Fahimi HD. Induction of focal hemopoiesis in adult rat liver by glucan, a macrophage activator. Lab Invest 42:217-224, 1980.

16. Williams DL, Sherwood ER, Browder IW, McNamee RB, Jones EL, DiLuzio NR. Pre-clinial safety evaluation of soluble glucan. Int J Immunopharmacol 10:405-414, 1988.

17. Landauer MR, Davis HD, Dominitz JA, Weiss JF. Dose and time relationship of the radioprotector WR-2721 on locomotor activity in mice. Pharmacol Biochem Behav 27:573-576, 1987.

18. Palmer TE, Glaza SM, Dickie BC, Weltman RH, Greenspun KS. Toxicity studies on the radioprotective agent WR-2721 in CDF mice and beagle dogs. Toxicol Pathol 13:58-65, 1985.

19. DiLuzio NR, Williams DL, McNamee RB, Edwards BF, Kitahama A. Comparative tumor-inhibitory and anti-bacterial activity of soluble and particulate glucan. Int J Cancer 24:773-779, 1979.

20. Schulz J, Almond PR, Cunningham JR, Holt JG, Loevinger R, Suntharalingam N, Wright KA, Nath R, Lempert D. A protocol for the determination of absorbed dose from high energy photon and electron beams. Med Phys 10:741-771, 1983.

21. Weibel ER. Stereological Methods: Vol. 1, Practical Methods for Biological Morphometry. London: Academic Press, p9, 1979.

22. Deimann W, Fahimi HD. Hepatic granulomas induced by glucan. An ultrastructural and peroxidase-cytochemical study. Lab Invest 43:172-181, 1980.

23. Yamada M, Naito M, Takahashi K. Kupffer cell proliferation and glucan induced granuloma formation in mice depleted of blood monocytes by strontium-89. J Leukocyte Biol 47:195-205, 1990.

24. Groeneveld PHP, Koopman G, van Rooijen N. The effects of LPS on the cellular composition of the splenic white pulp in responder C3H/He and non-responder C3H/HeJ mice. Virchows Arch [B] 49:183-193, 1985.

25. Steinman RM, Kaplan G, Witmer MD, Cohn ZA. Identification of a novel cell type in peripheral lymphoid organs of mice. V. Purification of spleen dendritic cells, new surface markers and maintenance in vitro. J Exp Med 149:1-16, 1979.

26. Sherwood ER, Williams DL, McNamee RB, Jones EL, Browder IW, DiLuzio NR. Enhancement of interleukin-1 and interleukin-2 production by soluble glucan. Int J Immunopharmacol 9:261-267, 1987.

27. Deimann W, Fahimi HD. The appearance of transition forms between monocytes and Kupffer cells in the liver of rats treated with glucan. J Exp Med 149:883-897, 1979.

28. Pospisil M, Tkadlecek L, Netikova J, Pipalova I, Viklicka S, Kozubik A, Vacha J, Jary J. Interstrain differences in the responsiveness of mice to glucan with respect to hematological effects and manifestations of late damage. Exp Pathol 33:27-36, 1988.

Comparison of apical and basal surfaces of confluent endothelial cells: patch-clamp and viral studies

MARGARET COLDEN-STANFIELD, EVA B. CRAMER, AND ELAINE K. GALLIN

Department of Physiology, Armed Forces Radiobiology Research Institute, Bethesda, Maryland 20889-5145; and Department of Anatomy and Cell Biology, State University of New York Health Science Center at Brooklyn, Brooklyn, New York 11203

Colden-Stanfield, Margaret, Eva B. Cramer, and Elaine K. Gallin. Comparison of apical and basal surfaces of confluent endothelial cells: patch-clamp and viral studies. *Am. J. Physiol.* 263 (*Cell Physiol.* 32): C573–C583, 1992.—The distribution of inwardly rectifying (K_i) and calcium-activated (K_{Ca}) potassium channels on the apical and basal surfaces of bovine aortic endothelial cells (BAECs) was examined by inverting BAEC monolayers onto polylysine-coated cover slips. To monitor cellular polarity, we examined human red blood cell adherence (hemadsorption) to the influenza virus protein, hemagglutinin (HA), and virus budding on the surface of infected BAECs. Hemadsorption and virus budding occurred on the apical surface but were not apparent on the basal surface of monolayers 1 and 5 h after inversion, although cellular HA antigen localization confirmed that all monolayers were infected. In contrast, by 9.5 and 24 h after inversion, hemadsorption was evident on the "new" apical surface. Single-channel patch-clamp analysis revealed the presence of both K_i and K_{Ca} channels on the apical surface and basal surface of BAEC monolayers 2–5 h after inversion. K channel conductance and kinetics were similar regardless of the surface monitored. This nonenzymatic mechanical technique of exposing the basal surface of endothelium provides a useful tool to study the distribution of ion channels in endothelium and in other polarized cell types grown in tissue culture.

cell polarity; potassium channels; influenza virus infection; hemagglutinin

PATCH-CLAMP STUDIES of cultured vascular endothelial cells indicate that although voltage-sensitive Ca or Na channels are absent (4, 26), several types of K channels are prevalent in the plasma membrane of these cells. These include a voltage-dependent inwardly rectifying K channel (K_i channel) (3, 26), K channels activated by shear stress and acetylcholine (17, 18), and Ca-activated K channels (K_{Ca} channels) induced by bradykinin and purinergic receptor occupation (3, 22). Although K_{Ca} channels are seldom spontaneously active, circulating Ca-mobilizing agents such as bradykinin, thrombin, ATP, and histamine induce channel openings, hyperpolarizing the membrane and increasing the driving force for Ca influx (12, 23). Although the distribution of K_{Ca} channels in confluent endothelial cell cultures has not been examined, the presence of similar K_{Ca} channels on subconfluent tracheal epithelial cells and the absence of these channels on confluent cells suggest that in tracheal epithelial cells K_{Ca} channels are asymmetrically distributed on the basolateral surface (31, 32).

Although a comparison of the ion channels present in confluent and subconfluent monolayers provides indirect evidence about channel distribution in polarized cells, direct observation of ion channel activity is required to conclusively demonstrate asymmetric channel behavior and distribution on the basal surface of polarized cells. This requires that the basal surface of cultured cells in adherent monolayers be accessible to patch electrodes. Several methods involving enzymatic and mechanical techniques have been used to record ion channel activity on basolateral surfaces of epithelial cells in intact tissues (8, 27, 31). In contrast, ion channel activity has not been recorded on the exposed basal membranes of polarized cell monolayers grown in tissue culture.

Muller and Gimbrone (15) recently demonstrated that the basal surface of confluent endothelial cells can be made accessible to biochemical probes by simply inverting endothelial cell monolayers onto polylysine-coated cover slips. Using this technique, they were able to show that the basal surface contains several radioiodinated proteins that are absent from the apical surface and that this asymmetry is maintained for up to 24 h after inversion of the monolayers. Their findings were consistent with other studies that described polarization of transport functions in confluent endothelial cells. For example, release of a platelet-derived-like growth factor (35) and the von Willebrand factor from endothelial cells (24, 29) preferentially occurs in the basolateral space. Similarly, the ability of angiotensin-converting enzyme to metabolize circulating bradykinin and angiotensin (potent modulators of blood pressure homeostasis) is optimized by an apical localization of the enzyme in endothelial cells (7, 16), while Na^+-K^+-ATPase appears to be exclusively located in the basal membrane of endothelial cells (1, 7).

In this study we demonstrate that the inversion technique of Muller and Gimbrone (15) can be used to record ion channel activity on the basal surface of confluent endothelial cells, and we examine the effects of the inversion procedure on cell viability, membrane potential, and gap junction permeability. Sidedness of influenza virus budding occurs preferentially from the apical surface of infected endothelial cells (13) and, when used as a functional monitor of cellular polarity, we show that the viral hemagglutinin (HA) protein on the apical surface of confluent cells does not begin to redistribute to the exposed basal surface until 9.5 h after inversion. Patch-clamp studies of the apical and basal surfaces of uninfected endothelial cells reveals similar K_{Ca} and K_i channels on both surfaces of the endothelial plasmalemma.

MATERIALS AND METHODS

Isolation and Identification of Bovine Aortic Endothelial Cells

Endothelial cells were dislodged from the vessel wall of bovine aorta (Mount Airy Meat Locker, Mount Airy, MD) by incubating with a 0.03% collagenase-phosphate-buffered saline (PBS) solution (type II, Worthington Biochemical, Freehold, NJ) for

10 min at 37°C. Cells were sloughed off by rinsing the lumen of the vessel with Dulbecco's modified Eagle's medium (DMEM, GIBCO, Grand Island, NY) and collecting the effluent in centrifuge tubes. Complete DMEM containing 10% heat-inactivated fetal bovine serum (Hyclone Laboratories, Logan, UT), penicillin (100 U/ml), streptomycin (100 µg/ml), neomycin (200 µg/ml), 2 mM glutamine (all from GIBCO), heparin (100 µg/ml) (Sigma, St. Louis, MO), and ascorbate (50 µg/ml; Sigma) was added to the tubes for centrifugation at 1,000 revolutions/min for 5 min. Pellets were resuspended in complete DMEM, plated in 60-mm tissue culture dishes, and placed in a 37°C 95% air-5% CO_2-humidified incubator. Cells were gently refed ~2-3 h later to reduce contamination by smooth muscle cells and fibroblasts. Primary endothelial cells were isolated 24 h later with cloning cylinders (Bellco Glass, Vineland, NJ) to eliminate remaining contaminating cells. Experimental data were obtained from bovine aortic endothelial cells (BAECs) in their second to eighth passage and 4-7 days postconfluency.

A pure population of endothelial cells was confirmed by 1) the characteristic "cobblestone," nonoverlapping morphology of confluent monolayers (Fig. 1A), 2) the presence of uniformly distributed acetylated low-density lipoprotein identified with the fluorescent probe 1,1'-diotadecyl-1-3-3-3'-3'-tetramethyl-indocarbocyanine perchlorate [DiI-Ac-LDL; Fig. 1B; Biomedical Technologies, Stoughton, MA (30)], and 3) the presence of high angiotensin-converting enzyme activity [determined by a microvial radioassay; Ventrex Laboratories, Portland, MN (21)]. The vascular smooth muscle cell line from rat aorta, A7r5 (American Type Culture Collection, Rockville, MD), did not accumulate DiI-Ac-LDL and had a 66-fold lower angiotensin-converting enzyme activity than BAEC monolayers (data not shown).

Inversion Procedure

BAEC monolayers were inverted to expose the basal surface of the cells, using the procedure described by Muller and Gimbrone (15). A poly-L-lysine-coated [1 mg/ml in Hanks' balanced salt solution (HBSS); Sigma] glass cover slip (Bellco) was placed on a confluent monolayer of BAECs after the monolayer was washed several times with HBSS warmed to 37°C (see schematic in Fig. 2). Within seconds, the cover slip was lifted up with the accompanying inverted monolayer and placed in a culture dish containing complete DMEM. The inverted BAECs were either immediately tested electrophysiologically or placed in a 5% CO_2-humidified incubator at 37°C for 2-5 h and then patch clamped. Successful inversion of the monolayer required that cells be plated on uncoated plastic culture dishes (Becton Dickinson, Lincoln Park, NJ) for at least 4 days postconfluency.

Viability of Inverted Monolayers

Cell viability. The viability of inverted monolayers was tested by exposing the monolayer to a PBS solution containing 0.05% ethidium bromide and 0.002% acridine orange 10 s or 30 min after inversion and visualizing the fluorescence with fluorescein optics (450-490 nm excitation/520 nm emission/510 nm dichroic mirror; Zeiss, Thornwood, NJ). Live cells fluoresce green (with acridine orange), and dead cells fluoresce red (with ethidium bromide).

A fluorescein isothiocyanate (FITC)-labeled dextran (100,000 mol wt; Sigma) incorporation assay was also used to determine whether the inversion procedure extensively disrupted the BAEC membrane. At 10 s or 30 min after a monolayer was inverted, it was exposed to FITC-dextran (20 mg/ml) in PBS for 1 or 10 min. The cultures were then gently washed with PBS before the cells were observed with fluorescein optics.

Gap junctions. Previous studies using lucifer yellow dye transfer and the passage of current between cells have demonstrated
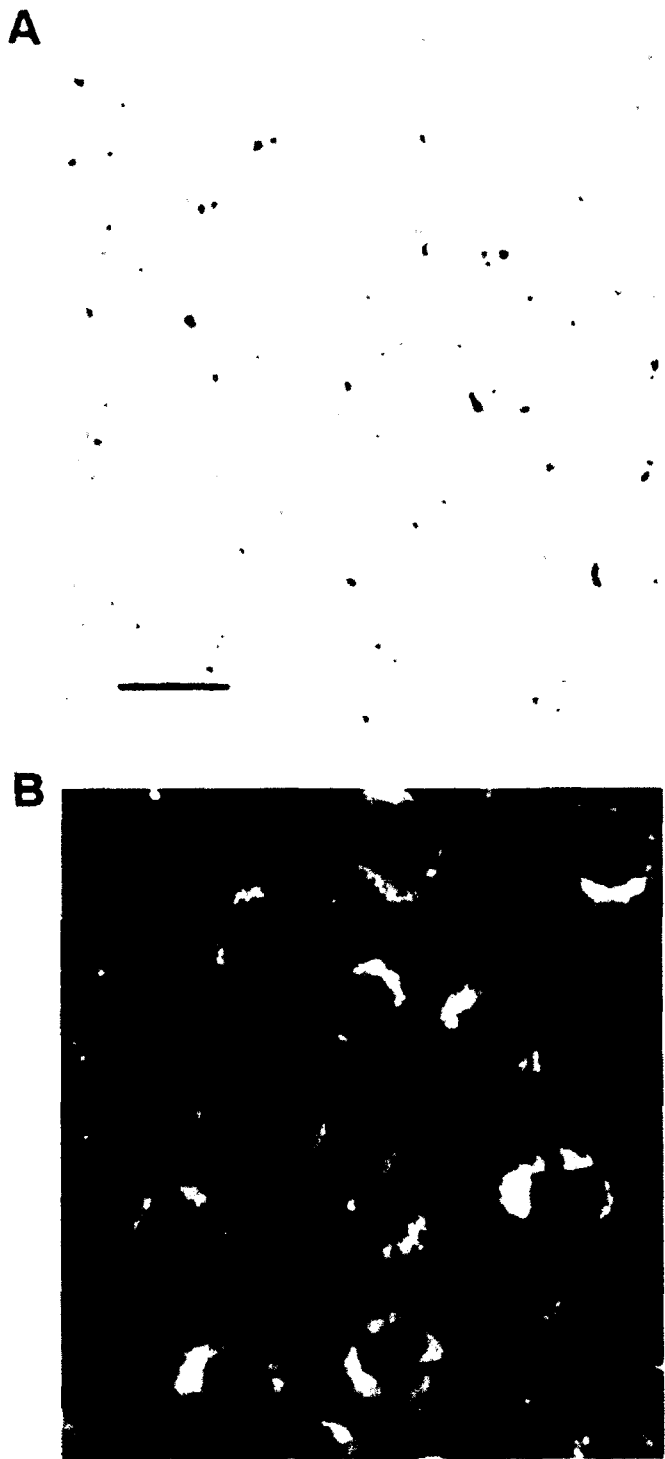
Fig. 1. A: photomicrograph of apical surface of a postconfluent bovine aortic endothelial cells (BAEC) monolayer. B: fluorescence micrograph demonstrating uniform uptake and perinuclear distribution of DiI-Ac-LDL into the same BAEC monolayer. Bar, 40 µm

that endothelial cells are electrically coupled through gap junctions (11). Lucifer yellow dye transfer was monitored in noninverted monolayers as well as in monolayers inverted for 0-5 h by using patch electrodes containing 1% lucifer yellow in high KCl solution (see *Patch-Clamp Technique* for composition) during whole cell recordings. Once the whole cell configuration was established, the pipette contents were allowed to diffuse passively into the cell for 5 min. Dye transfer was then visualized
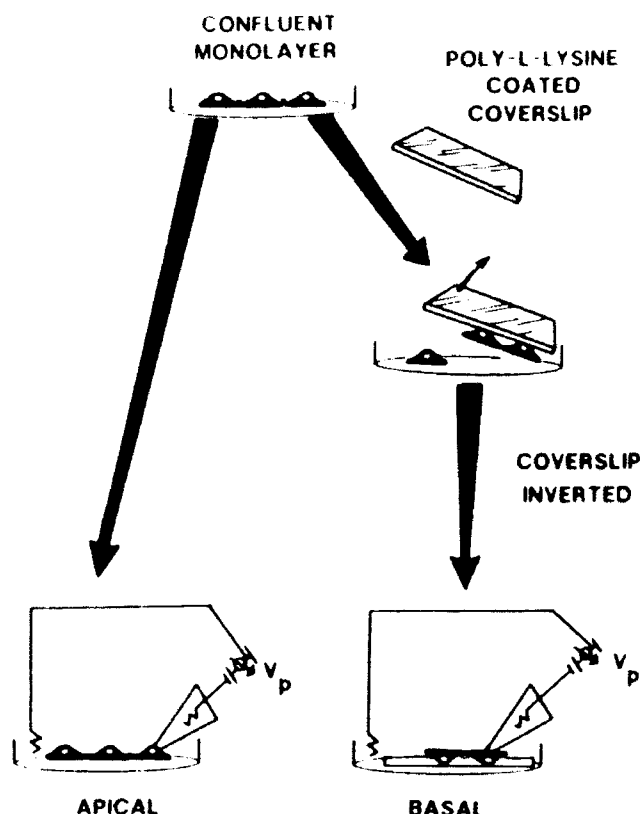
Fig. 2. Schematic of technique used to invert BAEC monolayers and to record electrical activity from either apical or basal endothelial cell surface.

with fluorescein optics and photographed on Ektachrome Tungsten 160 film (Eastman Kodak, Rochester, NY).

Polarity of BAEC Membranes

Hemadsorption on noninverted monolayers. The WSN (H1N1) strain of influenza virus was grown in the MDCK cell line as previously reported (20). Stock virus was titered at 2×10^9 plaque-forming units/ml and stored in liquid nitrogen until needed. Endothelial cells were infected by adding influenza virus (multiplicity of infection = 24 unless otherwise noted) in complete DMEM to noninverted monolayers. After 1 h, the medium was aspirated, and fresh complete DMEM was added to the dishes. Hemadsorption was used to indicate surface expression of viral HA protein on infected monolayers (19). At 1-25 h postinfection (pi), red blood cells (RBCs; 0.5% in Gey's balanced salt solution) were added to BAEC cultures for 30 min at 37°C in a 5% CO_2-humidified incubator. Monolayers were rinsed carefully in Gey's solution to remove nonadherent RBCs before the endothelial monolayers and adherent RBCs were fixed in 2% paraformaldehyde for 1 h on ice. After fixation, monolayers were rinsed in PBS with 50 mM NH_4Cl, examined on a Zeiss inverted microscope, and photographed. The number of RBC aggregates (≥3 RBCs in contact with each other) within five 0.075 mm^2 areas was counted by microscopic observation, and an average was determined.

Hemadsorption on inverted monolayers. Hemadsorption was performed 8 h after infection of monolayers that had been inverted for 1, 5, 9.5, and 24 h. To ensure a pi time of 8 h for all inverted monolayers, monolayers inverted for 1 and 5 h were infected 7 and 3 h, respectively, before the monolayer was inverted. Monolayers inverted for 9.5 and 24 h were infected 1.5 and 16 h, respectively, after inversion. After the hemadsorption
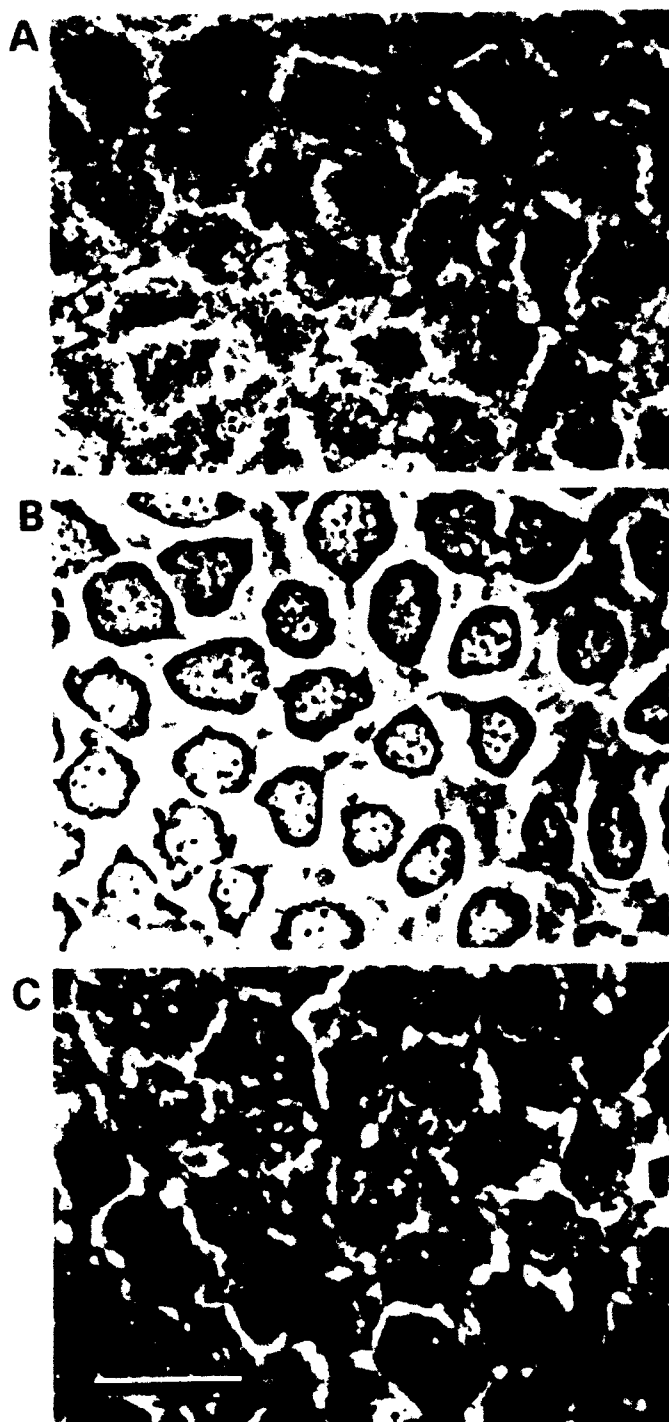

Fig. 3. Bright-field micrographs of apical surface of a BAEC monolayer (*A*), a monolayer within 1 h of inversion (*B*), and an inverted monolayer returned to culture conditions for 2 h (*C*). Bar, 40 μm.

assay, adherent RBC aggregates and monolayers were fixed and permeabilized for subsequent immunostaining.

Indirect Immunofluorescence

Monolayers were fixed in 2% paraformaldehyde in PBS (7.4) for 30 min on ice, permeabilized in -20°C acetone for 3 min, rinsed in PBS-50 mM NH_4Cl, and stored overnight at 4°C. The monolayers were then washed in PBS with 1% bovine serum albumin (BSA) for 30 min at room temperature, incubated with
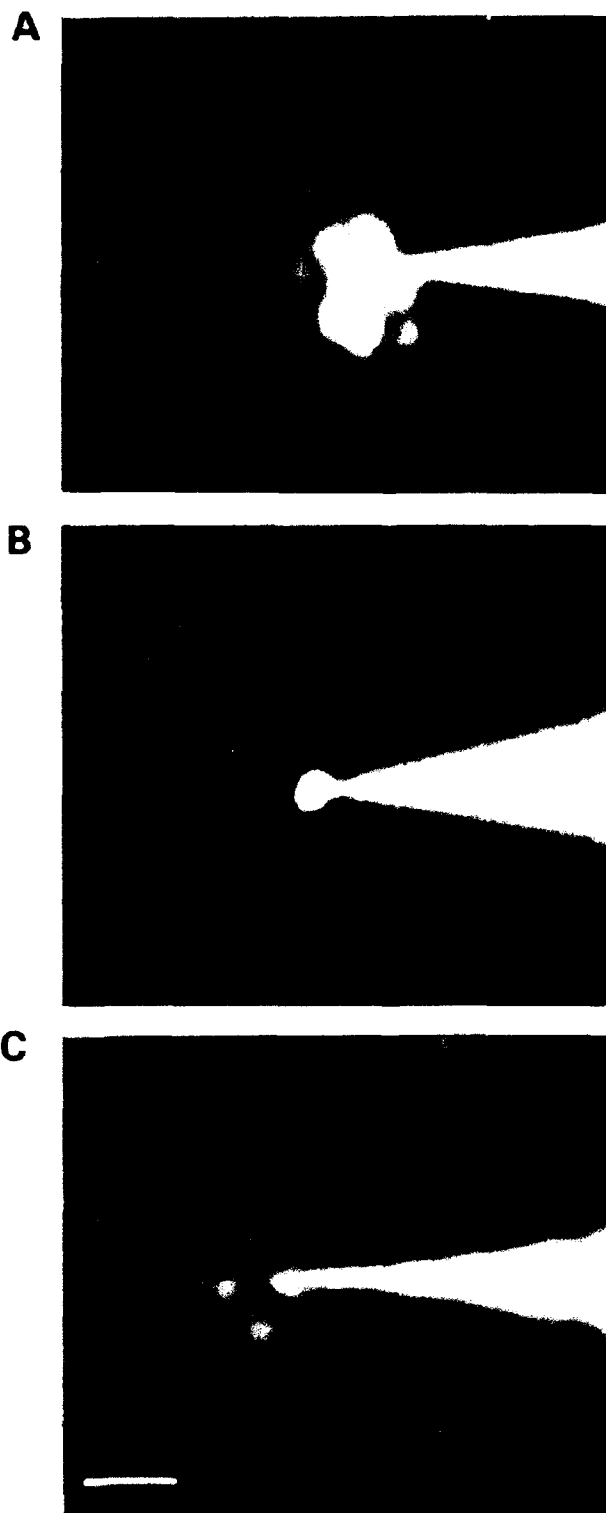
A

B

C

Fig. 4. Fluorescence micrographs of lucifer yellow dye transfer between cells of a noninverted monolayer (A), a monolayer within 1 h of inversion (B), and a monolayer 2 h after inversion (C). Bar, 40 μm.

a mouse anti-HA [monoclonal antibody H17-L19, immunoglobulin (Ig) G1, 1:20] for 1 h at room temperature, rinsed with PBS-1% BSA, and incubated with a rhodamine-conjugated goat anti-mouse IgG (heavy and light chain specific; 1:100; Cappel,

Cooper Biomedical, Malvern, PA). After a 1-h incubation at room temperature in the dark with the secondary antibody, BAEC monolayers were washed, monitored for fluorescence with rhodamine optics (546-610 nm excitation/590 nm emission/580 nm dichroic mirror), and photographed.

Ultrastructural Analysis

Inverted (1, 5, 9.5, and 24 h postinversion) and noninverted monolayers infected for 8 h with influenza virus (multiplicity of infection = 48) were fixed in 2.5% glutaraldehyde in 0.1 M phosphate buffer (pH 7.4) for 1 h. The monolayers were washed in 0.1 M phosphate buffer, postfixed for 1 h in 1% osmium in 0.1 M phosphate buffer, washed in 0.9% saline, dehydrated, and embedded in Epon 812. The thin sections were stained with lead citrate and uranyl acetate and examined on a JOEL (Peabody, MA) 100C electron microscope.

Patch-Clamp Technique

Single-channel recordings. Single-channel recordings were obtained from noninverted and inverted BAEC monolayers with an Axopatch-1A amplifier (Axon Instruments, Burlingame, CA). Low-resistance (3-5 MΩ) electrodes were fabricated from thick-walled glass (TW150-F, World Precision Instruments, New Haven, CT) and coated with Sylgard (Brownell Electro, Norfolk, VA) to reduce background noise. All single-channel experiments were performed at room temperature (22-25°C) in the cell-attached mode with the pipette containing (in mM) 145 KCl, 2.2 ethylene glycol-bis(β-aminoethyl ether)-N,N,N',N'-tetraacetic acid (EGTA), 2 CaCl (pCa 6), and 10 N-2-hydroxyethylpiperazine-N'-2-ethanesulfonic acid (HEPES), pH adjusted to 7.2 with KOH, and the bath containing (in mM) 137 NaCl, 5.4 KCl, 1 MgCl$_2$, 2 CaCl$_2$, 10 dextrose, and 10 HEPES, pH adjusted to 7.3 with NaOH.

Pressure application of drugs to individual cells was performed by imposing an air pressure of 4 kg/cm² to a pipette with a tip diameter of 1-2 μm via a Picospritzer II (General Valve, Fairfield, NJ). Resting membrane potential was recorded in the current-clamp mode by applying further suction to cell-attached patches to gain access to the intracellular space. The whole-cell configuration was verified by an increase in the amplitude of capacitative transients and an increase in background noise level.

Data analysis. Data were filtered at 500-1,000 Hz and recorded on an FM tape recorder at a bandwidth of 2.5 or 5 kHz (Hewlett-Packard, Rockville, MD) for subsequent digitization at a sampling frequency of 1,000-2,000 Hz. Unitary channels were measured using computer programs in which events were detected by a threshold discriminator (14). Percentages of open

Table 1. *Red blood cell aggregation to influenza virus-infected BAEC monolayers*

Time postinfection, h	No. of RBC aggregates
0 (control, uninfected)	0
1	0
3	0
5	0.1±0.1
7	12.5±2.2*
9	32.8±1.8*
11	43.2±1.5*
25	27.4±0.6*

Values are means ± SE. Triplicate cultures of BAEC monolayers were infected with influenza virus in complete DMEM (multiplicity of infection = 24). Hemadsorption assay was performed at various times after infection. RBC, red blood cell. * Significantly greater than control, $P \leq 0.05$.

Non-Inverted Monolayer
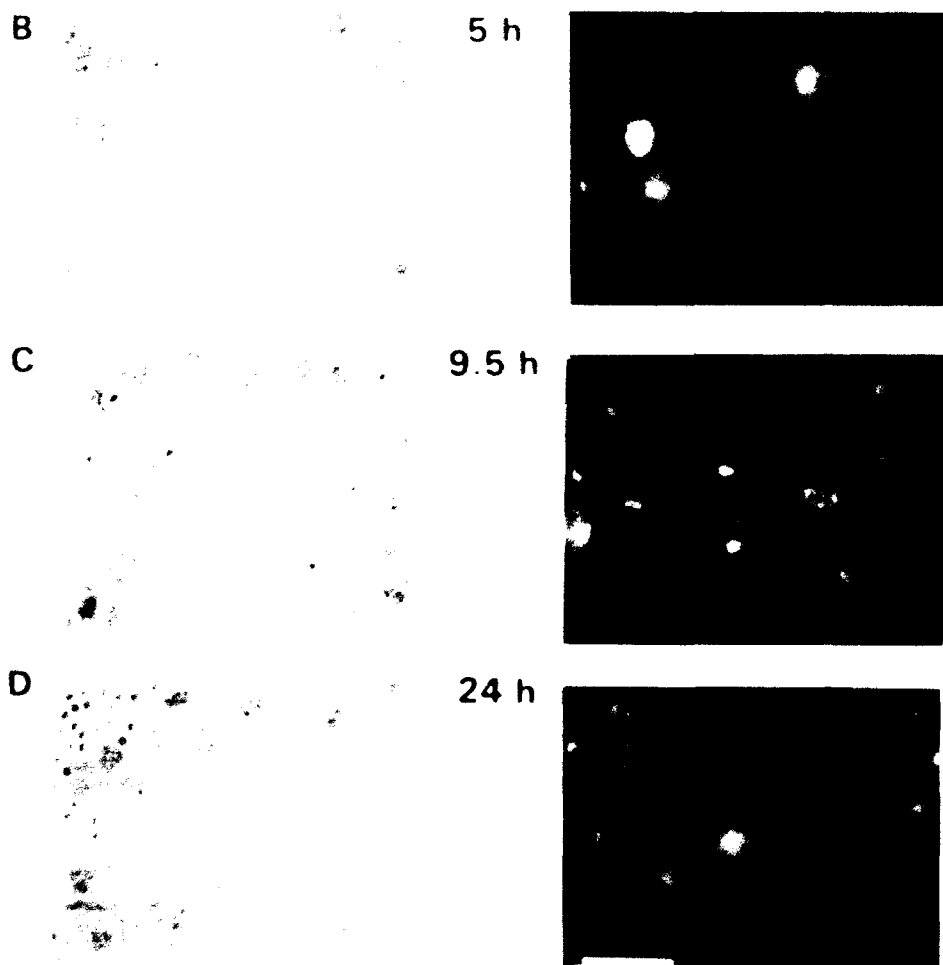

Inverted Monolayers

B   **5 h**

Fig. 5. Bright-field (*left*) and fluorescence (*right*) micrographs examining colocalization of red blood cell aggregates and cellular hemagglutinin antigen on noninverted monolayers (*A*) and monolayers inverted for 5 h (*B*), 9.5 h (*C*), and 24 h (*D*). Hemadsorption was performed on all monolayers 8 h postinfection. No positive hemagglutinin staining occurred in uninfected BAEC monolayers. Bar, 35 μm.

C   **9.5 h**

D   **24 h**

and closed times of channels were generated from the digitized data via computer programs (14).

Resting membrane potential and channel conductance measurements recorded from the apical surface were compared with the same parameters on the inverted surface using the Mann-Whitney test with statistical significance set at $P \leq 0.05$. The occurrence of channel activity recorded from both BAEC surfaces was compared using the χ^2 test for proportionality with statistical significance set at $P \leq 0.05$.

RESULTS

Inverted Monolayers

Morphology and viability. While noninverted endothelial cell monolayers had a characteristic cobblestone appearance (Fig. 3A), the process of inversion resulted in time-dependent changes in cell morphology. Although endothelial cells remained in contact with one another,

they retracted immediately after inversion (Fig. 3B). To determine whether these cells were damaged, inverted monolayers were treated with viability stains, ethidium bromide and acridine orange. Exposure to these stains 10 s or 30 min after inversion indicated that 100% of the cells were viable (data not shown). Damage was also assessed with a FITC-dextran incorporation assay after the monolayers were inverted. No labeled dextran was detected in the inverted cells, confirming that the inversion procedure did not result in extensive membrane disruption (data not shown).

Resting membrane potential. Although viability staining and incorporation of FITC-dextran demonstrated no extensive cellular damage, inversion of the monolayer resulted in a large depolarization. Resting membrane potential of cells in monolayers within 1 h of inversion was -19.9 ± 2.3 (SE) mV ($n = 33$) compared with -65.9 ± 0.5 mV ($n = 80$) recorded from cells in noninverted monolayers. However, if inverted monolayers were placed back in the incubator for 2-5 h, cells retracted less (Fig. 3C), and their resting membrane potential approached that of noninverted cells (-60.0 ± 1.6 mV; $n = 41$).

Gap junctions. Lucifer yellow dye transfer experiments illustrated that while dye was rapidly transferred between cells in noninverted monolayers (Fig. 4A, 4 monolayers tested), no dye was transferred between cells in monolayers within 1 h of inversion (Fig. 4B, 3 monolayers tested). However, dye transfer occurred after inverted monolayers were placed back in the incubator for at least 2 h (Fig. 4C, 4 monolayers tested). Thus cell-to-cell communication, resting membrane potential, and morphology of inverted monolayers recovered ~2 h after inversion.

Polarization of Influenza Virus Budding

Hemadsorption, which correlates with the expression of surface viral HA, was used to monitor endothelial cell polarization. Data obtained over a 25-h period on the apical surface of influenza virus-infected BAECs are summarized in Table 1. No RBC adherence was detected on uninfected endothelial cell monolayers. Similarly, hemadsorption was absent on monolayers 1, 3, and 5 h pi. However, at 7 h pi hemadsorption was apparent, and it peaked at 11 h pi and was still evident at 25 h pi. RBC aggregates bound specifically to the apical surface of BAECs, which immunostained for cellular HA antigen (Fig. 5A). Electron-microscopic examination of monolayers infected for 8 h revealed virus budding from the apical surface of the cells (Fig. 6A). Therefore studies designed to determine whether budding of influenza virus remains polarized after inversion were carried out on inverted monolayers 8 h after viral infection. These monolayers showed cellular HA staining but no RBC aggregates 1 or 5 h (Fig. 5B) after inversion. Electron-microscopic examination of monolayers inverted for 5 h showed virus still budding from the apical surface and a basal lamina on the exposed basal surface (Fig. 6B). RBC aggregates became apparent on the exposed basal surface at 9.5 h (Fig. 5C) and increased in number at 24 h (Fig. 5D) after inversion of infected BAEC monolayers. Therefore, in terms of influenza virus budding, by 9.5 h the basal surface began to revert to an apical membrane.

Expression of K Channels in BAEC Membranes

K channels in apical cell membranes. When recording from confluent BAECs in the cell-attached mode with high KCl in the patch electrode and NaCl in the bath, single-channel activity was observed in 57% of the patches (30 of 53 studied). These patches contained two different types of K channels that have been described previously: the K_i and K_{Ca} channels (3, 22). Spontaneous K_i channels with long open times (%open time = 94) were recorded in 17 patches when the patch membrane was hyperpolarized (Fig. 7A). The current-voltage relationship shown in Fig. 7B illustrates the inward rectification and ion selectivity of the channel. In this cell-attached patch the current through the channel was zero at approximately +65 mV applied potential. Under these recording conditions, equilibrium potential for K was ≅0 mV and resting membrane potential of the cell was −67 mV. Thus K carried the current through this channel, because other permeant ions had very different reversal potentials under these experimental conditions. The single-channel conductance of the K_i channel was 30.5 ± 3.2 pS ($n = 9$) in the applied voltage range of 0 to −40 mV.

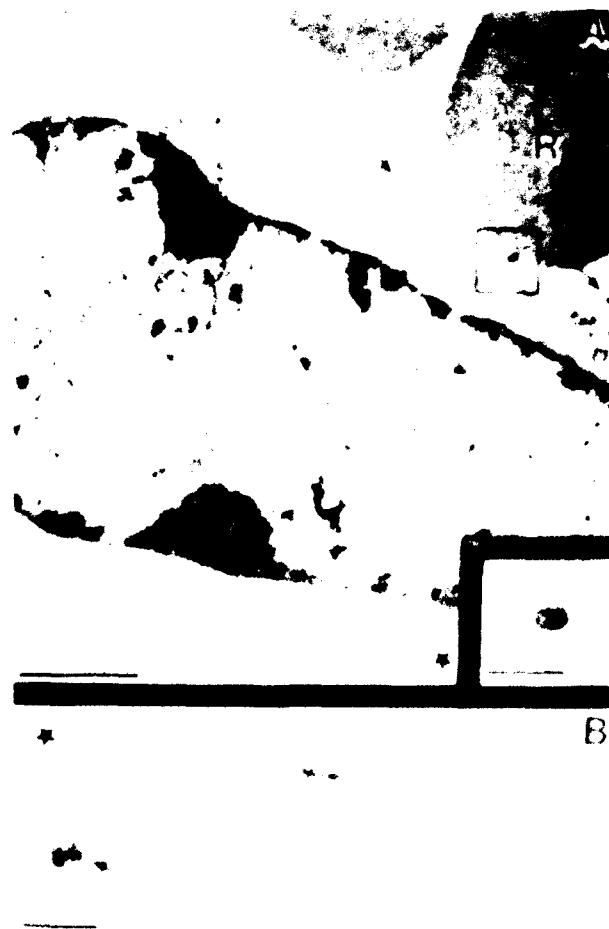
Fig. 6. Electron micrographs of a noninverted endothelial cell monolayer (A) with bound red blood cells (R) and a 5-h inverted monolayer (B). Both monolayers were infected for 8 h and show basal lamina (*) on their basal surface and virus budding from their apical surface (arrow). Inset: high magnification of red blood cell binding to budding virion. Bars, 1.0 (A), 0.3 (inset), and 2.0 (B) µm.
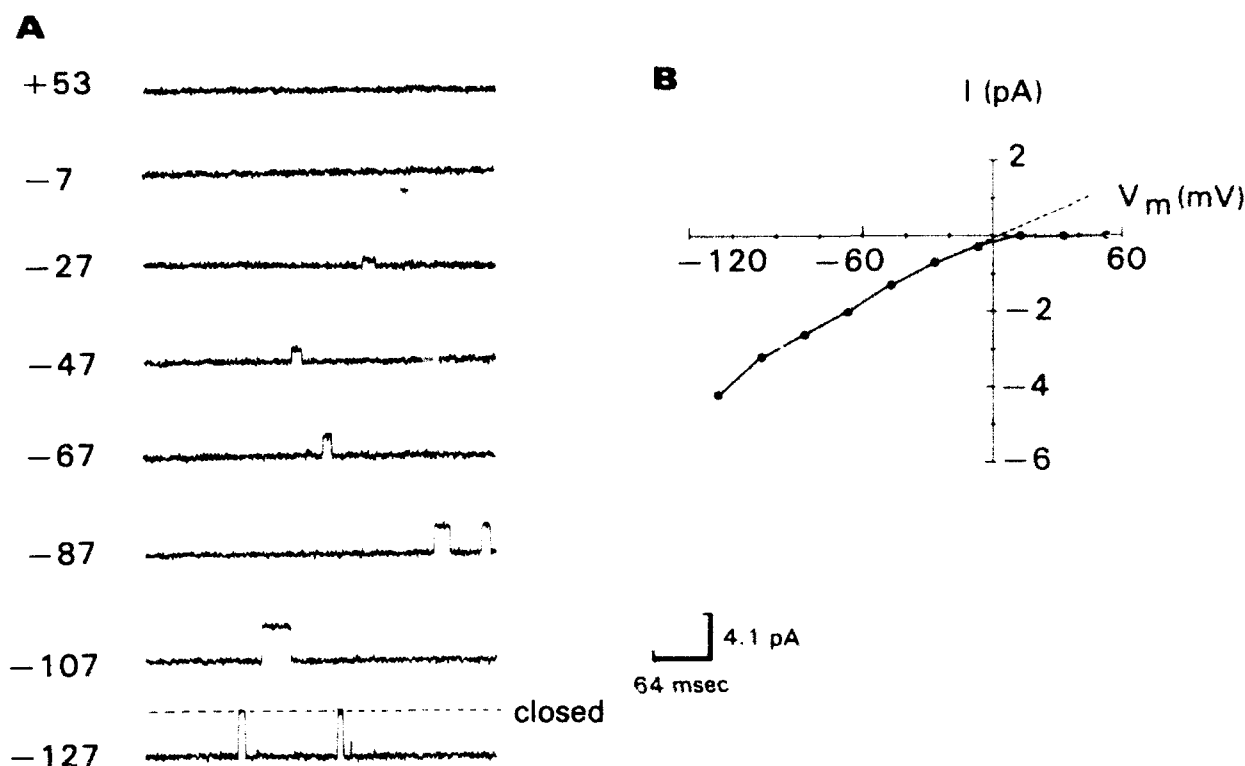
A

+53

−7

−27

−47

−67

−87

−107

−127

B

I (pA)

V_m (mV)

−120   −60   60

2

−2

−4

−6

4.1 pA

64 msec

closed

Fig. 7. Spontaneous inwardly rectifying K (K_i) single-channel currents from a cell-attached patch. A: a family of digitized current records from apical surface of monolayer at indicated membrane potentials (V_m = applied voltage + resting membrane potential). B: current-voltage (I-V) relationship of K_i channel. Resting membrane potential measured in current-clamp mode was −67 mV.

K_{Ca} channels were present spontaneously on the apical surface in 21 of 53 patches of BAEC monolayers. Although these channels were present in 40% of the patches studied, few channel openings were recorded because the channel was in a closed state 94% of the time. Exposing the patched cell to either 1 μM ionomycin or bradykinin, Ca-mobilizing agents, significantly increased K_{Ca} channel activity by reducing the percent closed time of the channel from 94 to 65 (Fig. 8). Ionomycin or bradykinin increased K_{Ca} channel openings in 39 of 42 patches studied regardless of whether single-channel activity was present during the control period (15% of patches had both spontaneous K_i and K_{Ca} channels). The current-voltage relationship of a bradykinin-induced K_{Ca} channel demonstrates a mild inward rectification with slope conductances of 54.7 ± 1.4 pS ($n = 9$) for inward current and 9.8 ± 1.3 pS ($n = 8$) for outward current in the applied voltage ranges of 0 to −40 mV and +90 to +120 mV, respectively (Fig. 8B).

K channels in basal cell membranes. As shown in Fig. 9, A-C, the general characteristics and current-voltage relationships of the two K channels on the basal surface within 1 h of inversion were similar to our observations on the apical membrane of BAECs. Under our recording conditions, no other ion channel activity was present spontaneously or when the cells were activated by bradykinin or ionomycin. However, because it required at least 2 h to restore junctional permeability and the resting membrane potential of inverted monolayers, a detailed comparison was made between noninverted monolayers and monolayers that had been inverted for 2-5 h. For

inverted monolayers allowed to recover at least 2 h, 11 of 30 patches were quiescent, and 23% of the patches possessed spontaneous K_i channel activity (Fig. 9D). Similar to the K_i channel in the apical membrane, the channel was open 92% of the time with a slope conductance of 26.0 ± 2.1 pS ($n = 5$) in the applied voltage range of 0 to −40 mV (Fig. 9F).

Although spontaneous K_{Ca} channels were present in 15 of 30 patches studied, they were in a closed state 97% of the time. Increased K_{Ca} channel openings occurred in 20 of 23 patches when the cells were exposed to 1 μM ionomycin or bradykinin (%closed time = 61; Fig. 9E). The slope conductance of the K_{Ca} channel was 54.9 ± 3.0 pS ($n = 4$) in the inward direction and 13.0 ± 1.7 pS ($n = 3$) in the outward direction (Fig. 9F), which was not significantly different from the conductance measurements obtained for the K_{Ca} channel on the apical surface. In summary, the occurrence and behavior of both K channels were the same on the apical and basal surfaces (Table 2).

DISCUSSION

Endothelial cells form a polarized monolayer with an asymmetric secretion of substances and distribution of proteins (2, 6). Unlike epithelial cells (for review see Ref. 34), relatively little is known about the distribution of ion channels in endothelial cells. Recent patch-clamp data have described ion channel activity on the apical surface of both subconfluent and confluent endothelial cells (for review see Ref. 25), but no one has directly examined ion channels on the basal surface of these cells. In the present study, we used Muller and Gimbrone's (15) technique of
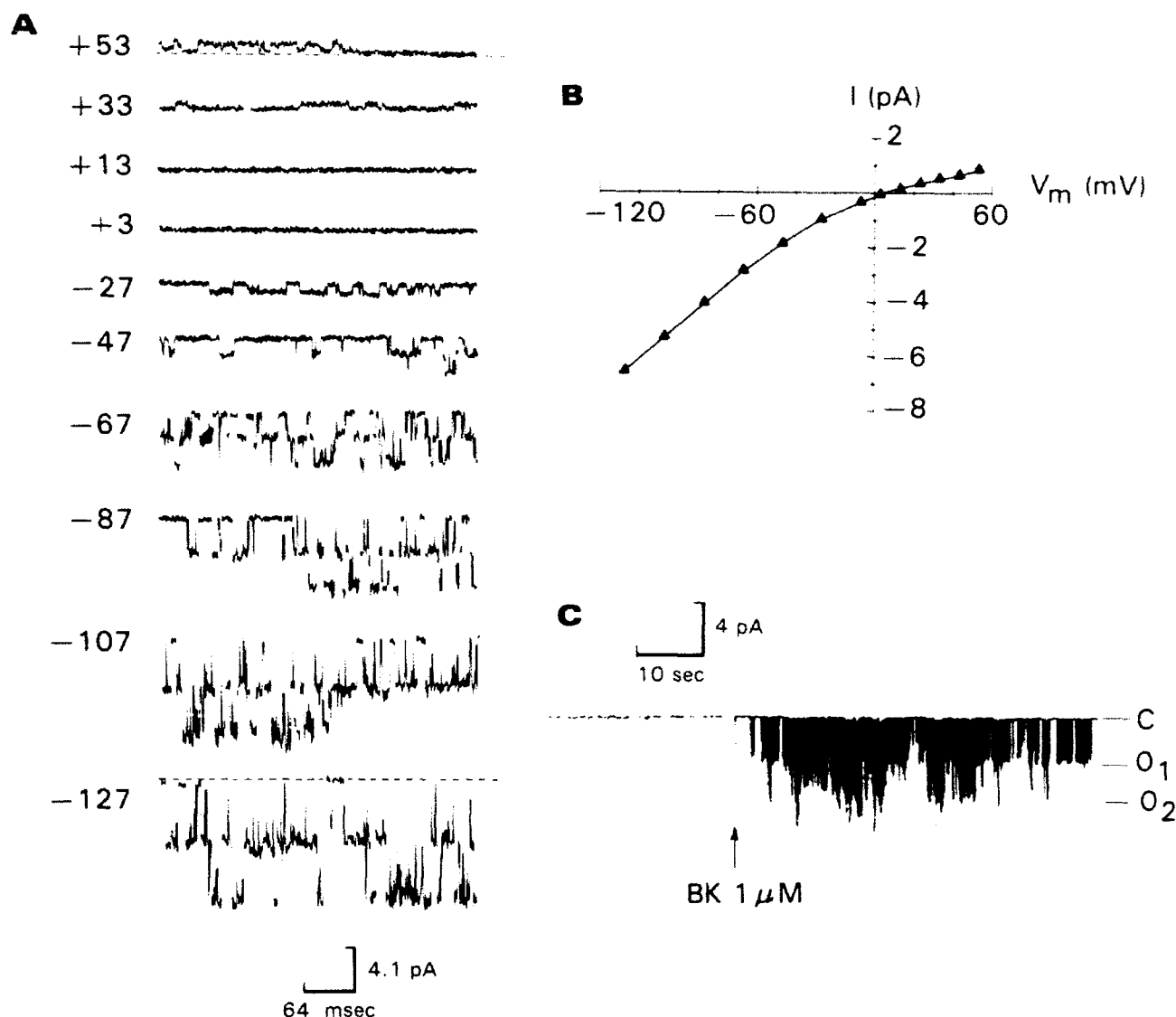
Fig. 8. Bradykinin (BK)-stimulated calcium-actuated K (K_{Ca}) channels from a cell-attached patch. *A*: a family of digitized current records on apical surface at indicated V_m after a brief exposure to bradykinin (1 μM). Dashed line indicates closed level of the channel. *B*: *I-V* relationship of a bradykinin-stimulated K_{Ca} channel. *C*: slower chart speed recording of channel activity before and after bradykinin exposure at a V_m of -67 mV. Resting membrane potential of this cell was -67 mV. Downward deflection denotes inward channel activity with at least 3 open-state levels.
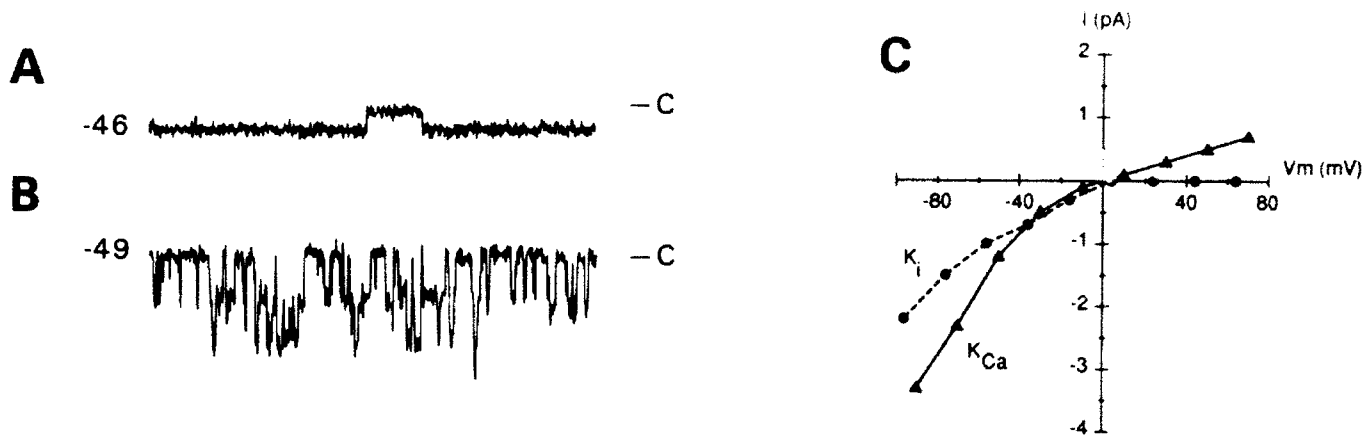
inverting confluent monolayers to compare ion channel activity in the apical and basal membranes of polarized endothelial cells.

Behavior of Inverted Monolayers

The condition of endothelial cell monolayers after inversion was assessed by observing *1*) vital staining, *2*) electrical coupling, and *3*) resting membrane potential. Although viability assays detected no membrane damage or disruption, cells retracted from each other, and electrical coupling was absent for at least 1 h after inversion. By 2 h after inversion, endothelial monolayers were again electrically coupled. This time course was paralleled by a return of the inverted monolayer to a more cobblestone-like morphology. A similar time course of morphological recovery was noted after scrape wounding or glass bead permeabilization of vascular endothelial cells (5, 10). In

the present study, resting membrane potential of noninverted monolayers was found to be -66 mV, while cells in monolayers within 1 h of inversion were depolarized. The activity of K_i and K_{Ca} channels in monolayers within 1 h of inversion was similar to that in noninverted monolayers. Therefore the large depolarization induced by inversion was probably not due to alterations in the activity of these channels but rather to changes in intracellular ionic concentrations and/or an increase in activity of either leak or other ionic channels. Because permeabilized endothelial cells undergo a transient increase in internal Ca that is predominantly due to Ca entry from extracellular medium (33). Ca influx through nonselective cation channels (9) may have caused the depolarization. Nonetheless, resting membrane potential returned to more negative values (-60 mV) when inverted endothelial monolayers were allowed to recover 2-5 h.

Inverted 1 h

A

B

C

Inverted 3 h
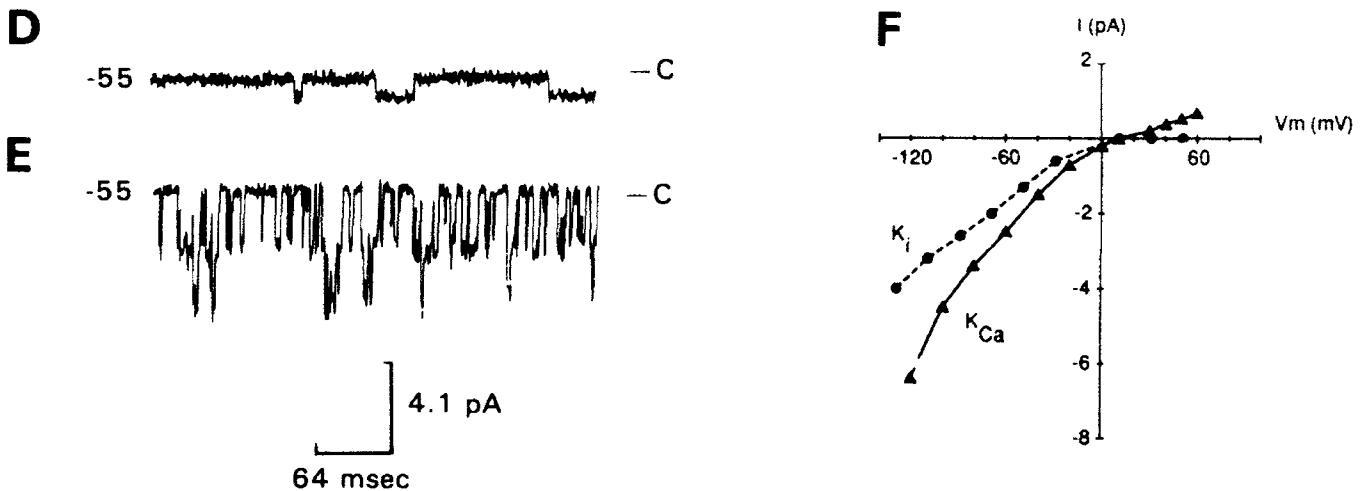
D

E

4.1 pA

64 msec

F

Fig. 9. Spontaneous K_i and bradykinin-stimulated (1 μM) K_{Ca} channels from 4 different cell-attached patches at 1 and 3 h postinversion. At 1 h postinversion, K_i (A) and bradykinin-stimulated K_{Ca} (B) channel activity are shown at indicated V_m with I-V relations for both channels (C). Resting membrane potential was −6 (A) and −9 mV (B) in cells in a monolayer at 1 h postinversion. At 3 h postinversion, K_i (D) and bradykinin-induced K_{Ca} (E) channel activity are shown at indicated V_m with I-V relations for both channels(F). Resting membrane potential was −55 (D) and −55 mV (E) in cells within a monolayer inverted for 3 h. Downward deflection denotes inward channel activity, and −C denotes closed state of the channel.

Asymmetric Hemadsorption and Virus Budding

Influenza virus budding has been shown to preferentially occur from the apical surface of infected endothelial cells (13). This process can be monitored by following the binding of human RBCs to viral HA protein present on the plasma membrane of infected cells (19). In the present study, hemadsorption was not detectable until 7 h and peaked at 11 h after influenza virus infection of noninverted BAEC monolayers. Although cellular HA expression 8 h pi could be detected in inverted monolayers, hemadsorption did not occur on monolayers inverted for up to 5 h. These findings were supported by ultrastructural observations of the inverted monolayers. Monolayers inverted for up to 5 h still showed virus budding from

the original apical surface. However, by 9.5 h postinversion, endothelial monolayers began to exhibit surface HA, and at 24 h postinversion, HA expression on the inverted surface was similar to that noted on infected noninverted cells. In comparison, Muller and Gimbrone (15) demonstrated that, while at 24 h postinversion (the earliest time observed after inversion) redistribution of surface proteins began to occur, the apical pattern of iodinated surface protein was not fully attained until 3 days postinversion. Thus, in inverted monolayers, redistribution of the viral budding patterns appears to occur more rapidly than redistribution of radioiodinated surface proteins. Nevertheless, our viral budding data together with the observations of Muller and Gimbrone (15) indicate that when

Table 2. *Patches with K channel activity in BAEC membrane surfaces*

Channels	Patches with Channel Activity, %	
	Apical	Basal*
K_i	32 (17/53)	23 (7/30)
K_{Ca}	40 (21/53)	50 (15/30)
K_{Ca}-stimulated in silent patches†	91 (21/23)	64 (7/11)

Channel activity was measured as channel openings during cell-attached recordings. Values in parentheses are no. of patches exhibiting channel activity/total number of patches studied. Occurrence of channel activity recorded from both BAEC surfaces was compared using the χ^2 test for proportionality. $P \leq 0.05$. * Monolayers 2-5 h after inversion. † Cells exposed to 1 µM ionomycin or bradykinin during patch recordings. K_i, inwardly rectifying K channel; K_{Ca}, calcium-actuated K channel.

endothelial cells are patch clamped 1-5 h after inversion, the membrane that is being patch clamped retains at least several (and possibly all) of the properties of polarized cells.

Expression of K Channels

Perhaps the best-characterized ion channels in endothelial cells are the K_i and K_{Ca} channels (for review see Ref. 25). While K_i channel activity has been well characterized in many cell types, there is no evidence in other cell types that it is asymmetrically distributed. In contrast, a channel similar to the K_{Ca} channel in endothelial cells appears to be present only on the basolateral surface of canine tracheal epithelial cells (32). Therefore we chose to examine both the K_i and K_{Ca} channels in polarized endothelial cells, hypothesizing that while K_i channels might be symmetrically distributed, K_{Ca} channels might be asymmetrically distributed. Contrary to our expectations, we provide evidence supporting the view that both K_i and K_{Ca} channels are localized on both apical and basal surfaces of the plasma membrane of confluent BAECs. It should be noted that our data do not exclude the possibility that there may be subtle differences in K_i and K_{Ca} channel density between apical and basal surfaces. This technique is valuable in demonstrating the presence and behavior of ion channels on the surfaces of polarized cell types, but it is not necessarily the choice for delineating small differences in channel density because extensive numbers of patches would be required.

K_i channels with similar characteristics to those described in these studies have been described in other vascular endothelial cell lines grown under subconfluent conditions (26). These studies extend those observations by characterizing K_i channel activity on both apical and basal surfaces of confluent BAEC monolayers. Although spontaneous K_i channel activity was recorded from no more than a third of the patches obtained from both surface membranes, when active these channels were open 90% of the time at the resting membrane potential. The presence of K_i channel activity at rest (3, 26) strongly suggests that the K_i channel functions to set the resting membrane potential (−66 mV) in BAECs as it does in other cells (14).

In previous work, Colden-Stanfield et al. (3) described another K channel with a Ca sensitivity and faster kinetics than the K_i current in confluent BAEC monolayers. This K_{Ca} channel, which is modulated by pH and membrane potential, has been recorded from the apical surface of both subconfluent and confluent BAEC monolayers (3, 22, 28). K_{Ca} channels can be activated by exposing endothelial cells to bradykinin and ATP. In the studies presented here, the occurrence of the K_{Ca} channel was identical when we recorded from the apical surface of BAEC monolayers or from the inverted basal surface (45% of patches). In both our noninverted and inverted monolayers, the percent closed time of the K_{Ca} channel was 94 at rest, indicating that intracellular Ca was not elevated in inverted monolayers. Furthermore, the lack of channel activity in patches of cells not exposed to stimuli indicates that these channels probably do not contribute to the resting K+ permeability of these cells. However, after addition of a stimulus, such as bradykinin, that increases intracellular Ca, K_{Ca} channels then open, hyperpolarizing the cell and increasing the driving force for Ca entry (12, 23).

In summary, our data indicate that both the apical and basal surfaces of confluent cultures of endothelial cells can be patch clamped. Furthermore, we show that K_i and K_{Ca} channels are present on both the apical and inverted basal surface of confluent cells at a time when the inverted surface still retains polarized virus budding. This technique will be useful in examining the distribution of other ion channels in confluent endothelial cells and other polarized cells.

Address for reprint requests: M. Colden-Stanfield, Dept. of Physiology AFRRI, Bethesda, MD 20889-5145.

REFERENCES

1. Betz, A. L., J. A. Firth, and G. W. Goldstein. Polarity of the blood-brain barrier: distribution of enzymes between the luminal and antiluminal membranes of brain capillary endothelial cells. *Brain Res* 192: 17-28, 1980.
2. Birdwell, C. R., D. Gospodarowicz, and G. L. Nicolson. Identification, localization, and role of fibronectin in cultured bovine endothelial cells. *Proc Natl Acad Sci USA* 75: 3273-5277, 1978.
3. Colden-Stanfield, M., W. P. Schilling, L. D. Possani, and D. L. Kunze. Bradykinin-induced potassium current in cultured bovine aortic endothelial cells. *J Membr Biol* 116: 227-238, 1990.
4. Colden-Stanfield, M., W. P. Schilling, A. K. Ritchie, S. G. Eskin, L. T. Navarro, and D. L. Kunze. Bradykinin-induced increases in cytosolic calcium and ionic currents in cultured bovine aortic endothelial cells. *Circ Res* 61: 632-640, 1987.
5. Fennell, D. F., R. E. Whatley, T. M. McIntyre, S. M. Prescott, and G. A. Zimmerman. Endothelial cells reestablish functional integrity after reversible permeabilization. *Arteriosclerosis Thromb* 11: 97-106, 1991.
6. Haudenschild, C. C., D. Zahniser, J. Folkman, and M. Klagsbrun. Human vascular endothelial cells in culture. Lack of response to serum growth factors. *Exp Cell Res* 98: 175-183, 1976.
7. Jaffe, S., P. D. Oliver, S. M. Farooqui, P. L. Novak, N. Sorgente, and V. K. Kalra. Separation of luminal and abluminal membrane enriched domains from cultured bovine aortic endothelial cells: monoclonal antibodies specific for endothelial cell plasma membranes. *Biochim Biophys Acta* 898: 37-52, 1987.
8. Kawahara, K., M. Hunter, and G. Giebisch. Potassium channels in *Necturus* proximal tubule. *Am J Physiol* 253 (Renal Fluid Electrolyte Physiol 22): F488-F494, 1987.

9. **Lansman, J. B., T J. Hallam, and T. J. Rink.** Single stretch activated ion channels in vascular endothelial cells as mechanotransducers? *Nature Lond.* 325: 811–813, 1987.

10. **Larson, D. M., and C. C. Haudenschild.** Junctional transfer in wounded cultures of bovine aortic endothelial cells. *Lab Invest* 59: 373, 1988.

11. **Larson, D. M., E. Y. Kam, and J. D. Sheridan.** Junctional transfer in cultured vascular endothelium: I. Electrical coupling. *J Membr Biol* 74: 103–113, 1983.

12. **Laskey, R. E., D. J. Adams, A. Johns, G. M. Rubanyi, and C. van Breemen.** Membrane potential and Na$^+$-K$^+$ pump activity modulate resting and bradykinin-stimulated changes in cytosolic free calcium in cultured endothelial cells from bovine atria. *J Biol Chem* 265: 2613–2619, 1990.

13. **Lombardi, T., R. Montesano, and L. Orci.** Polarized plasma membrane domains in cultured endothelial cells. *Exp Cell Res* 161: 242–246, 1985.

14. **McKinney, L. C., and E. K. Gallin.** Inwardly rectifying whole-cell and single-channel K currents in the murine macrophage cell line J774.1. *J Membr Biol* 103: 41–53, 1988.

15. **Muller, W. A., and M. A. Gimbrone, Jr.** Plasmalemmal proteins of cultured vascular endothelial cells exhibit apical-basal polarity: analysis by surface-selective iodination. *J Cell Biol* 103: 2389–2402, 1986.

16. **Nakache, M., H. E. Gaub, A. B. Schreiber, and H. M. McConnell.** Topological and modulated distribution of surface markers on endothelial cells. *Proc Natl Acad Sci USA* 83: 2874–2878, 1986.

17. **Olesen, S., D. E. Clampham, and P. F. Davies.** Haemodynamic shear stress activates a K$^+$ current in vascular endothelial cells. *Nature Lond.* 331: 168–170, 1988.

18. **Olesen, S., P. F. Davies, and D. E. Clampham.** Muscarinic-activated K$^+$ current in bovine aortic endothelial cells. *Circ Res* 62: 1059–1064, 1988.

19. **Ratcliffe, D. R., S. L. Nolin, and E. B. Cramer.** Neutrophil interaction with influenza-infected epithelial cells. *Blood* 72: 142–149, 1988.

20. **Rodriguez-Boulan, E.** Polarized assembly of enveloped viruses from cultured epithelial cells. *Methods Enzymol* 98: 486–501, 1983.

21. **Rosen, E. M., J. P. Noveral, S. N. Mueller, and E. M. Levine.** Regulation of angiotensin I-converting enzyme activity in serially cultivated bovine endothelial cells. *J Cell Physiol* 122: 30–38, 1985.

22. **Sauve, R., L. Parent, C. Simoneau, and G. Roy.** External ATP triggers a biphasic activation process of a calcium-dependent K$^+$ channel in cultured bovine aortic endothelial cells. *Pfluegers Arch* 412: 469–481, 1988.

23. **Schilling, W. P.** Effect of membrane potential on cytosolic calcium of bovine aortic endothelial cells. *Am J Physiol* 257 (*Heart Circ Physiol* 26): H778–H784, 1989.

24. **Sporn, L. A., V. J. Marder, and D. D. Wagner.** Differing polarity of the constitutive and regulated secretory pathways for von Willebrand factor in endothelial cells. *J Cell Biol* 108: 1283–1289, 1989.

25. **Takeda, K., and M. Klepper.** Voltage-dependent and agonist-activated ionic currents in vascular endothelial cells: a review. *Blood Vessels* 27: 169–183, 1990.

26. **Takeda, K., V. Schini, and H. Stoeckel.** Voltage-activated potassium, but not calcium currents in cultured bovine aortic endothelial cells. *Pfluegers Arch* 410: 385–393, 1987.

27. **Taniguchi, J., K. Yoshitomi, and M. Imai.** K$^+$ channel currents in basolateral membrane of distal convoluted tubule of rabbit kidney. *Am J Physiol* 256 (*Renal Fluid Electrolyte Physiol* 25): F246–F254, 1989.

28. **Thuringer, D., A. Diarra, and R. Sauve.** Modulation by extracellular pH of bradykinin-evoked activation of Ca$^+$-activated K$^+$ channels in endothelial cells. *Am J Physiol* 261 (*Heart Circ Physiol* 30): H656–H666, 1991.

29. **van Buul-Wortelboer, M. F., H. M. Brinkman, J. H. Reinders, W. G. van Aken, and J. A. van Mourik.** Polar secretion of von Willebrand factor by endothelial cells. *Biochim Biophys Acta* 1011: 129–133, 1989.

30. **Voyta, J. C., D. P. Via, C. E. Butterfield, and B. R. Zetter.** Identification and isolation of endothelial cells based on their increased uptake of acetylated-low density lipoprotein. *J Cell Biol* 99: 2034–2040, 1984.

31. **Wehner, F., L. Garretson, K. Dawson, Y. Segal, and L. Reuss.** A nonenzymatic preparation of epithelial basolateral membrane for patch clamp. *Am J Physiol* 258 (*Cell Physiol* 27): C1159–C1164, 1990.

32. **Welsh, M. J., and J. D. McCann.** Intracellular calcium regulates basolateral potassium channels in a chloride-secreting epithelium. *Proc Natl Acad Sci USA* 82: 8823–8826, 1985.

33. **Whatley, R., G. Zimmerman, T. McIntyre, and S. Prescott.** Endothelium from diverse vascular sources synthesizes platelet activating factor. *Arteriosclerosis* 8: 321–331, 1988.

34. **Wills, N. K., and A. Zweifach.** Recent advances in the characterization of epithelial ionic channels. *Biochim Biophys Acta* 906: 1–31, 1987.

35. **Zerwes, H., and W. Risau.** Polarized secretion of a platelet-derived growth factor-like chemotactic factor by endothelial cells in vitro. *J Cell Biol* 105: 2037–2041, 1987.

An *in Vitro* Method for Radiolabeling Proteins with ^{35}S

John F. Kalinich and David E. McClain

Radiation Biochemistry Department, Armed Forces Radiobiology Research Institute, Bethesda, Maryland 20889-5145

The radiolytic decomposition products of [^{35}S]-methionine have been used to radiolabel proteins *in vitro*. The process occurs in a time-, temperature-, and pH-dependent manner. Maximum labeling of bovine serum albumin occurs after a 24 h incubation at 37°C and pH 8.5. Once incorporated, the radiolabel cannot be removed by extended incubation at various temperatures, multiple freeze/thaw cycles, or boiling, indicating that the ^{35}S moiety is covalently attached to the protein. A wide variety of proteins have been radiolabeled. The method is simple to perform and yields radiolabeled proteins of high specific activity.

There are a variety of methods available for radiolabeling proteins *in vitro*. Several of the more widely used procedures include reductive methylation with tritiated sodium borohydride (1) or with [^{14}C]formaldehyde and sodium cyanoborohydride (2), iodination (3), and ^{35}S labeling with *t*-butoxycarbonyl-L-[^{35}S]methionine *N*-hydroxysuccinimidyl ester (4).

Previous work has shown that a consequence of *in vivo* protein labeling with [^{35}S]methionine is the production of a highly reactive water-soluble compound (5,6). It is probable that this volatile decomposition by-product is methylmercaptan (6,7). We have developed a procedure that uses the radiolytic decomposition products of [^{35}S]methionine to radiolabel proteins *in vitro*.

MATERIALS AND METHODS

Materials. L-[^{35}S]Methionine was purchased from New England Nuclear (Boston, MA). Bovine serum albumin, Pentex fraction V, was obtained from Miles Laboratories (Kankakee, IL). Other proteins and reagents were purchased from Sigma (St. Louis, MO).

Protein labeling conditions. L-[^{35}S]Methionine (3 µl of >1000 Ci/mmol) was added to 1 mg of BSA[1] in a total final volume of 100 µl. Reactions were performed at the

---

[1] Abbreviations used: BSA, bovine serum albumin; TCA, trichloroacetic acid; SDS, sodium dodecyl sulfate; Hepes, *N*-2-hydroxyethylpiperazine *N*-2-ethanesulfonic acid; Pipes, piperazine-*N*,*N*-bis(2-ethanesulfonic acid); DTT, dithiothreitol.

temperatures and times indicated in the tables. Other additions to the reactions are as described in the tables. To terminate the reaction and to separate the unreacted label from the radiolabeled protein, the reaction mixture was passed through a Sephadex G-25 column. Alternatively, the mixture could be separated in a Centricon C-10 microconcentrator (W. R. Grace & Co., Beverly, MA).

TCA precipitation. The radiolabeled BSA (5 µl) was precipitated by the addition of 1 ml of ice-cold 25% TCA/2% casein hydrolysate. The mixture was left on ice for 30 min, after which it was vacuum filtered through a Whatman GF/A glass microfiber filter. The filter was washed three times with 3 ml of ice-cold 5% TCA and one time with ice-cold acetone and air dried. The filter was placed in a liquid scintillation vial with 5 ml of Ecoscint A scintillation fluid (National Diagnostics, Manville, NJ) and the incorporated radioactivity determined using a Beckman Model LS5801 Liquid Scintillation Counter.

Gel electrophoresis. Radiolabeled protein samples (5 µl) were prepared for electrophoresis by adding 20 µl of SDS sample buffer (50 mM Tris-HCl, pH 6.8, 2% SDS, 2 mM EDTA, 140 µM 2-mercaptoethanol, 10% glycerol, and 0.05% bromphenol blue) and boiling for 3 min. Electrophoresis on SDS-polyacrylamide gels was performed as described (8). After electrophoresis, gels were prepared for fluorography using sodium salicylate (9) and exposed to Kodak X-Omat film at −80°C.

Laser densitometry. X-ray films were scanned with a Pharmacia/LKB laser densitometer and exposure densities integrated using the associated software. Only exposure densities within the linear range of the film (<2.5 AU) were included in calculations. Data were calculated as the density volume (AU × mm²) and normalized to the control reaction in each experiment.

Thin layer chromatography. Amino acids alone, reaction mixtures of amino acids and [^{35}S]methionine, and acid-hydrolyzed ^{35}S-labeled BSA samples were chromatographed in two dimensions on silica gel 60 thin-layer plates. The first-dimension solvent was chloro-

TABLE 1

Stability of ³⁵S Association with BSA

Freeze/thaw		24-h incubation	
Cycle	Percentage of control	Temperature (°C)	Percentage of control
1	99.2	4	98.1
3	90.1	22	106.4
5	91.2	37	97.1
10	95.3		

Note. BSA (1 mg) was radiolabeled with [³⁵S]methionine (3 μl) at 37°C for 24 h in 10 mM Hepes, pH 7.4 (total volume, 100 μl). Samples were then run through multiple freeze/thaw cycles or incubated for 24 h at the indicated temperatures. Samples were electrophoresed and the gels prepared for fluorography, dried, and exposed to X-ray film. The films were quantified by laser densitometry and the exposure densities of the treated samples normalized to control values. Data represent $N = 3$.

FIG. 1. Association of ³⁵S with BSA increases over time. Labeling reactions (3 μl [³⁵S]methionine, 1 mg BSA, 10 mM Hepes, pH 7.4, 100 μl total volume) were run at 37°C for 1, 3, 6, 12, 18, and 24 h. Samples (5 μl) were electrophoresed on 10% SDS polyacrylamide gels. The gels were prepared for fluorography, dried, and exposed to X-ray film. (A) The film of a representative time-course experiment. The films were quantified by laser densitometry and the data normalized to the value obtained for the 24-h sample. (B) A graph of the association of label with BSA over time.

form/methanol/17% (w/w) ammonia (2/2/1). The solvent for chromatography in the second dimension was phenol/water (75/25, w/w). Amino acids were detected with ninhydrin and radioactive species by exposing the thin-layer plate to Kodak X-Omat film at −80°C.

RESULTS

When incubated at physiological temperatures, [³⁵S]-methionine decomposes to form a highly reactive water-soluble compound and a variety of other products (5–7). We have utilized this decomposition reaction to radiolabel proteins *in vitro* with ³⁵S. Less than 2% of the total radioactivity initially added to the reaction mixture was incorporated into a TCA-precipitatable form after a 24-h incubation at 37°C. Increasing the amount of [³⁵S]-methionine in the reaction mixture increased the amount of label associated with the protein, but did not increase the percentage of label incorporated. This indicates that the limiting factor in this procedure is the rate of decomposition of the [³⁵S]methionine and not the availability of labeling sites.

To determine the stability of the interaction of ³⁵S with BSA several experiments were conducted. Radiolabeled BSA was subjected to multiple freeze/thaw cycles or 24 h incubation at various temperatures. Samples were then electrophoresed on SDS–polyacrylamide gels and the gels prepared for fluorography, dried, and exposed to X-ray film. The radiolabeled BSA bands were scanned by laser densitometry and normalized to control (no freeze/thaw, no incubation). The results in Table 1 show that once the ³⁵S is associated with the protein, the label is stable and cannot be removed by freezing and thawing or by extended incubation. Boiling the sample before electrophoresis also has no effect on the association of the ³⁵S with the protein. These results
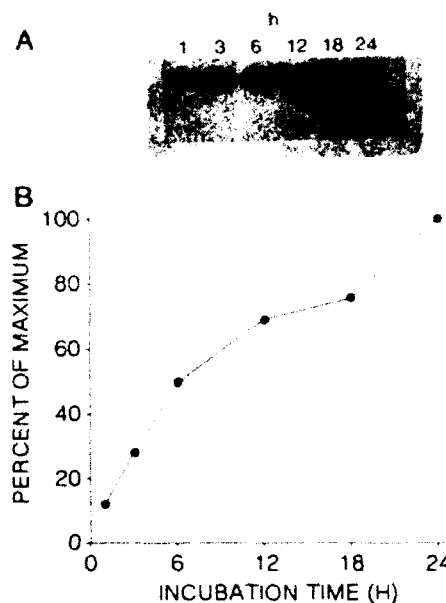
indicate that the interaction of the radioactive [³⁵S]-methionine decomposition product(s) with the protein is a covalent one.

The results of a time course experiment conducted at 37°C are shown in Fig. 1. Figure 1A represents a time-course film. Following laser densitometry and normalization of the data to the 24-h value, the graph in Fig. 1B, which shows that the labeling of BSA occurs in a time-dependent manner, is obtained. The effect of incubation temperature on ³⁵S labeling is shown in Table 2.

TABLE 2

Effect of Temperature on BSA Labeling with ³⁵S

Temperature (°C)	Percentage of 37°C
4	2.7
15	9.5
22	21.5
30	71.3
37	100.0

Note. Labeling reactions were run at the indicated temperatures for 24 h as described in the note to Table 1 and processed as described under Materials and Methods. The resulting X-ray films were quantified by laser densitometry and the exposure densities normalized to the value obtained for 37°C. Data represent $N = 6$.
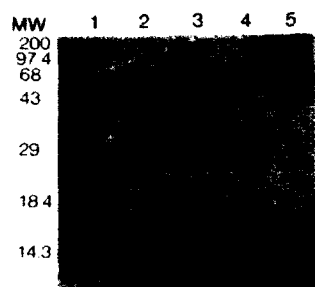
FIG. 2. ^{35}S labeling of proteins. Labeling reactions, gel electrophoresis, and fluorography were performed as described in the legend to Fig. 1, except that the reaction time was 24 h. Each lane contains 1 μg of protein. Lane 1, α-lactalbumin (14.2 kDa); lane 2, carbonic anhydrase (29 kDa); lane 3, chicken egg albumin (43 kDa); lane 4, bovine serum albumin (66 kDa); lane 5, β-galactosidase (116 kDa). Molecular mass markers (Bethesda Research Laboratories) are myosin H-chain, 200 kDa; phosphorylase b, 97.4 kDa; bovine serum albumin, 68 kDa; ovalbumin, 43 kDa; carbonic anhydrase, 29 kDa; β-lactoglobulin, 18.4 kDa; and lysozyme, 14.3 kDa. The molecular masses indicated in the figure reflect the apparent molecular weights of the prestained markers as reported by the supplier.

The labeling reaction was incubated for 24 h at the indicated temperatures before electrophoresis and laser densitometry. Exposure densities were normalized to the 37°C value. The temperature-dependent labeling of BSA is in agreement with the [^{35}S]methionine decomposition conditions found by others (5–7).

Our preliminary experiments investigating this labeling phenomenon utilized BSA as a test protein. In order to ensure that our results were not due to some unique characteristic of BSA we labeled several other proteins. These results are shown in Fig. 2. α-Lactalbumin, carbonic anhydrase, chicken egg albumin, and β-galactosidase can all be radiolabeled by this procedure. The following specific activities were obtained for these radiolabeled proteins: α-lactalbumin, 72 mCi/mmol; carbonic anhydrase, 62 mCi/mmol; chicken egg albumin, 303 mCi/mmol; bovine serum albumin, 42 mCi/mmol; and β-galactosidase, 754 mCi/mmol. In addition BSA concentrations as low as 10 ng/ml could be successfully labeled using this method (data not shown).

The labeling of BSA with ^{35}S shows a dramatic pH effect (Fig. 3). Virtually no labeling occurs when the reaction is run below pH 6. A pH plateau is reached between pH 7.4 and 9.6 with maximum labeling occurring at pH 8.5. A slight decrease in the labeling of BSA is found when the pH of the reaction mixture reaches pH 11.0 and 11.5.

Table 3 shows the effect of various agents, commonly used in protein isolation, on the radiolabeling reaction. Significant labeling occurs in the presence of cations (Na^+, Ca^{2+}, Mg^{2+}, K^+), reducing agents (2-mercaptoethanol, DTT), sucrose, detergents (Triton X-100, SDS), chelators (EDTA), and low concentrations of glycerol. However, substantial inhibition of the labeling reaction

was observed when the reaction was run in the presence of compounds containing primary or secondary amines. Urea, ammonium sulfate, or guanidine HCl inhibited the reaction. Concentrations of Tris buffer (pH 7.4) greater than 50 mM also decreased ^{35}S incorporation. No effect was apparent at lower concentrations. When the labeling reaction was run at pH 7.4 in increasing concentrations of Hepes, a tertiary amine compound, no difference in the amount of labeling was observed (data not shown). Similar results occur when proteins are labeled by reductive methylation with sodium cyanoborohydride and [^{14}C]formaldehyde (2).

The inhibition of BSA labeling that occurs in the presence of excess amines suggests that amine groups are involved in the labeling reaction. However, preliminary experiments investigating what amino acid residues are labeled by this procedure suggest that amine-mediated labeling does not occur. Individual amino acids were incubated with [^{35}S]methionine for 24 h at 37°C, chromatographed on silica gel thin-layer plates in two dimensions, and autoradiographed. After R_f values for each radiolabeled species were determined and those contributed by the decomposition products of [^{35}S]-methionine subtracted, the ability of each amino acid to be labeled by this procedure could be ascertained. The R_f values obtained from these experiments were then compared to the values from the chromatograph of acid-hydrolyzed ^{35}S-labeled BSA. From these investigations it was determined that only tyrosine, tryptophan, histidine, and cysteine residues were radiolabeled in this procedure (Fig. 4). To our surprise neither lysine or arginine was labeled, suggesting a mechanism different than that for the reductive methylation procedure.
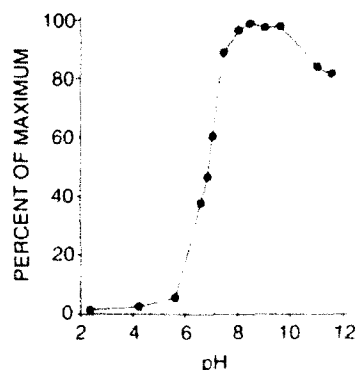

FIG. 3. The effect of pH on the radiolabeling of BSA with ^{35}S. Labeling reactions (1 mg BSA, 3 μl [^{35}S]methionine, 100 μl total volume) were conducted at 37°C for 24 h in the presence of 10 mM of the appropriate buffer. The following buffers were used: glycine, pH 2.3; acetate, pH 4.2; citrate, pH 5.5; Pipes, pH 6.5; Tris, pH 6.8, 7.0, 7.4, 8.0, 9.0, and 11.0; Hepes, pH 7.4; glycine, pH 8.0; borate, pH 8.5; carbonate, pH 9.6 and 11.5. Labeled BSA samples were electrophoresed and prepared for fluorography as described in the legend to Fig. 1. X-ray films were quantified by laser densitometry and data normalized to the maximum value (pH 8.5).

TABLE 3

Effect of Various Substances on BSA Labeling

	Percentage of control		Percentage of control		Percentage of control
NaCl (mM)		DTT (mM)		Urea (M)	
50	82	1	137	4	24
100	97	10	91	8	5
250	90				
		β-Me (mM)		SDS (%)	
MgCl₂ (mM)		1	67	0.5	69
5	62	10	64	1.0	46
10	108				
25	82	EDTA (mM)		(NH₄)₂SO₄ (%)	
		1	90	5	4
CaCl₂ (mM)		10	148	25	4
5	62				
10	85	Glycerol (%)		Guanidine HCl (M)	
25	54	1	56	1	18
		10	6	5	1
KCl (mM)					
25	67	Triton X-100 (%)		Sucrose (mM)	
50	62	0.5	138	50	147
100	62	1.0	88	100	88
				250	72

Note. Labeling reactions (1 mg BSA, 3 μl [^{35}S]methionine, 10 mM Hepes, pH 7.4; total volume, 100 μl) were conducted at 37°C for 24 h as previously described except that the compounds listed in the table were present at the indicated final concentrations. The resulting X-ray films were quantified by laser densitometry and the exposure densities normalized to control (no additions to the reaction mixture). DTT is dithiothreitol and β-ME is β-mercaptoethanol.

DISCUSSION

Proteins can be radiolabeled *in vitro* with ^{35}S using the radiolytic decomposition products of [^{35}S]methionine. Specific activities approaching 40–42 mCi/mmol (6 μCi/ mg protein) can be achieved by incubating BSA (1 mg) with [^{35}S]methionine (3 μl) for 24 h at 37°C. The labeling reaction is time-, temperature-, and pH-dependent.

The limiting factor of the radiolabeling reaction appears to be the decomposition of the [^{35}S]methionine.

FIG. 4. Schematic diagram of the location of ^{35}S-modified amino acids following two-dimensional thin-layer chromatography on silica gel 60. Chromatography and solvents were as described under Materials and Methods. The ^{35}S-modified amino acids are denoted by their three-letter abbreviations. Radioactive species of unknown origin are denoted by a question mark.

Increasing the amount of [^{35}S]methionine in the reaction mixture increases the amount of radioactivity associated with the protein but does not increase the percentage of protein-associated label. The percentage of label incorporated remains at approximately 2% of the total amount of radioactivity added to the reaction. We have attempted to accelerate the decomposition of the [^{35}S]-methionine by incubation of the labeled methionine alone for 24 h at temperatures from 4 to 42°C before addition of the BSA. However, no increase in the degree of labeling was observed (data not shown). We believe that formation of methyl mercaptan, the putative volatile decomposition product (6), results in further decomposition reactions. It is likely that the protein acts as a "receptor" for this reactive by-product. Increasing the rate of breakdown of the [^{35}S]methionine in the presence of the protein should therefore increase the efficiency of labeling.

Once associated with the protein the radiolabel is stable. Multiple freeze/thaw cycles, boiling, and extended incubations (24 h) at various temperatures do not remove it. This suggests a covalent attachment of the radiolabel to the protein. Proteins can also be labeled in the presence of a variety of compounds commonly used in protein isolation and purification. However, in the presence of urea, ammonium sulfate, and guanidine HCl, substantial inhibition of the labeling reaction was observed. Also when the radiolabeling reaction was run in the presence of Tris (pH 7.4, 0–1 M), a
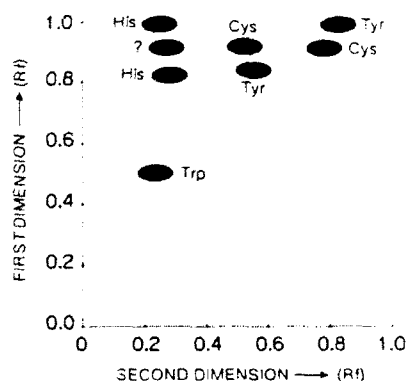
concentration-dependent decrease in labeling was observed above 50 mM. A similar experiment with Hepes (pH 7.4, 0–1 M) showed no effect on labeling. These results indicate that primary and secondary amine-containing compounds interfer with labeling, leading us to postulate a reaction mechanism similar to that for reductive methylation (2). However, thin-layer chromatography data suggest that the only amino acids capable of being labeled are tyrosine, tryptophan, histidine, and cysteine. These data, along with the pH-dependent nature of the reaction, suggest a mechanism similar to a base-catalyzed addition to the double bonds of tyrosine, tryptophan, and histidine. The labeling of cysteine could be attributed to disulfide formation between the cysteine and the methyl mercaptan. However, this does not explain the inhibition seen with the amine-containing compounds. The actual reaction mechanism awaits further investigation.

In conclusion, we have developed a method to radiolabel proteins with ^{35}S. The procedure utilizes the radiolytic decomposition products of [^{35}S]methionine to label the proteins, possibly through addition to the double bonds of tyrosine, tryptophan, and histidine. The reaction is time-, temperature-, and pH-dependent and is applicable to a variety of proteins. The method is simple to perform and yields proteins of high specific activity.

REFERENCES

1. Tack, B. F., and Wilder, R. L. (1981) in Methods in Enzymology (Langone, J. J., and Van Vunakis, H., Eds.), Vol. 73, pp. 138–147, Academic Press, San Diego.
2. Jentoft, N., and Dearborn, D. G. (1979) J. Biol. Chem. 254, 4359–4365.
3. Bolton, A. E., and Hunter, W. M. (1973) Biochem. J. 133, 529–539.
4. Amersham (1987) Data Sheet No. 11814.
5. Meisenhelder, J., and Hunter, T. (1988) Nature 335, 120.
6. Amersham (1988) TechTip Publication No. 108.
7. Kopoldova, J., Kolousek, J., Babicky, A., and Liebster, J. (1958) Nature 182, 1074–1076.
8. Laemmli, U. (1970) Nature 227, 680–685.
9. Chamberlain, J. P. (1979) Anal. Biochem. 98, 132–135.

Possible potentiation of the emetic response to oral S(-) zacopride by various receptor ligands in the ferret

Gregory L. King and John K. Weatherspoon

Department of Physiology, Armed Forced Radiobiology Research Institute, Bethesda, Maryland, 20889-5145, USA

SUMMARY

Three classes of receptor ligands (the D2 receptor agonist (+) apomorphine, the cholinergic-nicotinic receptor agonists (-) nicotine and (+)-nicotine-(+)-di-p-toluoyltartrate ((+)-NDPT), and the nonspecific opioid receptor antagonist (-) naloxone) were evaluated for their ability to potentiate the emetic response to two different doses (0.003 and 0.30 mg/kg) of p.o. S(-) zacopride. These S(-) zacopride doses evoked responses from 4/6 and 7/10 ferrets, respectively. Prior treatment (s.c.) with nonemetic doses (n = 2-4) of (+) apomorphine (0.01 mg/kg), (-) nicotine (0.30 mg/kg), or (-) naloxone (3.0 mg/kg) appeared to potentiate the emetic response to the higher dose of S(-) zacopride by initiating an earlier onset (P < 0.05) of the response. (-) Naloxone also increased the overall duration of the emetic episodes to the higher dose of S(-) zacopride. These preliminary results suggest that ligands acting at D2, nicotinic, and opioid receptors can enhance the emetic response to S(-) zacopride. However, it is unclear from these studies whether that enhancement is mediated centrally or peripherally.

Potentialisation possible de la réponse émétique à la prise orale de S(-) Zacopride par divers ligands chez le furet.

Résumé: Trois classes de ligands (l'apomorphine: agoniste (±) des récepteurs D2, la nicotine (-) et le (+) nicotine-di-p-toluoyltartrate ((+)-NDPT): agonistes des récepteurs cholinergiques-nicotiniques, et le (-) naloxone: antagoniste non-spécifique des récepteurs opioides) ont été évaluées pour leur capacité à potentialiser la réponse émétique à 2 doses différentes (0,003 et 0,30 mg/Kg) de S(-) zacopride per os. Ces doses de S(-) zacopride ont induit des réponses chez respectivement 4/6 et 7/10 furets. Le traitement initial (s.c.) avec des doses non émétiques (n = 2-4) de (±) apomorphine (0,01 mg/Kg), de (-) nicotine (0,30 mg/Kg), ou de (-) naloxone (3,0 mg/Kg) est apparu comme potentialisant la réponse émétique à la plus forte dose de S(-) zacopride en provoquant un déclenchement plus précoce (P < 0,05) de la réponse. (-) Naloxone a aussi augmenté la durée totale des épisodes émétiques à la plus forte dose de S(-) zacopride. Ces résultats préliminaires suggèrent que les ligands agissant au niveau des récepteurs D2, nicotiniques et opioides peuvent augmenter la réponse émétique au (-) S zacopride. Cependant, ces études ne peuvent préciser si le niveau d'action de cette augmentation est central ou périphérique.

INTRODUCTION

The substituted benzamide zacopride (4-amino-N-[1-azabicyclo(2.2.2)oct-3-yl]-5-chloro-2-methoxybenzamide[E])-2-buteniodiate) is a serotonin (5-hydroxytryptamine; 5-HT) subtype-three ($5-HT_3$) receptor antagonist and antiemetic that also evokes emesis at therapeutic (*i.e.*, antiemetic) doses in the ferret (King, 1990b; Sancilio **et al.**, 1990). The emetic response to zacopride occurs regardless of whether zacopride is given i.v., i.p., i.m., or p.o., and also predominantly to the S(-) but not the R(+) enantiomer (King, 1990b; King & Landauer, 1990; Sancilio **et al.**, 1990, 1991; Middlefell & Price, 1991; Bhandari & Andrews, 1991). Although emesis to p.o. administration is abolished by prior abdominal vagotomy (King, 1990b), the response after all administration routes is mitigated by several classes of receptor ligands (King, 1990b; Sancilio **et al.**, 1990, 1991; Middlefell & Price, 1991; Bhandari & Andrews, 1991).

The previous studies used prior treatment with specific receptor ligands to *palliate* the emetic response. In contrast, the present study was designed to determine whether prior treatment with specific receptor ligands could *potentiate* the emetic response to p.o. S(-) zacopride. Results from such studies should further our understanding about the pharmacology of the emetic response to S(-) zacopride and perhaps emesis in general.

For our studies, three individual classes of receptor ligands were chosen. The first two classes, receptor agonists, were chosen based on our previous findings that either the dopaminergic subtype-two (D_2) receptor antagonist domperidone or the cholinergic-muscarinic receptor antagonist and racemate glycopyrrolate ameliorates the emetic response to p.o. S(-) zacopride (King, 1990b). Thus one compound selected was the racemic mixture of the D_2 receptor agonist ($\pm$) apomorphine. Two other compounds selected were the stereoisomers of the cholinergic-nicotinic receptor agonists, (-) nicotine and (+)-nicotine-(+)-di-p-toluoyltartrate ((+)-NDPT). These latter compounds were chosen because quaternary ammonium analogs of atropine (*e.g.*, glycopyrrolate; King, 1990b) exhibit nicotinic receptor antagonist properties (Brown, 1990). The third class of ligand chosen to challenge p.o. S(-) zacopride was the nonspecific opioid-receptor antagonist (-) naloxone, which has been previously shown to potentiate emesis to other emetic agents (Scherkl **et al.**, 1990; Barnes **et al.**, 1991).

METHODS

Subjects: All subjects were male, castrated, and descented ferrets (Fitch) from Marshall Farms (North Rose, NY). Ferrets were housed in the AAALAC-accredited animal facility at AFRRI and provided with water and ferret chow *ad libitum*.

Procedure: Five to 10 animals were injected s.c. with a challenging agent (($\pm$) apomorphine [0.01 mg/kg], (-) nicotine tartrate [0.30

mg/kg], (+)-NDPT [0.30 mg/kg], or (-) naloxone [0.30 or 3.0 mg/kg] before administering p.o. S(-) zacopride (0.003 or 0.30 mg/kg]. (+) Apomorphine and (-) naloxone were given 20 min before S(-) zacopride; (-) nicotine and (+)-NDPT, 5 min before. Following administration of p.o. S(-) zacopride, the ferrets were placed in a large, well-ventilated Plexiglas[R] box, and behaviors were observed and recorded on a personal computer for 1-1.5 hr, as previously described (King & Landauer, 1990). The doses of challenging agents were chosen from preliminary results (2-4 animals) showing that these doses, when tested alone, did not evoke retching or emesis over a 45-60 min observation period. A single group of control animals was given p.o. 0.003 (n = 6) or 0.30 mg/kg (n = 10) S(-) zacopride and used to compare their responses with those groups receiving a drug challenge. Each ferret was tested only once with p.o. S(-) zacopride because we had previously observed that ferrets quickly develop an aversion after a single (emetic) dose. That is, after given an emetic dose of zacopride, the animals struggled to avoid subsequent administration at later times. In addition, each ferret was given a challenging agent only once to avoid tachyphylaxis to that agent.

Drugs: (+) Apomorphine and (-) naloxone were purchased from Sigma (St. Louis, MO), and (-) nicotine and (+)-NDPT from RBI (Natick, MA). All compounds were made fresh in NaCl as vehicle and give.. in a final volume of less than 1 ml. S(-) zacopride (Wyeth-Ayerst, Princeton, NJ) was made fresh in 5% dextrose/water as vehicle and given in 1-3 ml volume.

Data Analysis: The latencies and durations of recorded behaviors of the various groups were compared and analyzed with nonparametric tests (Kruskall-Wallis Rank Sum test and Dunn's test), and the incidence and total number of behavioral events with parametric tests (ANOVA and Newman-Keul's multiple range test). When only two groups were compared, the Student's t-test or Mann-Whitney test was used, as appropriate. Comparison of the percentages of responding animals was made by analysis of proportions by a contingency table. Significance was accepted at $P < 0.05$.

RESULTS

Preliminary testing for emesis in response to the doses of challenging agents showed that, for these agents alone, the following proportion of animals showed an emetic response. For (+) apomorphine, 0/3 animals responded to a 0.01 mg/kg dose, whereas 3/4 retched or vomited to a 0.05 mg/kg dose. For (-) nicotine, 0/3 and 0/4 responded to respective doses of 0.10 and 0.30 mg/kg. In response to (+)-NDPT, 0/3 responded to a dose of 0.30 mg/kg. For (-) naloxone, 0/2 and 0/4 responded to respective doses of 0.30 and 3.0 mg/kg.

Table 1 shows that a nonemetic (0.01 mg/kg) dose of (+) apomorphine appeared to potentiate the emesis to a high dose (0.30 mg/kg) of p.o. S(-) zacopride. This potentiation by (+) apomorphine of the high-dose response to S(-) zacopride was expressed as an earlier onset of the response when compared with controls. (+) Apomorphine also seemed to reduce the latency of onset for the response to the lower zacopride dose but this was not significant.

Table 1. (±) APOMORPHINE[a] PRETREATMENT EFFECTS ON
EMETIC RESPONSE TO P.O. S(-) ZACOPRIDE

Drug dose (mg/kg)	Responders	Latency: 1st retch (min)[b]	Episode duration (min)	Number of retches
0.003 S(-) Zaco	4/6	24.4 ± 6.3	7.2 ± 3.0	36.2 ± 7.7
+ 0.01 Apo	6/6	11.7 ± 4.2	10.6 ± 5.0	48.0 ± 15.8
0.30 S(-) Zaco	7/10	7.6 ± 1.9[c]	4.2 ± 1.1	29.2 ± 6.9
+ 0.01 Apo	5/5	1.0 ± 0.4[c]	2.8 ± 1.0	24.0 ± 7.5

[a]Given s.c. 20 min before S(-) zacopride. [b]All values are mean ± SEM.
[c]$P < 0.05$ between groups.

Table 2 shows that only the greater dose of (-) nicotine (0.30 mg/kg) appeared to potentiate the emetic response to the high dose of p.o. S(-) zacopride. Again this potentiation was expressed as an earlier onset of the response. Note, however, that (-) nicotine and (+)-NDPT seemed to both reduce the latency to the first retch and increase the episode duration of the response to the lower dose uf S(-) zacopride.

As seen in Table 3, the greater dose (3.0 mg/kg) of (-) naloxone seemed to clearly potentiate the emesis to the greater dose of p.o. S(-) zacopride. In contrast to pretreatment with either (±) apomorphine or the nicotinic receptor agonists (-) nicotine, however, not only did the responses to the higher dose of S(-) zacopride occur with a shorter latency, but the overall duration of the episodes was greater. In addition, although not significant, (-) naloxone appeared to evoke a greater number of retching events.

Table 2. (-) NICOTINE[a] OR (+)-NDPT[a] PRETREATMENT
EFFECTS ON EMETIC RESPONSE TO P.O. S(-) ZACOPRIDE

Drug dose (mg/kg)	Responders	Latency: 1st retch (min)[b]	Episode duration (min)	Number of retches
0.003 S(-) Zaco	4/6	24.4 ± 6.3	7.2 ± 3.0	36.2 ± 7.7
+ 0.30 (-) Nico	4/6	18.7 ± 5.6	12.8 ± 4.4	35.7 ± 8.9
+ 0.30 (+)-NDPT	6/6	10.5 ± 2.3	21.6 ± 6.9	49.0 ± 7.6
0.30 S(-) Zaco	7/10	7.6 ± 1.9[c]	4.2 ± 1.1	29.2 ± 6.9
+ 0.30 (-) Nico	7/8	0.8 ± 0.1[c]	3.5 ± 0.7	30.4 ± 13.1
+ 0.30 (+)-NDPT	7/8	2.6 ± 1.7	4.4 ± 1.8	31.0 ± 8.3

[a]Given s.c. 5 min before S(-) zacopride. [b]All values are mean ± SEM.
[c]$P < 0.05$ between groups.

Table 3. (-) NALOXONE[a] PRETREATMENT EFFECTS ON EMETIC RESPONSE TO P.O. S(-) ZACOPRIDE

Drug dose (mg/kg)	Responders	Latency: 1st retch (min)[b]	Episode duration (min)	Number of Retches
0.003 S(-) Zaco	4/6	24.4 ± 6.3	7.2 ± 3.0	36.2 ± 7.7
+ 0.3 Nal	2/6	22.6 ± 8.6	0.8 ± 0.3	20.5 ± 3.5
+ 3.0 "	6/6	28.2 ± 8.3	11.6 ± 8.1	45.3 ± 11.1
0.30 S(-) Zaco	7/10	7.6 ± 1.9[c]	4.2 ± 1.1	29.2 ± 6.9
+ 0.3 Nal	8/10	3.6 ± 2.2	3.0 ± 1.3[d]	37.1 ± 15.1
+ 3.0 "	9/10	0.8 ± 0.3[c]	21.1 ± 7.2[d]	61.7 ± 19.2

[a]Given s.c. 20 min before S(-) zacopride. [b]All values are mean ± SEM. [c,d]$p < 0.05$ between groups.

DISCUSSION

The principal finding of these preliminary studies was that three different classes of receptor ligands appeared to potentiate the emetic response to a moderately high dose of S(-) zacopride. This potentiation was expressed primarily as a significant reduction in the latency to the first retching response. (-) Naloxone, however, also significantly increased the episode duration. Furthermore, in some cases, the latencies and durations to the lower dose of S(-) zacopride appeared to also be modified by these compounds. The reduced latencies to emesis reported here do not conclusively demonstrate an effect of these compounds. However, surgical procedures such as vagotomies ameliorate emetic responses by altering the latencies (Andrews et al., 1990; King and Landauer, 1990). This suggests that we have perturbed the system by pharmacological methods, but that further studies are warranted that use other doses of these compounds, as well as S(-) zacopride.

Two of the classes of ligands used here are receptor agonists and none bind at the 5-HT$_3$ receptor. These data thus suggest that activation of these receptor sites can modulate the emetic response to p.o. S(-) zacopride. The D$_2$ receptor agonist (±) apomorphine appeared to potentiate the emetic response, which further corroborates an earlier finding by this laboratory (King, 1990b) that a D$_2$ receptor antagonist ameliorates the emetic response. Our earlier finding of involvement of a cholinergic receptor in the emetic response was partially corroborated by the apparent potentiation of the emetic response with the nicotinic receptor agonist (-) nicotine. Although quaternary atropine derivatives such as glycopyrrolate also act at the nicotinic receptor (Brown, 1990), Alaranta et al. (1990) found that the ganglionic-blocking property of glycopyrrolate was 16x less potent than hexamethonium, one half as potent as tetraethylammonium, and 2x as potent as decamethonium. These latter data suggest that our previous results with glycopyrrolate are most likely due to muscarinic receptor antagonism. Finally, our finding that the opioid receptor antagonist (-) naloxone also potentiated the emetic response further corroborates the general role of the opioids in emetic events

Table 4. RECEPTOR LIGANDS THAT ALTER EMETIC RESPONSE
TO S(-) OR RS(±) ZACOPRIDE

Receptor ligand	Response to challenge		
	No effect	Attenuate	Potentiate
Serotonergic			
5-HT$_{1P}$			
antagonist	N-acetyl-5-HTP-DP[a]*	–	–
5-HT$_3$			
agonist	–	2-CH$_3$-5HT[b]**	–
antagonist	Granisetron[c]	Granisetron[b]	–
	R(+) Zacopride[d]	R(+) Zacopride[e,f]	–
	ICS 205-930[c]	Ondansetron[e]	–
5-HT$_4$			
agonist	–	–	–
antagonist	–	ICS 205-930[a,c]	–
	–	S(-) Zacopride[d,e,f]	–
Dopaminergic			
D$_2$			
agonist	–	–	(±) Apomorphine?
antagonist	–	Domperidone[b]	–
	–	Haloperidol[a]	–
	–	Prochlorperazine[a]	–
Cholinergic			
Muscarinic			
antagonist	Atropine[e]	Glycopyrrolate[b]	–
Nicotinic			
agonist	(+)-NDTP?***	–	–
	–	–	(-) Nicotine?
Opioid			
antagonist			
δ,k,μ,σ	–	–	(-) Naloxone?

*N-acetyl-5-hydroxytryptophyl-5-tryptophan amide. **2-methyl-serotonin. ***(+)-nicotine-(+)-di-p-toluoyltartrate.
[a]Sancilio, et al., 1990; [b]King, 1990; [c]Bhandari and Andrews, 1991; [d]King, in preparation; [e]Middlefell and Price, 1991; [f]Sancilio, et al., 1991.

(Costello & Borison, 1977). These latter results also suggest that more specific opioid receptor antagonists should be evaluated for their ability to modulate the emesis to p.o. S(-) zacopride.

From the present results it is unclear whether these compounds acted centrally or peripherally to potentiate the emesis to p.o. S(-) zacopride. Although we were careful to give nonemetic pretreatment doses of these agents, all three (apomorphine, nicotine, and naloxone) can evoke emesis when given either peripherally at higher doses or centrally (Kamerling et al, 1982; Spealman, 1983; Beleslin & Krstic, 1987; Gupta et al., 1989; Jovanivic-Micic et al., 1989; Torii et al., 1991; see review, King, 1990a). Our previous work (King, 1990b) used receptor antagonists that did not cross the blood-brain barrier, but the compounds used in the experiments reported here do not share that

property. For example, within 5-10 min after injection, the brain concentrations of both (-) nicotine and (-) naloxone considerably exceed those of the serum (Applegren **et al.**, 1962; Tsujimoto **et al.**, 1975; Tepper **et al.**, 1979; Berkowitz **et al.**, 1975; Ngai **et al.**, 1976). Even after s.c. administration, higher brain concentrations are seen for both (-) nicotine and (+)-NDPT (Martin **et al.**, 1983). Thus the site of potentiating action of these three compounds could be central in nature. Such central action by these compounds could be at the *area postrema* (chemoreceptor trigger zone), as ablations of this region can abolish the emesis to centrally administered apomorphine and nicotine, but not (-) naloxone (see King, 1990a). Other behavioral responses to nicotine imply a generalized central excitation that may be possible to detect from measures of locomotor activity. We have not yet analyzed the vertical locomotor activity of the ferrets in this study. Nevertheless, this behavioral measure has detected sedative-like effects of RS(±) and S(-) zacopride (*e.g.*, reduced vertical locomotor activity) (King & Landauer, 1990; King, in preparation).

(±) Apomorphine, (-) nicotine, and (+)-NDPT could be acting peripherally at the *area postrema* to potentiate the emetic response to p.o. S(-) zacopride. Depending on the species (see King, 1990a), *area postrema* ablations will fully or partially abolish the emetic response to peripherally administered apomorphine and nicotine. (Such studies have not been done with (-) naloxone). A predominantly peripheral action of apomorphine is supported by the work of Burkman **et al.** (1974) who found that, after an i.v. bolus of apomorphine, its plasma content remained approximately 23x greater than that of the brain for up to 50 min.

Dopaminergic, nicotinic-cholinergic, and opioid receptor binding sites are also found within the ganglia of the enteric nervous system (Costa **et al.**, 1987). Thus the three compounds could also be acting at or near the vagal afferent endings that respond to the actions of p.o. S(-) zacopride (King, 1990b). Applegren **et al.** (1962) found both immediate nicotine binding in the gastric mucosa after an i.v. bolus and preliminary evidence for binding at sympathetic ganglionic sites. With respect to nicotine, however, its immediate binding after a bolus injection is greater in the adrenal cortex than in the brain (Tsujimoto **et al.**, 1975; Tepper **et al.**, 1979). This suggests the possibility that nicotine may release catecholamines from the adrenal cortex, which in turn could modulate the emesis to S(-) zacopride.

Table 4 summarizes those receptor ligands that have been shown to modify the emetic response to S(-) or RS(±) zacopride. That several receptor agonists or antagonists can affect the response suggests that there are multiple receptor sites that can modulate the response. In those studies in which atropine or a quaternary derivative were used, the results are contradictory. It also remains unclear as to which 5-HT receptor the S(-) enantiomer binds to elicit the emetic response. For example, it has been suggested that the emetic response could be mediated by binding at either the 5-HT$_3$ or 5-HT$_4$ receptor. This question is further confounded by a lack of agreement as to whether the reported pharmacological (*i.e.*, 5-HT$_{1P}$ and 5-HT$_4$ receptor antagonist) properties of N-acetyl-5-HTP-DP are similar (Wade **et al.**,

1991; Andrade & Chaput, 1991). As further example, the 5-HT₃ receptor antagonist Granisetron mitigated zacopride-induced emesis during the first 30 min of a 1 hr observation period (King, 1990a), but had no effect when the observation period was extended to 2 hr (Bhandari & Andrews, 1991). Likewise, some, but not others, have found that the R(+) enantiomer of zacopride mitigated the emetic response.

Some of the results obtained from these *in vivo* studies also raise questions about the appropriate experimental design for such studies. For example, the reported antiemetic properties of the R(+) enantiomer for S(-) zacopride would confound those studies in which the RS(±) racemate is used as the emetic stimulus. Likewise, the antiemetic properties of th' S(-) enantiomer for its own emetic response would confound those studies in which a cumulative dosing regimen is used to test for its emetic properties. Because the experimental designs and the routes of administration used have varied considerably among all these studies, resolving the question at which receptor the S(-) enantiomer is acting to evoke the emetic response will require further study.

In summary, we have presented preliminary data suggesting that three different classes of receptor ligands (a D_2 receptor agonist, nicotinic receptor agonists, and an opioid receptor antagonist) appeared to potentiate the emetic response to p.o. S(-) zacopride. Some of these results confirm our previous findings showing that activation of non-5-HT₃ receptor sites can modulate the emetic response to p.o. S(-) zacopride. This provides further insight into the complex interactions of neurotransmitters in evoking emesis.

REFERENCES

Alaranta, S., Kling, E., Patsi, T., & Sjostrand, N.O. (1990): Inhibition of nicotine-induced relaxation of the bovine retractor penis muscle by compounds known to have ganglion-blocking properties. *Br. J. Pharmacol.* 101, 472-476.

Andrade, R., & Chaput, Y. (1991): 5-Hydroxytryptamine₄-like receptors mediate the slow excitatory response to serotonin in the rat hippocampus. *J. Pharmacol. Exp. Ther.* 257, 930-937.

Andrews, P.R.L., Davis, C.J., Bingham, S., Davidson, H.I.M., Hawthorn, J., & Maskell, L. (1990): The abdominal visceral innervation and the emetic reflex: Pathways, pharmacology, and plasticity. *Can. J. Physiol. Pharmacol.* 68, 325-345.

Applegren, L.-E., Hansson, E., & Schmiterlow, C.G. (1962): The accumulation and metabolism of C^{14}-labelled nicotine in the brain of mice and cats. *Acta Physiol. Scand.* 56, 249-257.

Barnes, N.M., Bunce, K.T., Naylor, R.J., & Rudd, J.A. (1991): The actions of fentanyl to inhibit drug-induced emesis. *Neuropharmacology,* 30, 1073-1083.

Beleslin, D.B. & Krstic, S.K. (1987): Further studies on nicotine-induced emesis: nicotinic mediation in area postrema. *Physiol. Behav.* 39, 681-686.

Berkowitz, B.A., Ngai, S.H., Hempstead, J., & Spector, S. (1975): Disposition of naloxone: Use of a new radioimmunoassay. *J. Pharmacol. Exp. Ther.* 195, 499-504.

Bhandari, P., & Andrews, P.L.R. (1991): Preliminary evidence for

the involvement of the putative 5-HT$_4$ receptor in zacopride- and copper sulphate-induced vomiting in the ferret. *Eur. J. Pharmacol.* 204, 273-280.

Brown, J.H. (1990): Atropine, scopolamine, and related antimuscarinic drugs. In *The Pharmacological Basis of Therapeutics*, ed. A.G. Gilman, T.W. Rall, A.S. Nies & P. Taylor, pp. 150-165. New York: Pergamon Press.

Burkman, A.M., Notari, R.E., & Van Tyle, W.K. (1974): Structural effects in drug distribution: Comparative pharmacokinetics of apomorphine analogues. *J. Pharm. Pharmac.* 26, 493-507.

Costa, M., Furness, J.E., & Llewellyn-Smith, I.J. (1987): Histochemistry of the enteric nervous system. In *Physiology of the Gastrointestinal Tract*, ed. L.R. Johnson, pp. 1-40. New York: Raven Press.

Costello, D.J., & Borison, H.L. (1977): Naloxone antagonizes narcotic self-blockade of emesis in the cat. *J. Pharmacol. Exp. Ther.* 203, 222-230.

Gupta, Y.K., Bhandari, P., Chugh, A., Seth, S.D., Dixit, K.S., & Bhargava, K.P. (1989): Role of endogenous opioids and histamine in morphine induced emesis. *Indian J. Exp. Biol.* 27, 52-54.

Jovanivic-Micic, D., Strbac, M., Krstic, S.K., Japundzic, N., Samardzic, R., & Beleslin, D.B. (1989): Ablation of the area postrema and emesis. *Metab. Brain Dis.* 4, 55-60.

Kamerling, S.G., Wettstein, J.G., Sloan, J.W., Su, T.P., & Martin, W.R. (1982): Interaction between nicotine and endogenous opioid mechanisms in the unanesthetized dog. *Pharmacol. Biochem. Behav.* 17, 733-740.

King, G.L.: The antiemetic and other properties of R(+)-zacopride in the ferret. (in preparation).

King, G.L. (1990a): Animals models in the study of vomiting. *Can. J. Physiol. Pharmacol.* 68, 260-268.

King, G.L. (1990b): Emesis and defecations induced by the 5-hydroxytryptamine (5-HT$_3$) receptor antagonist zacopride in the ferret. *J. Pharmacol. Exp. Ther.* 253, 1034-1041.

King, G.L., & Landauer, M.R. (1990): Effects of zacopride and BMY25801 (batanopride) on radiation-induced emesis and locomotor behavior in the ferret. *J. Pharmacol. Exp. Ther.* 253, 1026-1033.

Martin, B.R., Tripathi, H.L., Aceto, M.D., & May, E.L. (1983): Relationship of the biodisposition of the stereoisomers of nicotine in the central nervous system to their pharmacological actions. *J. Pharmacol. Exp. Ther.* 226, 157-163.

Middlefell, V.C., & Price, T.L. (1991): 5-HT$_3$ receptor agonism may be responsible for the emetic effects of zacopride in the ferret. *Br. J. Pharmacol.* 103, 1011-1012.

Ngai, S.H., Berkowitz, B.A., & Yang, J.C. (1976): Pharmacokinetics of naloxone in rats and man. *Anesthesiology* 44, 398-401.

Sancilio, L.F., Pinkus, L.M., Jackson, C.B., & Munson, H.R., Jr. (1990): Emetic activity of zacopride in ferrets and its antagonism by pharmacological agents. *Eur. J. Pharmacol.* 181, 303-306.

Sancilio, L.F., Pinkus, L.M., Jackson, C.B., & Munson, Jr., H.R. (1991): Studies on the emetic and antiemetic properties of zacopride and its enantiomers. *Eur. J. Pharmacol.* 192, 365-369.

Scherkl, R., Hashem, A., & Frey, H.H. (1990): Apomorphine-induced emesis in the dog -- routes of administration, efficacy and

synergism by naloxone. *J. Vet. Pharmacol. Ther.* 13, 154-158.
Spealman, R.D. (1983): Maintenance of behavior by postponement of scheduled injections of nicotine in squirrel monkeys. *J. Pharmacol. Exp. Ther.* 227, 154-159.
Tepper, J.M., Wilson, J.R., & Schlesinger, K. (1979): Relations between nicotine-induced convulsive behavior and blood and brain levels of nicotine as a function of sex and age in two inbred strains of mice. *Pharmacol. Biochem. Behav.* 10, 349-353.
Torii, Y., Saito, H., & Matsuki, N. (1991): Selective blockade of cytotoxic drug-induced emesis by 5-HT$_3$ receptor antagonists in *Suncus murinus*. *Jpn. J. Pharmacol.* 55, 107-113.
Tsujimoto, A., Nakashima, T., Tanino, S., Dohi, T., & Kurogocn. (1975): Tissue distribution of [^{3}H]nicotine in dogs and rhesus monkeys. *Toxicol. Appl. Pharmacol.* 32, 21-31.
Wade, P.R., Mawe, G.M., Branchek, T.A., & Gershon, M.D. (1991): Use of stereoisomers of zacopride to analyze actions of 5-hydroxytryptamine on enteric neurons. *Am. J. Physiol.* 260, G80-G90.

ACKNOWLEDGMENTS

226

SYNTHETIC TREHALOSE DICORYNOMYCOLATE AND ANTIMICROBIALS INCREASE SURVIVAL FROM SEPSIS IN MICE IMMUNOCOMPROMISED BY RADIATION AND TRAUMA

G. D. Ledney*, G. S. Madonna, M. M. Moore,
T. B. Elliott, and I. Brook

Department of Experimental Hematology Armed Forces
Radiobiology Research Institute, Bethesda, MD

Abstract

When mammalian antimicrobial defenses are compromised by
radiation, death from sepsis may occur. Tissue trauma in irradiated hosts
significantly increases mortality from bacterial infections and makes

---

*Send reprint requests to: Dr. G.D. Ledney, Department of Experimental
Hematology Armed Forces Radiobiology Research Institute, Bethesda,
MD 20889-5145.

antimicrobial treatments more difficult than when individuals are
subjected to trauma or radiation alone. We determined that
postirradiation therapy with the immunomodulator synthetic trehalose
dicorynomycolate (S-TDCM) and antimicrobials increases survival in
mice after lethal irradiation and tissue trauma. Single agent therapy with
systemic oxacillin, gentamicin, ofloxacin, and S-TDCM did not increase
survival. Topical treatment of the injury with gentamicin cream in
addition to systemic therapy with oxacillin or S-TDCM was necessary to
enhance survival. Therapy with gentamicin and S-TDCM had a syner-
gistic effect on survival. Therapies combining augmentation of non-
specific host defense mechanisms with antimicrobials may be valuable in
treating irradiated patients also sustaining tissue trauma.

Introduction

When a host's antimicrobial defenses are severely compromised
by radiation, death from sepsis may occur (Brook, 1988). Trauma
inflicted on irradiated hosts significantly increases the difficulty of
treating bacterial infections, compared with treating trauma or radiation
exposure alone (Madonna *et al.*, 1991). Penicillin therapy contains but
does not eradicate penicillin-sensitive *Staphylococcus aureus* from
infected muscle wounds in sublethally irradiated mice (Brook and Elliott,
1989; Elliott *et al.*, 1990).

The power reactor disaster in Chernobyl and the atomic deton-
ations at Hiroshima and Nagasaki underscore the need for effective
therapies for infection in humans subjected to nuclear radiation and
physical trauma. Newly synthesized antimicrobials and immunomodu-
lators may effectively treat infections in severely immunocompromised
hosts. For example, we recently showed that the immunomodulator S-
TDCM, when injected into γ-irradiated mice either alone or with the
third-generation cephalosporin ceftriaxone, increased survival from
induced lethal *Klebsiella pneumoniae* infection (Madonna *et al.*, 1989a).
Using S-TDCM with the fluoroquinolone ofloxacin to treat acquired
infections after γ irradiation and skin wound trauma also increased
survival times of mice (Madonna *et al.*, 1989b).

In the current study, we present our findings on the survival of
irradiated-wounded mice treated with S-TDCM and antimicrobials for
endogenously acquired infections. We show that survival from lethal
irradiation-wounding is possible when topical antimicrobials are used in

conjunction with systemic treatments with antimicrobials or the immunomodulator S-TDCM.

Materials and Methods

C3H/HeN female mice were obtained from the National Cancer Institute Animal Breeding Facility, Frederick, MD and were maintained as previously described (Madonna *et al.*, 1991). Research was conducted in a facility accredited by the American Association for Accreditation of Laboratory Animal Care, and all procedures involving animals were reviewed and approved by our institutional animal care and use committee.

C3H/HeN mice were irradiated unilaterally at 40 cGy/min to a total dose of 8.0 Gy with a ^{60}Co Theratron unit. All irradiations of mice were done in aerated Plexiglas restrainers. The tissue/air ratio was 0.98 for the radiation conditions.

Mice were anesthetized by inhalation of methoxyflurane before wounding. Full-thickness, nonlethal skin injuries (15% total-body surface area) were inflicted after irradiation by removing a 1-inch by 1.5-inch section of dorsal skin and underlying paniculous carnosus muscle with a steel punch. Details for inflicting skin wounds were previously published (Madonna *et al.*, 1991).

Cultures of wounds were performed by a sterile swab technique; liver cultures were performed on homogenized tissue (Madonna *et al.*, 1991). Bacteria found in irradiated mice, wounded mice, or irradiated-wounded mice were isolated on phenylethanol agar or MacConkey's agar and were identified by standard techniques using Gram's stain, colonial morphology, and specific biochemical assays (Lennette *et al.*, 1985).

S-TDCM was a gift of Ribi ImmunoChem Research, Inc., Hamilton, MT. S-TDCM's chemical formulation results in a molecular weight of about 1,250 daltons. Briefly, S-TDCM is prepared by the condensation of 32-carbon-atom mycolic acid residues with sugar trehalose. Before use, stock S-TDCM concentrations were prepared using pyrogen-free materials by dissolving in hexane and drying under nitrogen. The dried product was then homogenized in 0.2% Tween 80 and 0.9% NaCl, and sonicated. Endotoxin levels in 1 mg/mL S-TDCM samples were < 0.006 ng/mL, as determined by the limulus lysate assay. A dose of 200 μg S-TDCM was injected i.p. into mice in 0.5 mL volumes.

Oxacillin sodium (Bactocill; Beecham Labs, Division of Beecham, Inc., Bristol, TN), gentamicin sulfate (Elkins-Sinn, Inc., Cherry Hill, NJ), and ofloxacin (a gift of R. W. Johnson, Pharmaceutical Research Institute, Raritan, NJ) were prepared in pyrogen-free water, and 0.1 mL was injected s.c. above the right or left gluteus medius alternately in each mouse once daily for ten consecutive days. The daily doses of oxacillin were 150 mg/kg; of gentamicin, 7.5 mg/kg; and of ofloxacin, 40 mg/kg. Silvadene cream™ (1% silver sulfadiazine; Marion Labs Inc., Kansas City, MO), Garamycin cream™ (0.1% gentamicin sulfate; Schering Corp., Kenilworth, NJ); and a generic 0.1% gentamicin sulfate (Goldline Labs, Fort Lauderdale, FL) were applied once daily for ten consecutive days in 0.5 to 0.7 g amounts sufficient to cover the wounded site.

Survival data of mice in experimental groups were obtained for 30 days after irradiation. Statistical analyses were made by the generalized Savage (Mantel-Cox) procedure. Asterisks (*) in figures indicate significance at the 0.05 level when compared with control-treated mice.

Results

Bacteria colonized the wound site in wounded and lethally irradiated-wounded mice (Table I). The predominant bacteria species on all wounds were gram-positive staphylococci and streptococci. In addition, gram-negative bacteria, common members of mouse intestinal microflora, were found on the wound site and apparently translocated to the liver within four to five days. At six to seven days, all irradiated-wounded mice died from sepsis. In lethally irradiated mice, bacterial translocation, indicated by positive liver cultures, occurred just prior (day 11) to death. Systemic ofloxacin and gentamicin, antimicrobials effective against gram-negative bacteria, increased survival times, while systemic S-TDCM decreased the survival time of lethally irradiated-wounded mice (Figure 1). Topical treatment of the wound site of lethally irradiated-wounded mice by either gentamicin sulfate cream or silver sulfadiazine cream increased survival (Figure 2). Silver sulfadiazine is effective against gram-negative and gram-positive bacteria as well as many fungi. Combined modality therapy of lethally irradiated-wounded mice with systemic oxacillin, effective against staphylococci, and topical gentamicin resulted in full recovery (Figure 3). Topical treatment of lethally

TABLE I

Isolated Bacteria From Wound and Liver of Irradiated-Wounded Mice*

Condition	Day of Culture			
	4 to 5		6 to 11	
	Wound	Liver	Wound	Liver
8.0 Gy γ + 15% wound	S. aureus S. faecium E. coli P. mirabilis	P. mirabilis	Dead	Dead
Wounded only	S. aureus S. xylosus Streptococcus spp. S. epidermidis	None	S. aureus S. xylosus Streptococcus spp.	None
Irradiated only (9 Gy γ)	NA	None	NA	S. aureus E. coli K. oxytoca

NA = not applicable

*C3H/HeN mice were wounded 1 h after irradiation. Mice (3-8) in each group were euthanized either on day 4, 5, 6, 8, or 11 after irradiation and injury, and the wound site and liver were cultured to identify the bacteria. Bacteria are listed in order of frequency of isolation in each group/time. Gram-positive bacteria (> 100 colonies/plate) were cultured from all wounded or irradiated-wounded mice. Gram-negative bacteria (> 100 colonies/plate) were cultured from all irradiated-wounded mice. In wounded mice, gram-negative bacteria were cultured in variable numbers; the colony incidence (0-100) was less than that for gram-positive organisms.
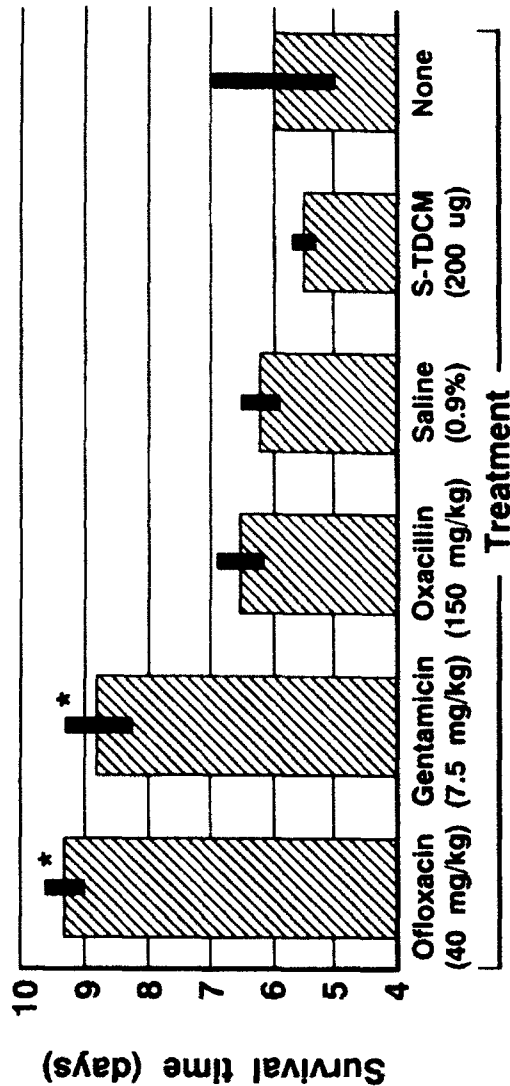
Figure 1.: Systemic antimicrobials enhance survival of lethally irradiated mice inflicted with wound trauma. Groups of 20 C3H/HeN mice were given 8.0 Gy γ radiation 1 h before inflicting 15% skin wound trauma. Mice that were not treated with S-TDCM received 0.5 mL 0.9% saline after wound trauma. Antimicrobials or water were provided once daily commencing two days after skin wound trauma and for nine or ten consecutive days thereafter. Ofloxacin and gentamicin significantly increased survival times (p < 0.05) of irradiated-wounded mice, compared with all other treatment groups. All antimicrobials significantly increased survival times (p < 0.05) of irradiated-wounded mice, compared with survival times of mice given S-TDCM. The mean survival time for mice given 8.0 Gy radiation and not wounded was 12.8 ± 0.4 days. Survival of 70% was recorded for mice given 200 μg S-TDCM i.p. 1 h after 8.0 Gy radiation.
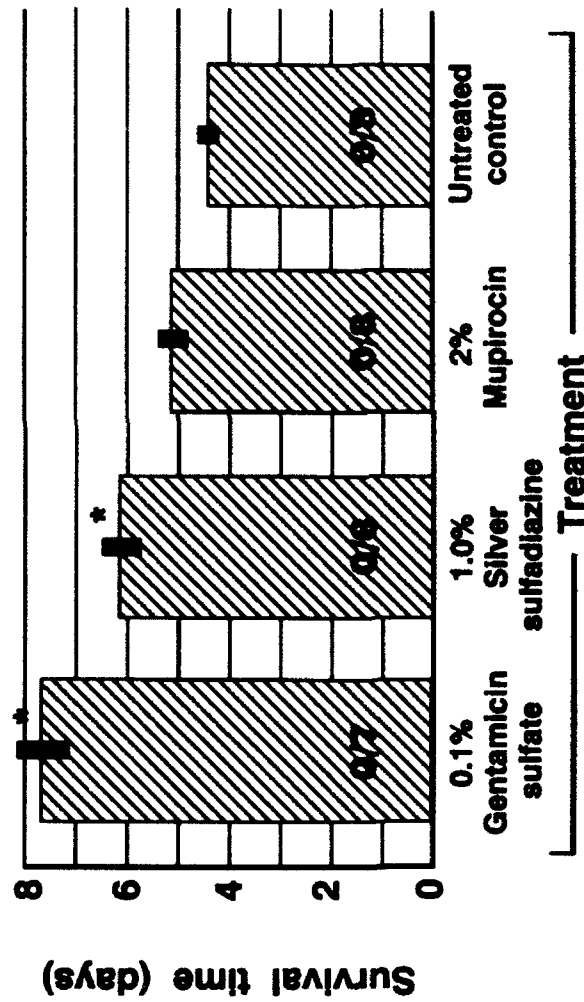
Figure 2.: Topical application of gentamicin sulfate (0.1%) or silver sulfadiazine (1.0%) increases survival in mice after irradiation and wounding. C3H/HeN mice (seven to eight per group) were wounded 1 h after 8.0 Gy γ irradiation. Treatment with each topically applied antimicrobial commenced 4 h after wounding and was applied for five consecutive days.
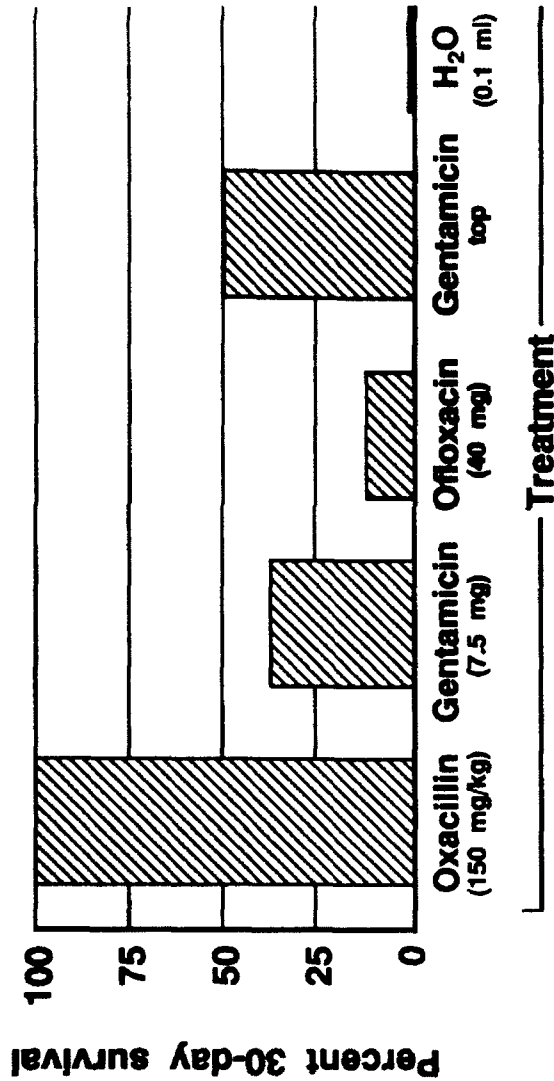
Figure 3.: Combined therapy with topical (top) 0.1% gentamicin sulfate and systemic antimicrobials increases survival in irradiated mice inflicted with wound trauma. C3H/HeN mice were wounded 1 h after irradiation. Antimicrobial therapies commenced 4 h after injury and were provided daily for ten days. Groups of 16 mice (given γ radiation) were treated topically with 0.1% gentamicin sulfate and s.c. with either 150 mg/kg/day of oxacillin, 7.5 mg/kg/day of gentamicin, or 40 mg/kg/day of ofloxacin. Control groups were treated with 0.1 mL sterile water plus gentamicin cream or were given no antimicrobial therapy. In this experimental series, topical gentamicin alone or with systemic oxacillin and gentamicin significantly increased survival ($p < 0.05$) compared with ofloxacin.
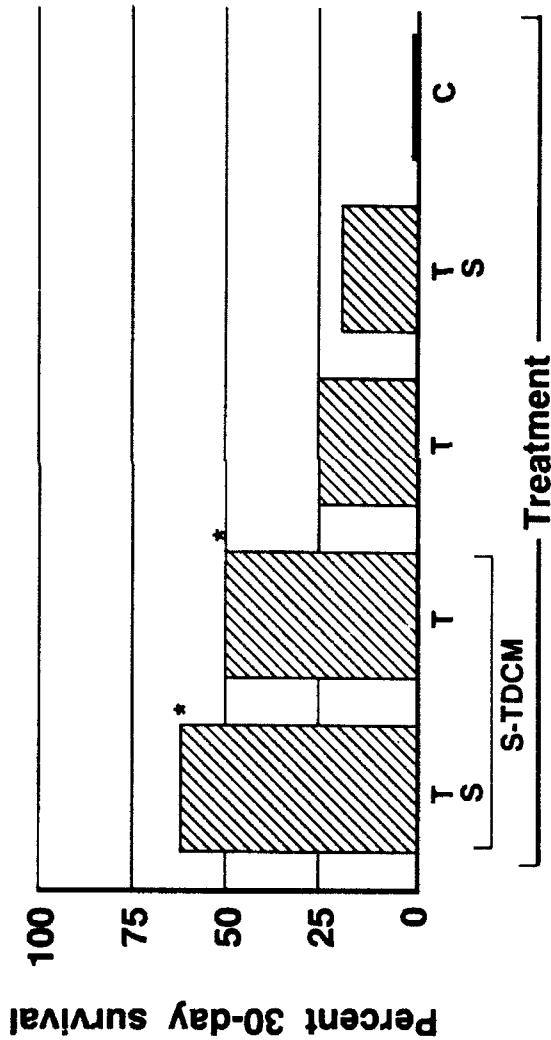
Figure 4.: Combined therapy with topical 0.1% gentamicin sulfate and S-TDCM increases survival in irradiated mice inflicted with wound trauma. C3H/HeN mice were wounded 1 h after 8-Gy irradiation. S-TDCM (200 μg i.p.) was given immediately after wound trauma. Gentamicin therapy was applied topically and/or given s.c. starting 4 h after injury and daily thereafter for nine days. Groups of 16 mice given γ radiation were treated as indicated. T = topical 0.1% gentamicin sulfate; S = systemic 7.5 mg/kg gentamicin sulfate; C = control. Systemic gentamicin sulfate with S-TDCM but without topical gentamicin was not evaluated in irradiated mice. In irradiated mice, topical gentamicin therapy with S-TDCM (with or without systemic gentamicin therapy) significantly increased survival (p < 0.05), compared with all other treatment groups.

irradiated-wounded mice with gentamicin sulfate in combination with S-TDCM or with gentamicin sulfate used systemically provided anti-bacterial coverage and resulted in 50 to 60% survival (Figure 4).

Discussion

Radiation accidents and subsequent mortality at Chernobyl, USSR, and Goiania, Brazil, point to the need for developing effective broad-spectrum antimicrobial therapies for victims of radiation accidents. In Chernobyl patients, *Staphylococcus epidermidis* may have contributed to terminal septicemia (Browne, 1990). *Klebsiella* sp. were found in several patients who died in Goiania (Brandao-Mello *et al.*, 1991).

Our studies reported here indicate that gram-negative and gram-positive bacteria colonize the wound site of irradiated mice. The same species were later found in the liver, suggesting that the bacteria translocated either from the wound site or from the intestinal tract. Alternatively, the gut may have been the source of septicemia, which caused simultaneous colonization of both the wound and the liver. It is not known if gram-positive bacteria colonized the intestinal tract prior to radiation, or radiation and wounding. Such bacterial species are normally found on the surface of the body and are not indigenous within the intestinal tract. Clearly, immunocompromising the host with radiation alone or with subsequent wound trauma resulted in gram-positive bacterial growth in the liver (Table I). A similar phenomenon was observed in severely burned rats (Maejima *et al.*, 1984) and total-body-irradiated mice (Brook *et al.*, 1986), resulting in the translocation of both gram-positive and gram-negative bacteria from the intestinal tract to the mesenteric lymph nodes, liver, and spleen.

Our data demonstrate that the topical application of antimicrobial creams on the wound site and systemic use of antimicrobials extend the survival time of lethally irradiated mice. Combined modality therapy with topical and systemic antimicrobials may be necessary to allow sufficient time for the radiation-damaged hematopoietic system to recover. Hematopoietic recovery in irradiated hosts is essential for long-term survival. Bone marrow transplantation was attempted in the victims of the Chernobyl accident (Baranov *et al.*, 1989), while the growth factor granulocyte-macrophage colony-stimulating factor (GM-CSF) was used in the Goiania victims (Brandao-Mello *et al.*, 1991). GM-CSF had some value because peripheral blood circulating cells increased.

In our work, we used S-TDCM because it enhances nonspecific host resistance to bacterial infections and increases hematopoiesis in irradiated mice (Madonna *et al.*, 1989a). Unlike GM-CSF, which requires multiple dosing, S-TDCM is effective after a single post-irradiation treatment. Also, S-TDCM activates macrophages, radio-resistant cells that are known to debride wounds, kill bacteria, and produce physiologic concentrations of other growth factors necessary for wound healing and reconstitution of immunohemopoiesis (Madonna *et al.*, 1989a). In the present study, a synergistic effect on survival was achieved by combining S-TDCM and gentamicin (Figure 4).

In conclusion, the individual exposed to radiation and inflicted with additional tissue trauma is at jeopardy to disseminated sepsis from a variety of opportunistic micro-organisms. Combined modality treatments with antimicrobials and immunomodulators or cell growth factors hold promise for developing therapies for individuals severely injured by radiation and trauma.

References

Baranov, A., Gale, R. P., Guskova, A., Piatkin, E., Selidovkin, G., Muravyova, L., Champlin, R. E., Danilova, N., Yevseeva, L., Petrosyan, L., Pushkareva, S., Konchalovsky, M., Gordeeva, A., Protasova, T., Reisner, Y., Mickey, M. R. and Terasaki, P. I. (1989).: Bone marrow transplantation after the Chernobyl nuclear accident. N. Engl. J. Med. *321*: 205-212.

Brandao-Mello, C. E., Oliveira, A. R., Valverde, N. J., Farina, R. and Cordeiro, J. M. (1991).: Clinical and hematological aspects of [137]Cs: the Goiania radiation accident. Health Phys *60*: 31-39.

Brook, I. (1988).: Use of antibiotics in the management of postirradiation wound infection and sepsis. Radiat. Res. *115*: 1-25.

Brook, I. and Elliott, T. B. (1989).: Treatment of wound sepsis in irradiated mice. Int. J. Radiat. Biol. *56*: 75-82.

Brook, I., Walker, R. I. and MacVittie, T. J. (1986).: Effect of radiation dose on the recovery of aerobic and anaerobic bacteria from mice. Can. J. Microbiol. *32*: 719-722.

Browne, D. (1990).: Biomedical lessons from the Chernobyl nuclear power plant accident. J. U.S. Army Med. Dept. *PB8-90-9/10*: 25-29.

Elliott, T. B., Brook, I. and Steifel, S. M. (1990).: Quantitative study of wound infection in irradiated mice. Int. J. Radiat. Biol. *58*: 341-350.

Lennette, E. H., Balows, A., Hausler, W. J. and Shadony, H. J. (1985).: *Manual of Clinical Microbiology*. Fourth edition. American Society of Microbiology, Washington, DC.

Madonna, G. S., Ledney, G. D., Elliott, T. B., Brook, I., Ulrich, J. T., Myers, K. R., Patchen, M. L. and Walker, R. I. (1989a).: Trehalose dimycolate enhances resistance to infection in neutropenic mice. Infec. Immunity. *57*: 2495-2501.

Madonna, G. S., Ledney, G. D., Moore, M. M., Elliott, T. B. and Brook, I. (1991).: Treatment of mice with sepsis following irradiation and trauma with antibiotics and synthetic trehalose dicorynomycolate (S-TDCM). J. Trauma *31*: 316-325.

Madonna, G. S., Moore, M. M., Ledney, G. D., Elliott, T. B. and Brook, I. (1989b).: Combined therapy of septicemia with ofloxacin and/or synthetic trehalose dicorynomycolate (S-TDCM) in irradiated and wounded mice. Microecol. Therapy *19*: 135-139.

Maejima, K., Deitch, E. A. and Berg, R. D. (1984).: Bacterial translocation from the gastrointestinal tracts of rats receiving thermal injury. Infec. Immunity *43*: 6-10.

Serial Injections of MK 801 (Dizocilpine) in Neonatal Rats Reduce Behavioral Deficits Associated with X-Ray-Induced Hippocampal Granule Cell Hypoplasia

G. ANDREW MICKLEY,[1] J. LELAND FERGUSON AND THOMAS J. NEMETH

Behavioral Sciences Department, Armed Forces Radiobiology Research Institute, Bethesda, MD 20889-5145

MICKLEY, G. A., J. L. FERGUSON AND T. J. NEMETH. *Serial injections of MK 801 (Dizocilpine) in neonatal rats reduce behavioral deficits associated with X-ray-induced hippocampal granule cell hypoplasia.* PHARMACOL BIOCHEM BEHAV 43(3) 785-793, 1992.—MK 801 (NMDA antagonist) has been shown to protect newborns from hypoxia-induced brain damage. Here, we determined if (+)-5-methyl-10,11-dihydroxy-5h-dibenzo(a,d)cyclohepten-5,10-imine (MK 801) could attenuate behavioral deficits associated with early radiation-induced hypoplasia of fascia dentata granule cells. We pretreated neonatal rats (n = 20) with MK 801 (0, 0.1, or 0.2 mg/kg, IP) before each of eight fractionated, head-only doses of X-rays (13 Gy total) administered during the first 16 days postpartum. Other rats (n = 18) received the same drug treatments but were sham irradiated. At age 16 months, water-escape latencies to a submerged platform were measured in a water maze.

Irradiated rats with hippocampal damage exhibited impaired learning (longer latencies to find the platform) than did sham-irradiated subjects. Moderate doses of MK 801 (0.1 mg/kg) facilitated the learning of the water maze by irradiated subjects but did not enhance the number of their fascia dentata granule cells. Higher doses (0.2 mg/kg) of MK 801 provided no behavioral benefits. In fact, this dose significantly impaired the learning of the water maze by sham-irradiated rats and potentiated the granule cell hypoplasia observed in irradiated subjects. Thus, early MK 801 treatment produces dose-dependent behavioral protection for rats with radiation-induced hippocampal damage. Future studies may reveal the neuro-physiological and neuroanatomic substrates of this behavioral recovery.

Water maze   Hippocampus   Fascia dentata   MK 801   Dizocilpine   Behavior   Brain damage
Rats   X-rays   Ionizing radiation

X-IRRADIATION of partially shielded neonatal rat brain can cause selective hypoplasia of fascia dentata granule cells. Bayer and Peters (8) and others (43-45) utilized this technique to study the behavioral consequences of hippocampal damage. Lesions of hippocampal granule cells, whether through neonatal irradiation (68) or by colchicine treatment (66), effectively remove a major input to the hippocampus (through the perforant path from entorhinal cortex) and produce behavioral consequences similar to total hippocampalectomy (68). For example, Bayer et al. (7) described locomotor hyperactivity, reduced spontaneous alternation in a T maze, and retarded acquisition of a passive avoidance task in rats with early radiation-induced hippocampal damage. More recently, we (45) replicated and extended this work by revealing that rats with hypoplasia of the fascia dentata granule cells exhibit perseverative spontaneous turning, with few reversals, in a bowl-shaped apparatus. These data illustrate behavioral effects of early radiation exposure and suggest a role for hippocampal granule cells in working memory (54), response inhibition (2,17,33), and spatial mapping (51).

The primary mechanism producing radiation-induced hypoplasia of fascia dentata granule cells is presumed to be alteration of genetic material (27). However, recent data are consistent with the hypothesis that excitatory amino acid (EAA) neurotransmitters (e.g., glutamate) acting through NMDA receptors may also play a role in the production of hippocampal damage and/or behavioral alterations following X-irradiation. First, glutamate acts as a neurotransmitter at perforant path/granule cell synapses located at the site of radiation-induced hypoplasia (9). Second, behavioral effects of radiation-induced hippocampal damage are similar to those observed following NMDA-induced excitotoxic damage to

---

[1] Requests for reprints should be addressed to G. Andrew Mickley, Ph.D., Radiofrequency Radiation Branch, Directed Energy Division (OEDR), Armstrong Laboratory, Brooks AFB, TX 78235-5301.

hippocampal neurons (60,61) or acute antagonism of brain NMDA receptors (42,59,69,74). Third, because glia play an important role in glutamate metabolism (64) radiation-induced destruction of glia (65,67) may have the effect of potentiating EAA neurotoxicity. Fourth, ionizing radiation exposure alters glutamate dehydrogenase and produces time-dependent changes in neuronal glutamate levels (1,32,62). These alterations in EAA may be biologically important in neonates because glutaminergic systems are in flux, and therefore quite plastic, during the early postnatal period (73). For example, Erdo and Wolff (19) showed a dramatic rise in the levels of glutamate during postnatal weeks 2 and 3. Likewise, in the human hippocampus there is also a transient increase of NMDA binding sites during development (58). In fact, neonatal rat brain is significantly more sensitive to glutamate and NMDA excitotoxicity than is the adult brain (28,41). Thus, although the evidence is circumstantial, early X-ray-induced hippocampal granule cell hypoplasia, and accompanying behavioral deficits, may be mediated, in part, by alterations in EAAs acting through NMDA receptors. We tested this hypothesis further by administering an NMDA antagonist [(+)-5-methyl-10,11-dihydroxy-5h-dibenzo(a,d)cyclohepten-5, 10-imine (MK 801)] before each X-ray exposure and then recording behavioral and neuroanatomic changes in irradiated and sham-irradiated rats.

MK 801 is a phencyclidine (PCP)-like compound that displays even greater potency than PCP in binding to the PCP receptor and antagonizing the excitatory and toxic actions of NMDA (29). MK 801 can protect neurons against traumatic injury, ischemic, anoxic, or epilepsy-related brain damage (all of which are postulated to be NMDA receptor-mediated processes) (14,22,31,40,49,52,56). Here we administer MK 801 concurrently with partial-head exposures to X-rays to determine if this procedure might alter a) the radiation-induced hypoplasia of fascia dentata granule cells and/or b) the behavioral deficits associated with this neuropathology.

METHOD

Subjects

Pregnant rats [Crl: CD(SD)BR] obtained from Charles River Laboratories (Kingston, NY) and screened for evidence of disease were housed in a facility accredited by the American Association for Accreditation of Laboratory Animal Care (AAALAC). Temperature and relative humidity in the animal rooms were held at 19–21°C and 50 ± 10%, respectively, with ≥ 10 air changes/h. Full-spectrum lighting was cycled at 12-h intervals (lights on at 0600 h) with no twilight. Rats used in these experiments came from a total of 13 different litters. On the day of birth (day 1), litters were culled and up to eight males/litter were reared together. Based upon a random selection process, from 1 to 6 of these rats in each litter were actually used in the experiments reported here. All rats were weaned at the same time (on day 26 postpartum) and then individually housed in microisolator, polycarbonate cages on hardwood chip contact bedding. Rats were given ad lib Wayne Rodent Blox and acidified water (HCl, pH 2.5 to prevent the spread of *Pseudomonas*). Palatability studies indicate that animals do not prefer tapwater to acidified water and that there are no deleterious effects of this water treatment over the lifetime of the subject [for review, see (70)].

Irradiation

Subjects from each litter were randomly assigned to either the X-irradiated or the sham-irradiated (control) group. Irra-

diated rats received collimated X-rays (Phillips Industrial 300 kvp X-ray machine, Phillips, Inc., Mahwah, NJ; configured with 1.5 mm of copper filtration, with a half-value layer of 2.5 mm copper) delivered dorsally, in the coronal plane, through a narrow slot in a loose-fitting whole-body lead shield. X-rays were confined to that area of the head previously determined to contain the hippocampus. Determinations of the location of the hippocampal formation relative to external landmarks (e.g., snout, eyes, ears) were made during preliminary dissections of other neonatal rats. These external landmarks were subsequently used to set the position of the slot in the lead shield during our irradiation procedure. The measurements and anatomic landmarks we used for shield placement corresponded closely to those previously reported by Bayer and Peters (8). The slot in the shield was the opening between two movable lead strips (22.8 × 6.8 × 2 cm) suspended just above the heads of rats in the radiation exposure array. The opening extended laterally beyond the full width of each rat head and varied between 5–10 mm in the anterior/posterior plane to accommodate the growth of the head/brain over the course of the radiation treatment [see (8) for a complete explanation of this procedure]. Irradiated rats were exposed to 2.0 gray (Gy; 1 Gy = 100 rad) on postnatal days 1 and 2 (day of birth = postnatal day 1) and to 1.5 Gy on postnatal days 5, 7, 9, 12, 14, and 16 for a total partial-head-only dose of 13 Gy. Doses were determined by using Exradin 0.05 cc tissue-equivalent ion chambers with calibration traceable to the National Institute of Standards and Technology. X-rays were delivered at a rate of 0.49 Gy/min (total irradiation time = 3.0–4.0 min) at a depth of 2 mm in tissue. Sham-irradiated control rats were restrained for the same time period as irradiated rats but were not exposed to X-rays.

The entire anterior/posterior extent of the hippocampal formation was irradiated, as were brain areas dorsal and ventral to this structure [see (55) for a listing of these other brain areas]. Brain structures anterior and posterior to the slot in the lead were shielded. At the time of our postnatal radiation exposures, the rat brain contained three remaining populations of dividing (and therefore radiosensitive) cells: neuronal precursors of granule cells in the hippocampus, cerebellum, and olfactory bulbs (6,7). Two of these major neuronal precursor populations (in the cerebellum and olfactory bulbs) were covered by the radioopaque shielding. Unshielded were the mitotic (radiosensitive) granule cells of the dentate gyrus and the mature neurons in other brain structures residing in the same coronal plane as the hippocampus. This procedure produces selective hypoplasia of granule cells in the dentate gyrus (8,25) while sparing the radioresistant (13,26) mature neurons of other brain structures. The technique has been validated through a variety of neuroanatomic methods (6,25,75).

Drug Injections

Rats were randomly assigned to a drug treatment group. Within 5 min of the start of each irradiation or sham-irradiation procedure, rats were injected (IP) with either 0 (saline control), 0.1, or 0.2 mg/kg MK 801 in a volume of 0.03 ml. Therefore, each rat received eight injections during the first 16 days postpartum. Mortality resulting from the MK 801 treatments was not significantly different from that observed following saline control injections. See Table 1 for information about experimental group size.

Apparatus and Procedures

Following irradiation, rats were allowed to mature for approximately 17 months (see Table 1) before behavioral testing

TABLE 1

NUMBER, AGE, AND WEIGHT OF RATS AT THE TIME OF WATER MAZE TESTING

Radiation Treatment and Drug Administration	n	Age*	Weight†
Irradiated (saline)	8	507 ± 8	865 ± 51
Irradiated (0.1 mg/kg MK 801)	7	508 ± 7	877 ± 52
Irradiated (0.2 mg/kg MK 801)	5	512 ± 8	772 ± 38
Sham irradiated (saline)	7	502 ± 7	992 ± 70
Sham irradiated (0.1 mg/kg MK 801)	5	501 ± 5	959 ± 36
Sham irradiated (0.2 mg/kg MK 801)	6	508 ± 8	915 ± 74

*Ages are the mean days ± SEM for each group.
†Weights are mean g ± SEM for each group.

began. At this time, we recorded performance on a water maze (see below). We tested 17-month-old rats in the hopes of revealing hippocampally mediated deficits in spatial memory (20,57). Aged rats are more susceptible than young rats to drug-induced deficits in water maze performance (38). Thus, we expected radiation-induced deficits in performance of this spatial water maze task to be more prominent in old subjects. In a different time frame, other spontaneous behavior [i.e., spontaneous locomotion and rotation; see (45) for a description of these procedures] were also recorded. However, data from these other tests are not presented in this article.

Water maze. Water mazes have been used extensively to measure behavioral dysfunctions associated with hippocampal damage and NMDA receptor manipulation (42,47,59,61). In the current study, we measured water-escape latencies to a submerged platform located in a Morris-type water maze (47). The water maze was an oval stock-watering tank (manufactured by Rubbermaid, Inc., Frederick, MD) 140 × 90 × 60 cm deep. The tank was filled to 50 cm with clear water (27°C). The escape platform was a clear plastic disk (12.5 cm diameter × 1.2 cm) mounted on a clear plastic stand and submerged 2 cm below the surface of the water in the center of one of the tank's quadrants. Rats never showed evidence of detecting the platform unless they touched it. The tank rested on the floor of a 4.6 × 6.1-m room with overhead fluorescent lights and surrounded by a rich array of laboratory furnishings.

All trials lasted 30 s with 30 s between trials. Initial water acclimation consisted of two trials, the first with no platform. On the second trial, the rat was held facing the submerged platform (5 cm away) and released to climb up on it three times. Three to 4 weeks after this initial acclimation, rats were tested in the water maze. The test session consisted of eight trials. For each trial, the rat was placed in the water immediately facing the tank's wall at the middle of quadrant one or, on alternate trials, of quadrant 3. For the first and eighth trials, no platform was in the tank. For the second to the seventh trials, the platform was submerged in quadrant 4. The rat was given 30 s to locate and climb up on the platform. The rat remained on the platform for 2 s. If the rat did not find the platform in 30 s, it was guided to the goal. After the rat resided for 20 s on the platform, the subject was placed in a dry plastic holding box and given the next trial in 10 s (30 s total between trials). We recorded time spent in each quadrant, order of quadrants crossed, and latency to the platform.

Rats are natural swimmers and swim effectively when placed into the water for the first time. In these tests, no rat was in the water for more than 4 min and none shivered when removed. At the end of the session subjects were thoroughly dried with towels and a hair dry.. .

Body weights. Rats were weighed on 14 days during the

irradiation period (postnatal days 1, 2, and 5–16) and on 9 days after irradiation — but before weaning (days 17–24 and 26), as well as 2 days after weaning (days 27 and 28). Weights were also recorded at times associated with behavioral testing.

Histology

After behavioral testing, rats were anesthetized and perfused with heparinized saline followed by 10% buffered formalin. Brains were embedded in paraffin, serially sectioned (6 μm) (in the sagittal plane), and then stained with cresyl violet and luxol fast blue (37). All brains received a preliminary review to confirm radiation-induced damage to the dentate gyrus [for full documentation of this effect, see (44)]. In addition, some of the brains were analyzed in more detail (see Table 2). A single section (approximately 1.9 mm lateral to the midline) (55) was used for this analysis to (a) estimate the degree of fascia dentata injury and (b) survey the other brain areas (olfactory bulb and cerebellum) that, although shielded from irradiation, are known to contain granule cells mitotic at the time of radiation treatment. We counted the total number of granule cells that could be visualized in the single section of the dentate gyrus used in this analysis. Cell counts were accomplished under 250× total magnification by an observer blind to the experimental results. Nuclear cell counts were used to avoid the error caused by double or triple nucleoli. The size, cytoplasmic staining, and nuclear structure of granule cells usually makes them distinguishable from glial cells (4,63). However, the possibility cannot be ruled out that some of the astroglial cells may have also been counted. The impact of this possible error is reduced by the fact that the number of glial cells in the fascia dentata is extremely low (36). In addition, after neonatal irradiations similar to those described here Bayer and Altman (5) reported that the granule cell population remains significantly reduced into adulthood while the glia show an initial reduction in number followed by a complete regeneration to normal levels within 60–90 days (6). Thus, our cell counts in the fascia dentata of the 1-year-old adult rat would presumably not reflect a radiation-induced alteration in glial population. To confirm that the shielding of other brain areas was sufficient, we also counted granule cells in a 0.04 mm² area in the cerebellum and olfactory bulb. Further, we evaluated the sparing of other more mature, and therefore less radiosensitive, hippocampal structures by counting the thickness of the CA1 pyramidal cell layer that was dorsal to the dentate and directly in the path of the X radiation.

Statistical Analyses

Unless otherwise stated, data were analyzed within the framework of a two-way analysis of variance [ANOVA: radia-

TABLE 2

HISTOLOGICAL DATA DERIVED FROM ANALYSIS OF SAGITTAL SECTIONS OF RAT BRAIN

Radiation Treatment and Drug Administration	n	Anatomic Areas*			
		OB†	CB‡	DG§	CA1§
Irradiated (saline)	5	460.5	660.4	225.6	2.5
		(4.6)	(78.7)	(32.2)	(0.5)
Irradiated (0.1 mg/kg MK 801)	5	499.2	755.0	227.0	2.7
		(32.4)	(70.0)	(22.9)	(0.4)
Irradiated (0.2 mg/kg MK 801)	4	353.5	659.8	165.3#	2.7
		(96.7)	(105.0)	(25.7)	(0.5)
MEAN irradiated		442.5	694.0	219.6**	2.66
SEM irradiated		(34.2)	(45.9)	(17.8)	(0.23)
Sham irradiated (saline)	3	475.3	457.5	2153.0	3.0
		(29.2)	(159.5)	(143.0)	(0.3)
Sham irradiated (0.1 mg/kg MK 801)	4	474.0	725.0	2248.5	3.2
		(12.7)	(53.9)	(106.3)	(0.1)
Sham irradiated (0.2 mg/kg MK 801)	4	425.3	620.3	1873.8	3.7
		(48.4)	(54.2)	(291.4)	(0.8)
MEAN sham irradiated		459.8	618.3	2086.2	3.33
SEM sham irradiated		(17.05)	(38.8)	(119.7)	(0.27)

*OB, olfactory bulb; CB, cerebellum; DG, dentate gyrus of hippocampus; CA1, CA1 of hippocampus.
†Mean cell counts in 0.04 mm² area. Number in parentheses is the SEM.
‡Mean cell counts in total fascia dentata. Number in parentheses is the SEM.
§Mean pyramidal cell layer thickness (numbers of cells). Number in parentheses is the SEM.
#Significantly different from irradiated, saline-treated rats ($p < 0.05$, see text).
**DG cell counts in irradiated rats are significantly lower than those in sham-irradiated subjects ($p < 0.001$).

tion treatment (radiation/sham irradiation) × drug treatment (saline/0.1 mg/kg/0.2 mg/kg); $\alpha = 0.05$] (72). Either Newman-Keuls posthoc tests or t-tests [with the Bonferroni correction so as to reduce the probability of Type I errors, (46)] were used to specify the individual group differences. We also used t-tests to evaluate single a priori hypotheses (34).

RESULTS

MK 801, at a repeated dose of 0.1 mg/kg, produced an improvement in water maze acquisition. It did not, however, reverse the radiation-induced hypoplasia of fascia dentata granule cells.

Water Maze

During Trials 2-4 of the water maze task (early learning), there was not a significant difference between the treatment groups in their latency to arrive at the hidden platform (see Fig. 1). Thus, neither radiation-induced hippocampal damage nor early treatments with MK 801 altered the initial latencies to find the platform. However, during Trials 5-7 (late learning) several group differences appeared. During these trials, rats that had received X-ray treatments and saline control injections exhibited significantly longer latencies to arrive at the safe platform than did sham-irradiated rats with similar control injections, $t(13) = -3.67, p < 0.5$. Our low dose of MK 801 (0.1 mg/kg) protected irradiated rats from this behavioral deficit. Animals that received this drug treatment found the safe platform with latencies that were a) significantly less

than those exhibited by saline-treated irradiated rats but b) not significantly different from the latencies of sham-irradiated animals that received either saline or 0.1 mg/kg MK 801 [drug effect, $F(2, 32) = 7.508, p < 0.5$; drug × radiation treatments interaction, $F(2, 32) = 3.635, p < 0.05$; and Newman-Keuls tests, $p < 0.05$]. Conversely, the higher dose of MK 801 (0.2 mg/kg) provided no such behavioral benefit. Both irradiated and sham-irradiated rats that received this higher dose of MK 801 exhibited latencies comparable to those recorded from irradiated rats that received saline control injections as neonates. In fact, during training Trials 5-7 sham-irradiated rats that received serial doses of 0.2 mg/kg MK 801 took significantly longer to find the platform than did sham-irradiated rats that received control saline injections (Newman-Keuls, $p < 0.05$).

During Trials 1 and 8 (when no platform was present in the water maze), animals in all treatment groups spent similar amounts of time swimming in the quadrant of the maze where the safe platform was placed during trials 2-7. The total number of maze quadrants crossed during Trials 1 and 8 was also similar for our treatment groups. These data suggest that, independent of radiation or drug treatment history, animals showed similar characteristics of spatial exploration and swimming activity in the absence of a goal. We also determined the spontaneous locomotor activity (in a 1-h session) for some rats in this study ($n = 34$) [see (44) for details on this procedure]. The results from this measure were then correlated with each subject's latency to reach the hidden platform on Trials 5-7 of maze acquisition. This analysis revealed

a direct correlation between latency to find the hidden platform and locomotor activity, $r(32) = 0.38$, $p < 0.05$. This correlation suggests that hypoactivity may not be an important factor in the delayed acquisition of our water maze task.

Weight Data

Body weight at the time of maze testing did not correlate significantly with water maze learning [latency to arrive at the hidden platform, Trials 5-7) $r(36) = -0.18$]. However, as expected rat weight increased over time and this change was eventually modulated by radiation treatment history. Two repeated-measures ANOVAs [radiation treatment (radiated/sham irradiated) × drug dose (saline/0.1/0.2 mg/kg MK 801) × day] were calculated to determine weight changes during the irradiation procedure (postnatal days 1, 2, and 5-16) as well as following radiation treatments (days 17-24, 27, and 28). During postnatal days 1-16, there was a significant time effect, $F(13, 416) = 594.5$, $p < 0.5$ (suggesting growth), but neither radiation exposure nor drug treatment effects were statistically significant. Following the end of radiation treatments, body weight continued to increase over time, $F(10, 320) = 2130.24$, $p < 0.05$, and irradiated rats could eventually be differentiated from sham-irradiated subjects. A significant interaction between radiation treatment and time, $F(10, 320) = 17.27$, $p < 0.05$, was further explored by conducting two-way ANOVAs between treatment groups on particular days. When significant differences were found, t-tests [employing the Bonferroni correction, see (46)] were used to make paired comparisons. Within our measurement schedule, the first statistically significant radiation effect was observed on postnatal day 26, $F(1, 32) = 4.4$, $p < 0.05$, and persisted through the remainder of these early body weight assessments

[day 27, $F(1, 32) = 4.7$, $p < 0.05$; day 28, $F(1, 32) = 6.07$, $p < 0.05$]. Irradiated rats that received low (0.1 mg/kg) doses of MK 801 or control injections weighed significantly less than similarly dosed sham-irradiated subjects on each of these days, $t(9-13) = 1.94-2.24$, $p < 0.05$. However, a comparison between sham-irradiated rats that received 0.2 mg/kg MK 801 and the corresponding group of irradiated rats revealed no significant differences in body weight on postnatal days 24 and 26-28 ($p > 0.05$). This finding may be placed in perspective by the fact that both irradiated and sham-irradiated rats that received 0.2 mg/kg MK 801 had weights that approximated those of irradiated rats in other drug treatment conditions (i.e., received saline or 0.1 mg/kg MK 801) and were lighter than sham-irradiated rats in these groups. For example, on postnatal day 28 combined groups that received the high dose of MK 801 had significantly lower body weights than did rats that were either saline treated or 0.1 mg/kg treated and sham irradiated, $t(21) = -2.49$, $p < 0.05$.

Adult weight changes paralleled, in some ways, those observed in young rats. A comparison of rat body weights at the time of the maze test (see Table 1) revealed that radiation-induced weight reductions observed early in this experiment were also present 19 months later [two-way ANOVA, radiation effect, $F(1, 32) = 6.284$, $p < 0.05$. Further, early serial doses of MK 801 produced a consistent, but small (not statistically significant), reduction in body weight (compared to saline-injected controls) in our mature animals.

Histology

Exposure of a portion of the neonatal cerebral hemispheres to early, fractionated doses of ionizing radiation produced a selective reduction of granule cells of the hippocampal dentate
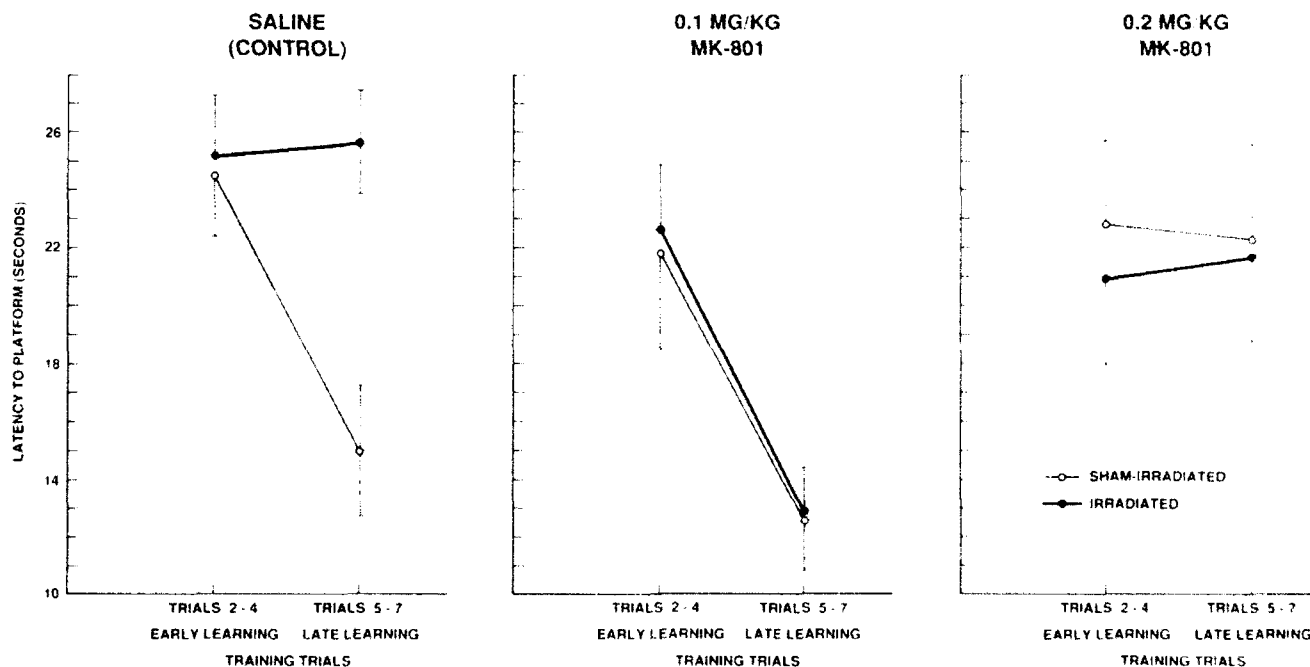

FIG. 1. Adult rat performance on a water maze task expressed as latencies (in seconds) to find a hidden platform. Data reflect mean latencies across three training trials (Trials 2-4 reflect early training; Trials 5-7 reflect late training). Radiation-induced hippocampal damage causes longer latencies to find a hidden platform late in maze learning. Repeated pretreatment of neonates with 0.1 mg/kg MK 801 (NMDA antagonist) eliminates this effect of radiation exposure. However, higher doses of MK 801 (0.2 mg/kg) retard maze learning in sham-irradiated controls. Variance indicators are SEM.

gyrus while sparing other brain areas (see Table 2). A two-way ANOVA (radiation treatment × drug treatment) revealed that exposure of the neonatal rat hippocampus to ionizing radiation produced a significant, $F(1, 24) = 308.17$, $p < 0.05$, depletion of dentate granule cells. Granule cell counts in the irradiated fascia dentata (mean = 219.6 ± 17.8) numbered approximately 11% of those observed in the hippocampus of sham-irradiated subjects (mean = 2,086.2 ± 119.7). Granule cell densities in the olfactory bulb and cerebellum were similar for subjects in both the irradiated and sham-irradiated groups. Likewise, the thickness of the pyramidal cell layer of CA1 was not altered by the radiation treatments. Using irradiation procedures similar to ours, Bayer and Peters (8) previously determined that X-irradiation destroys approximately 85% of the granule cells in the dentate gyrus of the hippocampus. As in our procedure, this technique spares a) hippocampal pyramidal cells and adjacent brain nuclei (e.g., caudate) in the path of the X-rays and b) shielded neurons anterior and posterior to the hippocampus (7,45).

A two-way ANOVA (radiation treatment × drug treatment) revealed that MK 801 treatments changed neither the CA1 pyramidal cell layer thickness nor the granule cell counts in the olfactory bulb or cerebellum. Likewise, serial injections of 0.1 mg/kg did not alter the number of fascia dentata granule cells in most treatment groups. Still, dentate granule cells were fewer in both irradiated and sham-irradiated rats that received 0.2 mg/kg MK 801. This reduction was statistically significant only in the case of irradiated rats treated with the higher dose of the drug [a priori, $t(7) = 2.11, p < 0.05$].

We calculated correlations between the anatomic data of saline-treated rats (irradiated and sham irradiated) and the results of their behavioral tests. This analysis revealed a significant relationship between the latency to find the hidden platform late in training (mean of Trials 5-7) and the number of cells in the fascia dentata, $r(6) = -0.69$, $p < 0.05$ (30). These data suggest that low granule cell numbers in the dentate gyrus predict long latencies (i.e., poor performance) late in water maze learning. There was not a corresponding statistically significant relationship between fascia dentata granule cell counts and early maze performance, $r(6) = 0.29$, $p > 0.05$. Likewise, none of the other anatomic parameters measured (e.g., cells in olfactory bulb, cerebellum, or CA1 cell layer thickness) correlated significantly with early or late maze performance.

DISCUSSION

Rats with radiation-induced hypoplasia of fascia dentata granule cells exhibited a learning deficit in the water maze. However, when irradiated neonatal rats were treated with our low dose of MK 801 (0.1 mg/kg) and then tested as adults their maze performance was not significantly different from sham-irradiated controls. These drug-induced behavioral benefits were observed despite the fact that radiogenic hippocampal damage in these animals was not significantly different from that of saline-treated irradiated rats. A higher dose of MK 801 (0.2 mg/kg) did not produce these behavioral benefits and, in fact, inhibited maze learning in control animals and potentiated hippocampal damage in irradiated subjects.

Our use of MK 801 in an attempt to antagonize radiation-induced hypoplasia of fascia dentata granule cells was not effective. Still, we observed significant *behavioral* benefits months after administration of the NMDA antagonist. This raises questions about the underlying physiological mechanisms of MK 801-induced antagonism of radiogenic learning deficits. While the current data do not speak to these points directly, our experimental paradigm has similarities to other experiments where MK 801 has been shown to modulate compensatory neural responses following sensory deprivation of the neonatal visual system. For example, blockade of NMDA receptors prevents the disconnection of deprived visual pathways and, when visual stimulation is reinstated, also prevents recovery of initially deprived afferents (16,23,35). Chronic MK 801 is effective in stimulating neuronal growth — especially in infant brain (22). Thus, NMDA receptor mechanisms are involved in the mediation of various forms of neuronal plasticity (10) including neuronal differentiation during organogenesis and the experience-dependent pruning of synaptic connections during early postnatal development (16). Other relevant studies have shown how, following transient cerebral ischemia, receptor binding on dentate granule cells can change dramatically in the absence of any cell loss (71). Perhaps MK 801's antagonism of NMDA activity modulates compensatory neuronal interconnections or receptor populations in such a way to allow maze learning in the presence of few fascia dentata granule cells (3,39).

Low doses (0.1 mg/kg) of MK 801 improved the water maze performance of irradiated rats. However, our higher dose (0.2 mg/kg) did not have this effect on irradiated rats and, in fact, inhibited maze learning in sham-irradiated control animals. Recent data suggest that NMDA receptors control neuronal plasticity in a way that is quite sensitive to the level of agonist present. For example, a high dose of NMDA induces retraction of retinal ganglion cell (RGC) neurites while low doses induce elongation of RGCs [(50; but also see (15)]. This dose-dependent modulation of neuronal growth could be an important tool of the developing nervous system.

It is difficult to fully explain the mechanisms by which our higher dose of MK 801 (0.2 mg/kg) lowered fascia dentata granule cell counts. We might point out, however, that under certain circumstances MK 801 has been shown to produce transient pathomorphological reactions in selected brain regions of the adult rat (53). Further, Duncan et al. (18) recently reported that a single 1-mg/kg (IP) dose of MK 801 causes inhibition of DNA synthesis in the neonatal brain. This inhibition may interfere with neurogenesis in the hippocampus. Thus, if NMDA antagonism is sufficiently strong functionally beneficial modulations of plastic neuronal interconnections (described above) may be replaced by significant changes in neurogenesis, gliogenesis, and the production of pathomorphological reactions.

Our observation that selective doses of MK 801 block radiation-induced learning deficits usually associated with fascia dentata granule cell hypoplasia is consistent with the hypothesis that NMDA receptors are involved in the brain's response to ionizing radiation. However, it may also be the case that some nonspecific physiological change produced by MK 801 could be playing a role in the behavioral radioprotection we report here. In particular, the hypothermia that accompanies MK 801 administration (11) has been shown to mediate some of the drug's antiischemic activity. This finding is not universal, however (24). MK 801-induced hypothermia may also play a role in its radioprotective actions since low temperature has been shown to reduce radiation-induced cell killing (21).

The changes in body weight reported here are of interest because, in many cases, they paralleled behavioral phenomenon [see also (15)]. For example, both reductions in weight and deficits in maze learning were observed in rats with fascia dentata granule cell hypoplasia; 0.1-mg/kg doses of MK 801 tended to normalize both body weights and maze acquisition

of irradiated animals; and higher drug doses (0.2 mg/kg) tended to produce weight reductions and selective impairments on water maze performance. These data might lead to the hypothesis that reduced body weights cause a lethargy or some other generalized debilitation that secondarily produces the deficits in maze learning that we report here. However, several findings do not support this notion. First, radiation-induced hippocampal damage such as that described here causes locomotor hyperactivity (44,45) and hyperresponsiveness to startle stimuli (43) rather than lethargy. Similarly, rats in all treatment groups in this study crossed a similar number of maze quadrants – thus suggesting similar swimming capabilities. Further, body weight did not correlate well with performance on the maze task. These data suggest that reduced body weight is neither a good indicator of lethargy nor an optimal predictor of water maze performance.

The long-term behavioral effects of repeated MK 801 administration in neonates may be compared and contrasted with those described following acute dosing of the NMDA antagonist in adult rats. A variety of studies indicate that MK 801 can produce acute a) sensorimotor disturbances (74), b) dose-dependent malaise (48), and c) impairment in the acquisition of hippocampal-dependent spatial learning tasks (12, 42,59) in adult rats. On the other hand, serial doses (0.2 mg/kg) of MK 801 in young rats (postnatal days 9–15) did not alter subsequent (day 36) motor activity, startle responsiveness, or water maze performance (42). These data are consistent with our findings in that we observed no long-term effects of serial neonatal doses of 0.1 mg/kg MK 801 on the water maze acquisition of our sham-irradiated control animals. However, neonatal doses of 0.2 mg/kg MK 801 produced marked deficits in maze learning that could be observed in adulthood. Because we did not test our animals as neonates/

young adults, and McLamb et al. (42) tested only young animals, we do not know the extent to which the phenomenon we observed is age dependent. Our earlier and more frequent dosing of MK 801 may also be factors in producing the late behavioral deficits we observed in mature rats. The importance of appropriate dose selection in both the acute and repeated administration of MK 801 is illustrated by the fact that a 0.2-mg/kg (IP) dose of MK 801 can produce an acute "gross intoxication" (74) while 0.1 mg/kg evoked no such effect.

Our results reflect long-term and/or long-latency behavioral changes following early, repeated exposure to an NMDA antagonist. They also suggest a role for NMDA receptors in behavioral dysfunctions associated with X-ray-induced hypoplasia of hippocampal granule cells. Future studies will explore neuroanatomic and neuropharmacological correlates of the behavioral phenomena reported here.

REFERENCES

1. Abu El Failat, R. R.; Moore, J. S.; Davies, J. V. The radiation inactivation of glutamate dehydrogenase. Radiat. Res. 93:62–70; 1983.
2. Altman, J.; Brunner, R. L.; Bayer, S. A. The hippocampus and behavioral maturation. Behav. Biol. 8:557–596; 1973.
3. Bailly, Y.; Rabacchi, S. A.; Delhaye-Bouchaud, N.; Mariani, J. NMDA receptor antagonist blocks synapse elimination during cerebellar development. Soc. Neurosci. Abstr. 17:1288; 1991.
4. Banks, W. J. Histology and comparative organology: A text atlas. Baltimore, MD: Williams and Wilkins; 1974.
5. Bayer, S. A.; Altman, J. Hippocampal development in the rat: Cytogenesis and morphogenesis examined with autoradiography and low-level x-irradiation. J. Comp. Neurol. 158:55–80; 1974.
6. Bayer, S. A.; Altman, J. Radiation-induced interference with postnatal hippocampal cytogenesis in rats and its long-term effects on the acquisition of neurons and glia. J. Comp. Neurol. 163:1–20; 1975.
7. Bayer, S. A.; Brunner, R. L.; Hine, R.; Altman, J. Behavioural effects of interference with the postnatal acquisition of hippocampal granule cells. Nature New Biol. 242:222–224; 1973.
8. Bayer, S. A.; Peters, P. J. A method for X-irradiating selected brain regions in infant rats. Brain Res. Bull. 2:153–156; 1977.
9. Bliss, T. V. P.; Douglas, R. M.; Errington, M. L.; Lynch, M. A. Correlation between long-term potentiation and release of endogenous amino acids from dentate gyrus of anaesthetized rats. J. Physiol. 377:391–408; 1986.
10. Brewer, G. J.; Cotman, C. W. NMDA receptor regulation of neuronal morphology in cultured hippocampal neurons. Neurosci. Lett. 99:268–273; 1989.
11. Busto, R.; Dietrich, W. D.; Globus, M. Y.; Valdes, I.; Scheinberg, P.; Ginsberg, M. D. Small differences in intraischemic brain

temperature critically determine the extent of ischemic neuronal injury. J. Cereb. Blood Flow Metab. 7:729–738; 1987.
12. Butelman, E. R. A novel NMDA antagonist, MK-801, impairs performance in a hippocampal-dependent spatial learning task. Pharmacol. Biochem. Behav. 34:13–16; 1989.
13. Cassarett, G. W. Radiation histopathology, vol. II. Boca Raton, FL: CRC Press; 1980.
14. Church, J.; Zeman, S.; Lodge, D. The neuroprotective action of ketamine and MK-801 after transient cerebral ischemia in rats. Anesthesiology 69:702–709; 1988.
15. Claiborne, B. J.; Felthauser, A. M. Effects of the NMDA antagonist MK-801 on behavior, body weight and dentate granule cell morphology in developing rat pups. Soc. Neurosci. Abstr. 16:845; 1990.
16. Collingridge, G. L.; Singer, W. Excitatory amino acid receptors and synaptic plasticity. Trends Pharmacol. Sci. 11:290–296; 1990.
17. Douglas, R. J. The hippocampus and behavior. Psychol. Bull. 67:416–442; 1967.
18. Duncan, C. P.; Seidler, F. J.; Slotkin, T. A. Effects of MK-801 on DNA synthesis in neonatal rat brain regions under normoxic and hypoxic conditions. Dev. Brain Res. 58:67–71; 1991.
19. Erdo, S. L.; Wolff, J. R. A comparison of the postnatal changes in aspartate and glutamate levels in cerebral cortex of the rat. Neurosci. Res. 4:51–56; 1989.
20. Gallagher, M.; Pelleymounter, M. A. Spatial learning deficits in old rats: A model for memory decline in the aged. Neurobiol. Aging 9:549–556; 1988.
21. Giambarresi, L.; Jacobs, A. J. Radioprotectants. In: Conklin, J. J.; Walker R. I., eds. Military radiobiology. Orlando, FL: Academic Press; 1987:265–301.
22. Gomez-Pinilla, F.; Tram, H.; Cotman, C. W.; Nieto-Sampedro,

M. Neuroprotective effect of MK-801 and U-50488H after contusive spinal cord injury. Exp. Neurol. 104:118-124; 1989.

23. Gu, Q.; Bear, M. F.; Singer, W. Blockade of NMDA-receptors prevents ocularity changes in kitten visual cortex after reversed monocular deprivation. Dev. Brain Res. 47:281-288; 1989.

24. Hattori, H.; Wasterlain, C. G. Hypothermia does not explain MK-801 neuroprotection in a rat model of neonatal hypoxic-ischemic encephalopathy. Neurology 41:330; 1991.

25. Hicks, S. P. Radiation as an experimental tool on mammalian developmental neurology. Physiol. Rev. 38:337-356; 1958.

26. Hicks, S. P.; D'Amato, C. J. Effects of ionizing radiation on mammalian development. In: Woollam, D. H. M., ed. Advances in teratology. London, UK: Logos Press; 1966:195-250.

27. Holahan, E. V. Cellular radiation biology. In: Conklin, J. J.; Walker, R. I., eds. Military radiobiology. Orlando, FL: Academic Press; 1987:87-110.

28. Ikonomidou, C.; Price, M. T.; Mosinger, J. L.; Frierdich, G.; Labruyere, J.; Salles, K. S.; Olney, J. W. Hypobaric-ischemic conditions produce glutamate-like cytopathology in infant rat brain. J. Neurosci. 9:1693-1700; 1989.

29. Iversen, L. L.; Woodruff, G. N.; Kemp, J. A.; Foster, A. C.; Gill, R.; Wong, E. H. F. Noncompetitive glutamate antagonists: Pharmacology and neuroprotective effects of the NMDA antagonist MK-801. In: Barnard, E. A.; Costa, E., eds. Allosteric modulation of amino acid receptors: Therapeutic implications. New York: Raven Press; 1989:347-356.

30. Johnson, R. Elementary statistics. Boston, MA: Duxbury Press; 1984:89-95, 532.

31. Kass, I. S.; Chambers, G.; Cottrell, J. E. The N-methyl-D-aspartate antagonists aminophosphonovaleric acid and MK-801 reduce anoxic damage to dentate granule and CA1 pyramidal cells in the rat hippocampal slice. Exp. Neurol. 103:116-122; 1989.

32. Kempner, E. S.; Miller, J. H. Radiation inactivation of glutamate dehydrogenase hexamer: Lack of energy transfer between subunits. Science 222:586-589; 1983.

33. Kimble, D. P. Hippocampus and internal inhibition. Psychol. Bull. 70:285-295; 1968.

34. Kirk, R. E. Experimental design: Procedures for behavioral sciences. Belmont, CA: Brooks/Cole; 1982.

35. Kleinschmidt, A.; Bear, M. F.; Singer, W. Blockade of "NMDA" receptors disrupts experience-dependent plasticity of kitten striate cortex. Science 238:355-358; 1987.

36. Laatsch, R. H.; Cowan, W. M. Electron microscopic studies of the dentate gyrus of the rat. I. Normal structure with special reference to synaptic organization. J. Comp. Neurol. 128:359-395; 1966.

37. LaBossiere, E. Histological processing for the neural sciences. Springfield, IL: Charles C. Thomas, 1976.

38. Linder, M. D.; Schallert, T. Aging and atropine effects on spatial navigation in the Morris water task. Behav. Neurosci. 102:621-634; 1988.

39. Manallack, D. T.; Lodge, D.; Beart, P. M. Subchronic administration of MK-801 in the rat decreases cortical binding of [^{3}H]D-AP5, suggesting down-regulation of the cortical N-methyl-D-aspartate receptors. Neuroscience 30:87-94; 1989.

40. McDonald, J. W.; Silverstein, F. S.; Cardona, D.; Hudson, C.; Chen, R.; Johnston, M. V. Systemic administration of MK-801 protects against N-methyl-D-aspartate- and quisqualate-mediated neurotoxicity in perinatal rats. Neuroscience 36:589-599; 1990.

41. McDonald, J. W.; Silverstein, F. S.; Johnston, M. V. Neurotoxicity of N-methyl-D-aspartate is markedly enhanced in developing rat central nervous system. Brain Res. 459:200-203; 1988.

42. McLamb, R. L.; Williams, L. R.; Nanry, K. P.; Wilson, W. A.; Tilson, H. A. MK-801 impedes the acquisition of a spatial memory task in rats. Pharmacol. Biochem. Behav. 37:41-45; 1990.

43. Mickley, G. A.; Ferguson, J. L. Enhanced acoustic startle responding in rats with radiation-induced hippocampal granule cell hypoplasia. Exp. Brain Res. 75:28-34; 1989.

44. Mickley, G. A.; Ferguson, J. L.; Mulvihill, M. A.; Nemeth, T. J. Progressive behavioral changes during the maturation of rats with early radiation-induced hypoplasia of fascia dentata granule cells. Neurotoxicol. Teratol. 11:385-393; 1989.

45. Mickley, G. A.; Ferguson, J. L.; Nemeth, T. J.; Mulvihill, M. A.; Alderks, C. E. Spontaneous perseverative turning in rats with radiation-induced hippocampal damage. Behav. Neurosci. 103:722-730; 1989.

46. Miller, G. Simultaneous statistical inference. 2nd ed. Berlin: Springer; 1981:6-8.

47. Morris, R. G. M.; Garrud, P.; Rawlins, J. N. P.; O'Keefe, J. Place navigation impaired in rats with hippocampal lesions. Nature 297:681-683; 1982.

48. Myhal, N.; Fleming, A. S. MK-801 effects on a learned food preference depends on dosage: Is it disruption of learning or a conditioned aversion? Psychobiology 18:428-434; 1990.

49. Novelli, A.; Reilly, J. A.; Lysko, P. G.; Henneberry, R. C. Glutamate becomes neurotoxic via the N-methyl-D-aspartate receptor when intracellular energy levels are reduced. Brain Res. 451:205-212; 1988.

50. Offermann, J.; Uchida, K.; Lipton, S. A. High dose NMDA induces retraction and low dose NMDA induces elongation of rat retinal ganglion cell (RGC) neurites. Soc. Neurosci. Abstr. 17:927; 1991.

51. O'Keefe, J.; Nadel, L. The hippocampus as a cognitive map. Oxford, UK: Oxford University Press; 1978.

52. Olney, J. W.; Ikonomidou, C.; Mosinger, J. L.; Frierdich, G. MK-801 prevents hypobaric-ischemic neuronal degeneration in infant rat brain. J. Neurosci. 9:1701-1704; 1989.

53. Olney, J. W.; Labruyere, J.; Price, M. T. Pathological changes induced in cerebrocortical neurons by phencyclidine and related drugs. Science 244:1360-1362; 1989.

54. Olton, D. S. Memory functions and the hippocampus. In: Seifert, W., ed. Neurobiology of the hippocampus. London, UK: Academic Press; 1983:335-373.

55. Paxinos, G.; Watson, C. The rat brain in stereotaxic coordinates. Sidney, Australia: Academic Press; 1982.

56. Peterson, S. L.; Boehnke, L. E. Anticonvulsant effects of MK-801 and glycine on hippocampal afterdischarge. Exp. Neurol. 104:113-117; 1989.

57. Rapp, P. R.; Rosenberg, R. A.; Gallagher, M. An evaluation of spatial information processing in aged rats. Behav. Neurosci. 101:3-12; 1987.

58. Represa, A.; Tremblay, E.; Ben-Ari, Y. Transient increase of NMDA-binding sites in human hippocampus during development. Neurosci. Lett. 99:61-66; 1989.

59. Robinson, G. S.; Crooks, G. B.; Shinkman, P. G.; Gallagher, M. Behavioral effects of MK-801 mimic deficits associated with hippocampal damage. Psychobiology 17:156-164; 1989.

60. Rogers, B. C.; Mundy, W. R.; Pediaditakis, P.; Tilson, H. A. The neurobehavioral consequences of N-methyl-D-aspartate (NMDA) administration in rats. Toxicologist 8:78; 1989.

61. Rogers, B. C.; Tilson, H. A. MK-301 prevents cognitive and behavioral deficits produced by NMDA receptor overstimulation in the rat hippocampus. Toxicol. Appl. Pharmacol. 99:445-453; 1989.

62. Rozanov, V. A.; Karpovich, G. A. Early changes in GABA and glutamate levels and aminotransferase activity in parts of the rat brain following whole-body gamma irradiation at an absolutely lethal dose. Radiobiologia 25:384-388; 1985.

63. Seress, L.; Pokorny, J. Structure of the granular layer of the rat dentate gyrus. A light microscopic and Golgi study. J. Anat. 133:188-195; 1981.

64. Simantov, R. Glutamate neurotoxicity in culture depends on the presence of glutamine: Implications for the role of glial cells in normal and pathological brain development. J. Neurochem. 52:1694-1699; 1989.

65. Switzer, R. C.; Bogo, V.; Mickley, G. A. High energy electron and proton irradiation of the rat brain induces degeneration detectable with the cupric silver stain. Soc. Neurosci. Abstr. 17:1460; 1991.

66. Tilson, H. A.; Rogers, B. C.; Grimes, L.; Harry, G. J.; Peterson, N. J.; Hong, J. S.; Dyer, R. S. Time-dependent neurobiological effects of colchicine administered directly into the hippocampus of rats. Brain Res. 408:163-172; 1987.

67. Van Cleave, C. D. Irradiation and the nervous system. New York: Rowman and Littlefield; 1983:210.

68. Wallace, R. B.; Kaplan, R. F.; Werboff, J. Behavioral correlates of focal hippocampal X-irradiation in rats. Exp. Brain Res. 24: 343–349; 1976.
69. Ward, L.; Mason, S. E.; Abraham, W. C. Effects of the NMDA antagonists CPP and MK-801 on radial arm maze performance in rats. Pharmacol. Biochem. Behav. 35:785–790; 1990.
70. Weisbroth, S. H. Bacterial and mycotic diseases. In: Baker, H. J.; Lindsey, R.; Weisbroth, S. H., eds. The laboratory rat. vol. 1. Biology and diseases. New York: Academic Press; 1979:206–208.
71. Westerberg, E.; Monaghan, D. T.; Kalimo, H.; Cotman, C. W.; Wieloch, T. W. Dynamic changes of excitatory amino acid receptors in the rat hippocampus following transient cerebral ischemia. J. Neurosci. 9:798–805; 1989.

72. Winer, B. J. Statistical principles in experimental design. 2nd ed. New York: McGraw-Hill; 1971.
73. Wong, P. T.-H.; McGeer, E. G. Postnatal changes of GABAergic and glutamatergic parameters. Dev. Brain Res. 1:519–529; 1981.
74. Wozniak, D. F.; Olney, J. W.; Kettinger, L.; Price, M.; Miller, J. P. Behavioral effects of MK-801 in the rat. Psychopharmacology (Berl.) 101:47–56; 1990.
75. Zimmer, J.; Sunde, N.; Sorensen, T. Reorganization and restoration of central nervous connections after injury: A lesion and transplant study of the rat hippocampus. In: Will, B. E.; Schmitt, P.; Dalrymple-Alford, J. C., eds. Brain plasticity, learning, and memory. London, UK: Plenum; 1985:505–518.

Anti-Cytokine Antibodies Reveal the Interdependence of Pro-inflammatory Cytokines in Protection from Lethal Irradiation

R. Neta and J.J. Oppenheim

*Department of Experimental Hematology, Armed Forces Radiobiology Research
Institute, Bethesda, MD 20814 and Laboratory of Molecular Immunoregulation
Biologic Response Modifiers Program, National Cancer Institute
Frederick, MD 21701, USA*

Ionizing radiation is particularly damaging to lymphoid and hematopoietic tissues, leading to anemia and decreased resistance to opportunistic infections, often resulting in death (1). Administration prior to irradiation of immunostimulatory/inflammatory agents that enhance host's defenses was shown several decades ago also to enhance survival (2,3). It is now known that virtually all of the pathophysiological effects elicited by such adjuvants are mediated by cytokines, hormone-like polypeptides that transmit signals from one cell to another (4,5). These include pluripotent inflammatory cytokines: IL 1, TNF, LIF, and IL 6, hematopoietic growth factors (CSF's), interferons, as well as the immunosuppressive TGFβ. The cytokines IL 1 and TNF have emerged as particularly important mediators of host defenses. Thus, our earlier findings that these two cytokines can confer radioprotection (6,7) is consistent with their role in protecting the host from damaging environmental agents.

Recently, IL 1 and TNF were shown to be produced by cells following exposure to ionizing radiation (8,9). These findings suggested that even endogenously produced cytokines may contribute to recovery from ionizing radiation. This hypothesis was examined using monoclonal antibodies to IL 1 receptor (IL 1R), to TNF, and to IL 6. These antibodies also enabled us to evaluate the contribution of IL 1 and TNF to LPS-induced radioprotection, and the relative contribution and relationship of IL 1, TNF, and IL 6 to one another in radioprotection.

Materials and Methods

Mice. CD2F1 male mice were purchased from the Animal Genetics and Production Branch, National Cancer Institute, NIH (Frederick, MD). Mice were quarantined on

arrival and screened for evidence of disease before being released from quarantine. They were maintained in an AAALAC-accredited facility in plastic Micro-isolator cages on hardwood chip contact bedding and given commercial rodent chow and acidified (HCl to a pH of 2.5) tap water <u>ad libitum</u>. Animal holding rooms were maintained at 70° ± 2° F with 50% ± 10% relative humidity using at least 10 air changes per hr of 100% conditioned fresh air. The mice were on a 12-hr light-dark full-spectrum lighting cycle with no twilight. Mice were 8-12 weeks of age when used. All cage cleaning, handling, and injections were carried out in a laminar flow clean air unit.

    <u>Reagents</u>. Protein-free LPS was prepared from E. coli K235 by phenol-water extraction. Human recombinant IL 1α and antibody to IL 1R (35F5), a rat anti-mouse monoclonal IgG1, were a generous gift from Drs. Peter Lomedico and Richard Chizzoneti of Hoffmann-La Roche (Nutley, NJ). TNF was obtained from Biogen (Cambridge, MA) and anti-TNF antibody (TN3.19.12), as well as control antibodies (all prepared in hamsters) were generously provided by Dr. Robert Schreiber (Washington University, St. Louis, MO). Control rat IgG was purchased from Sigma Chemical Co. (St. Louis, MO). Human IL 6 was a generous gift from Sandoz Pharma (Basel, Switzerland). Rat MAb to mouse rIL 6 (MP5 20F3) was prepared by Dr. Abrams (DNAX, Palo Alto, CA) using semi-purified Cos-7 mouse IL 6 as an immunogen. The isotype control, rat MAb to β-galactosidase (GL113) was used. TGFβ was kindly provided by Dr. Palladino (Genentech, S. San Francisco, CA). The antibody and the recombinant cytokines were diluted in pyrogen-free saline on the day of intraperitoneal injection.

    <u>Irradiation</u>. Mice were placed in Plexiglass containers and were given whole-body irradiation at 40 cGy/min by bilaterally positioned ^{60}Co elements. The radiation field was uniform within ±2%. The number of surviving mice was recorded daily for 30 days.

Results

    <u>The interaction of IL 1 and TNF in radioprotection.</u> IL 1 and TNF were shown by others to induce each other production (10-12). It was therefore of interest to examine whether IL 1-induced TNF and TNF-induced IL 1 contribute to radioprotection. Indeed, the use of antibody to IL 1R in TNF treated mice and antibody to TNF in IL 1-treated mice resulted in reduced radioprotection. This observation suggested that both cytokines were necessary for radioprotective response.

The contribution of IL 6 to IL 1 and TNF-induced radioprotection.   To assess the role of IL 6 in mediating the recuperative effects of IL 1 and TNF, mice were given anti-IL 6 antibody 6 to 20 hours prior to administration of IL 1 (100 ng) or TNF (5 μg).   The results indicate that anti-IL 6 antibody can completely block both IL 1- and TNF-enhanced survival from lethal irradiation, thus indicating that all three cytokines, IL 1, TNF and IL 6 are required to achieve radioprotection.

The contribution of IL 1, TNF and IL 6 to innate radioresistance.   Irradiation results in induction of IL 1 and TNF, documented by IL 1 activity released by irradiated macrophages (13), IL 1 detection in circulation of uv-irradiated rabbits (14) and IL 1 and TNF gene induction in x-irradiated cells (8,9).   The administration of each of these antibodies: anti-IL 1R antibody, anti-TNF antibody and anti-IL 6 antibody to mice receiving LD 40/30 doses of radiation (825 cGy) resulted in significantly decreased survival indicating that each of these cytokines, IL 1, TNF and IL 6 contribute to innate resistance to radiation.

The contribution of IL 1 and TNF to radioprotection with LPS.   Mice were pretreated with 200 μg of anti-IL 1R antibody or anti-TNF antibody, followed by treatment with 1 μg of LPS. Such pretreatment resulted in significantly reduced survival of LPS-pretreated and 950 cGy irradiated mice. The radioprotection with LPS was blocked entirely following combined pretreatment with the two antibodies.   These results demonstrate that IL 1 and TNF are essential for LPS-induced radioprotection.

Cytokines as sensitizers to radiation lethality. Previous studies using IFN or IL 6, each given alone before irradiation, sensitized mice and reduced their resistance to radiation lethality (15,16).   In the present studies, pretreatment with anti-IL 1R and anti-TNF antibody before LPS treatment revealed LPS to have a radiosensitizing effect in that mice receiving LPS together with antibody showed a significantly reduced minimal survival time (from 10.6 to 8.3 days). Similarly, reduction in survival was observed in mice receiving TGFβ either before or after irradiation (17).

Discussion

In vivo administration of the immunostimulatory/ inflammatory LPS results in the release of multiple cytokines, some of which, in turn, induce a cascade of additional cytokines, all of which may up- or down-

regulate the activity of the initiating agent. Thus our finding that administration of the antibody to both IL 1R and TNF completely blocks LPS induced radioprotection suggests that the two cytokines are critical for radioprotection. Although administration of IL 1 and TNF each results in significant radioprotection (6,7), their combined administration results in an additive or even synergistic radioprotective effect (7). Such a complementary radioprotective effect supports the view that the two cytokines employ distinct radioprotective pathways. On the other hand, anti-IL 1R antibody, given to mice before TNF administration, reduced the proportion of TNF- as well as IL 1-radioprotected mice, and similarly anti-TNF antibody reduced IL 1- as well as TNF-induced radioprotection (17). These results suggest that not only do IL 1 and TNF induce one another (10-12), but their subsequent interaction appears necessary to achieve optimal radioprotection.

IL 1 was also found to synergize with IL 6, GM-CSF and G-CSF in conferring radioprotection (7,16). However, since IL 1 was shown to induce the production of all three of the above cytokines (16,18-20), this synergy could be demonstrated only at suboptimal radioprotective doses of IL 1. The inability of the hematopoietic growth factors by themselves to protect against lethal doses of radiation (21), suggests that in addition to the stimulation of hematopoietic progenitor cells, other pathways and activities are required to achieve radioprotection. The unique capacity of IL 1 and TNF to stimulate production of some oxygen radical scavengers may be responsible for this difference. Both of these cytokines stimulate production of acute phase proteins with scavenging activities: ceruloplasmin and metallothionein (22,23), and a mitochondrial enzyme, MnSOD (24,25).

IL 6 not only fails to induce IL 1 or TNF, but actually has been reported to suppress their production (26,27). Thus, as we have previously observed, administration of IL 6 alone prior to irradiation, actually reduces survival from lethal irradiation (16). Despite this, injection of anti-IL 6 antibody also results in increased mortality of irradiated, normal mice as well as of irradiated TNF- or IL 1-treated mice (28). These observations suggest that IL 6 participates in both innate as well as IL 1- and TNF-induced resistance to radiation lethality. The failure of IL 6 by itself to improve radiation survival indicates that the protective activity of IL 6 only becomes manifest in the course of interaction with other cytokines. This hypothesis is supported by our earlier report that IL 6 given together

with suboptimal doses of IL 1, resulted in synergistically enhanced survival from lethal irradiation (16). Since radiation itself induces the production of endogenous IL 1 (9,13,14) and TNF (8), their presence would be expected to result in endogenous production of IL 6. Consequently, the interaction of all three cytokines, i.e., IL 1, TNF, and IL 6, would contribute to innate resistance of normal mice to radiation lethality.

As demonstrated by us and by others, some cytokines (known to be induced with LPS), actually down-regulate resistance to radiation (15-17). TGFβ, given either before or after irradiation, sensitizes mice to radiation lethality. This effect may be explained by several recognized activities of TGFβ. TGFβ down regulates IL 1R expression on bone marrow cells and lymphocytes (29), impairs IL 1 and TNF synthesis (30), and inhibits the proliferation of early hematopoietic progenitor cells (31) all of which can contribute to enhanced mortality. On the other hand, co-injection of TGFβ and IL 1 results in radioprotection (17) suggesting that the sensitizing properties of TGFβ can be overcome by the presence of pharmacological doses of IL 1. This may be due to slower kinetics of down regulation of hematopoiesis, or to the presence of saturating levels of IL 1 capable of compensating for the effects of TGFβ.

Other cytokines which also caused enhanced susceptibility to radiation include IFNα and β (15), and EGF (32). Cells pretreated with interferon α/β prior to exposure to ionizing radiation show reduced survival. Exposure of human squamous carcinoma cell lines to EGF before or after irradiation reduced plating efficency. It is not possible at this time to explain the greater radiation sensitivity of cells treated with IFNα or β. No experimental data has been presented to confirm that anti-proliferative properties of these cytokines may be the basis for the sensitizing effect.

Among the genes induced by irradiation (see review 33) those for cytokines are expressed within hours after irradiation. For example, TNFα mRNA transcripts and protein were detected in human tumor cell lines, sarcoma and myeloid leukemia cells, as well as in normal blood monocytes (8,33), but not in fibroblasts. Induction of IL 1 by ionizing radiation was first demonstrated by enhanced IL 1 bioactivity derived from irradiated macrophages (13), in sera of UV irradiated rabbits (14), and most recently at the transcriptional level in irradiated syrian hamster embryo cells (9). Enhanced expression of PDGF and bFGF transcripts has been detected in irradiated endothelial cells (34). Different cells

exhibited varied patterns of gene expression in response to ionizing radiation.

Treatment of different cell types with the same cytokire may actually lead to divergent results as shown for TNF (8,35). These opposing effects of TNF on different cell types may depend on inducibility in cells by IL 1 and TNF of Mn-SOD, a mitochondrial enzyme that catalyzes the conversion of the superoxide anion to hydrogen peroxide. Thus, the reported reduced ability of tumor cell lines to respond with Mn-SOD induction may account for their greater than normal susceptibility to the lytic effects of TNF and also for their enhanced susceptibility to radiation. In contrast, Mn-SOD induction by TNF may contribute to radioprotection, probably by reducing the levels of radiation induced oxygen intermediates.

It has been suggested that cytokines, such as bFGF can counteract the effects of lethal radiation by promoting repair processes. bFGF was shown to serve as an inducer of potential lethal radiation damage (PLRD) repair of bovine aortic endothelial cells (BAEC),(36). BAEC following radiation exposure when cultured in the presence or absence of bFGF differed in their clonogenic capacity. Whereas the slopes of the survival curves (determined by the inherent radiosensitivity of a given cell) did not differ significantly, complete elimination of the threshold shoulder in the bFGF-free culture was seen.

These findings suggest that autocrine/paracrine regulated restorative loops exist in cells and that cytokines may play an important role in initiating and promoting such restoration. Although the signal transduction pathways and the biochemical pathways leading to PLRD repair in different cells remain to be defined, it is likely that activation of genes for cytokines serves to reduce the damage due to radiation ini .t. Consequently, radioprotective as well as therapeutic effects of supplementary pharmacological doses of cytokines may act by amplification of pre-existing, radiation-induced endogenous cytokine-receptor loops that induce reparative processes.

Guide for the Care and Use of Laboratory Animals, prepared by the Institute of Laboratory Animal Resources, National Research Council.

References

1.   Bond, V.P., Fliedner, T.M. and Archambeau, J.O. Mammalian Radiation Lethality, Academic Press, New York, 1965.
2.   Ainsworth, E.J. and Chase, H.B. Proc. Soc. Exp. Biol. Med. 102: 483, 1959.
3.   Smith, W.W., Alderman, I.M. and Gillespie, R.I. Am. J. Physiol. 191: 124, 1957.
4.   Vogel, S.N. and Hogan, M.M. In: Immunophysiology, Role of Cells and Cytokines in Immunity and Inflammation (Eds. J.J. Oppenheim and E.N. Shevach), Oxford University Press, 1990, p. 238.
5.   Durum, S., Oppenheim, J.J. and Neta, R. In: Immunophysiology, Role of Cells and Cytokines in Immunity and Inflammation (Eds. J.J. Oppenheim and E. Shevach), Oxford University Press, 1990, p. 210.
6.   Neta, R., Douches, S.D. and Oppenheim, J.J. J. Immunol. 136: 2483, 1986.
7.   Neta, R., Oppenheim, J.J. and Douches, S.D. J. Immunol. 140: 108-111, 1988.
8.   Hallahan, D.E., Spriggs, D.R., Beckett, M.A., Kufe, D.W. and Weichselbaum, R.R. Proc. Natl. Acad. Sci. USA 86: 10104, 1989.
9.   Woloschak, G.E., Chiang-Liu, C.-M., Jones, P.S. and Jones, C.A. Cancer Res. 50: 339, 1990.
10. Bachwich, P.R., Chensue, S.W., Larrick, J.W. and Kunkel, S.L. Biochem. Biophys. Res. Commun. 136: 94, 1986.
11. Phillip, R. and Epstein, L.B. Nature 323: 86, 1986.
12. Dinarello, C.A. et al. J. Exp. Med. 163: 1433, 1986.
13. Geiger, B., Galily, R. and Gery, I. Cell. Immunol. 7: 177, 1973.
14. Ansel, J.C., Luger, T.A. and Green, I. J. Invest. Dermatol. 89: 32, 1987.
15. Gould, M.N., Kakria, R.C., Borden, E.C. and Olsen, S. J. Interf. Res. 4: 123-128, 1983.
16. Neta, R., Vogel, S.N., Sipe, J.D., Wong, G.G. and Nordan, R. P. Lymphokine Res. 7: 403, 1988.
17. Neta, R., Oppenheim, J.J., Schreiber, R.D., Chizzonite, R., Ledney, G.D. and MacVittie, T.J. J. Exp. Med. 173: 1177-1182, 1991.
18. Vogel, S.N., Douches, S.D., Kaufman, E.N. and Neta, R. J. Immunol. 138: 2143, 1987.
19. Zucali, J.R., Dinarello, C.A., Oblon, D.J., et al.

J. Clin. Invest. 77: 1857, 1986.

20. Bagby, G.C., Dinarello, C.A., Wallace, P., Wagner, C., Hefeneider, S. and McCall, E. J. Clin. Invest. 78: 1316, 1986.

21. Neta, R., Vogel, S.N., Oppenheim, J.J. and Douches, S.D. Lymphokine Res., 5: S105, 1986.

22. Neta, R. et al. In: Progress in Immunology, (Eds. B. Cinader and R.G. Miller), Academic Press, vol.6, 1986, p.900.

23. Karin, M., Imbra, R.J., Heguy, A. and Wong, G. Mol. Cell. Biol. 5: 2866, 1985.

24. Wong, G.H.W. and Goeddel, D.V. Science 242: 941, 1988.

25. Masuda, A., Longo, D., Kobayashi, Y. et al. FASEB J. 1: 3087, 1988.

26. Aderka, D., J. Le, and Vilcek, J. J. Immunol. 143: 3517. 1989.

27. Schindler, R., Mancilla, J., Endres, S., Ghorbani, R., Clark, S.C., and Dinarello, C.A. Blood 75:40, 1990.

28. Neta R., Perlstein, R., Vogel, S.N., Ledney, G.D., and Abrams, J. J. Exp. Med. 175, 689, 1992.

29. Dubois, C.M., Ruscetti, F.W., Palaszynski, E.W., Falk, L.A., Oppenheim, J.J. and Keller, J.R. J. Exp. Med. 172: 737, 1990.

30. Keller, J.R., Mantel, C. et al. J. Exp. Med. 168: 737, 1988.

31. Chantry, D., Turner, M., Abney, E. and Feldmann, M. J. Immunol. 142: 4295, 1989.

32. Kwok, T.T. and Sutherland, R.M. J. Nat. Canc. Inst. 81: 1020-1024, 1989.

33. Weichselbaum, R.R., Hallahan, D.E., Sukhatme, V., Dritschilo, A., Sherman, M.L. and Kufe, D.W. J. Natl. Cancer. Inst. 83: 480-484, 1991.

34. Witte, L., Fuks, Z. Haimovitz-Friedman, A., Vlodavsky, I., Goodman, A. and Eldor, A. Cancer Res. 49: 5066-5072, 1989.

35. Wong, G.H.W., McHugh, T., Weber, R. and Goeddel, D.V. Proc. Natl. Acad. Sci. USA 88: 4372-4376, 1991.

36. Haimovitz-Friedman, A., Vlodavsky, I., Chaudhuri, A., Witte, L. and Fuks, Z. Cancer Res. 51: 2552-2558, 1991.

Relationship between Vomiting and Taste Aversion Learning in the Ferret: Studies with Ionizing Radiation, Lithium Chloride, and Amphetamine

BERNARD M. RABIN[*,†] AND WALTER A. HUNT[*,1,2]

*Behavioral Sciences Department, Armed Forces Radiobiology Research Institute, Bethesda, Maryland 20889-5145; and †Department of Psychology, University of Maryland Baltimore County, Baltimore, Maryland 21228-5398

The relationship between emesis and taste aversion learning was stud ied in ferrets (Mustela putorius furo) following exposure to ionizing radiation (50–200 cGy) or injection of lithium chloride (1.5–3.0 mEq/kg, ip). When 10% sucrose or 0.1% saccharin was used as the conditioned stimulus, neither unconditioned stimulus produced a taste aversion, even when vomiting was produced by the stimulus (Experiments 1 and 2). When a canned cat food was used as the conditioned stimulus, lithium chloride, but not ionizing radiation, produced a taste aversion (Experiment 3). Lithium chloride was effective in producing a conditioned taste aversion when administration of the toxin was delayed by up to 90 min following the ingestion of the canned cat food, indicating that the ferrets are capable of showing long-delay learning (Experiment 4). Experiment 5 examined the capacity of amphetamine, which is a qualitatively different stimulus than lithium chloride or ionizing radiation, to produce taste aversion learning in rats and cats as well as in ferrets. Injection of amphetamine (3 mg/kg, ip) produced a taste aversion in rats and cats but not in ferrets which required a higher dose (>5 mg/kg). The results of these experiments are interpreted as indicating that, at least for the ferret, there is no necessary relationship between toxin-induced illness and the acquisition of a CTA and that gastrointestinal distress is not a sufficient condition for CTA learning. © 1992 Academic Press, Inc.

A conditioned taste aversion (CTA) is produced when an unconditioned stimulus (UCS) is paired with a novel food. As a result of this pairing, an organism will avoid ingestion of that food at a subsequent presentation. Taste aversions can be produced by both toxic (e.g., ionizing radiation or lithium chloride (LiCl)) and self-administered (e.g., amphetamine) stimuli. Although both types of stimuli produce similar avoidance behavior, the mechanisms underlying the acquisition of a CTA produced by treatment with a toxic UCS differ from those produced by treatment with self-administered compounds (Hunt & Amit, 1987; Parker, 1982, 1988).

Functionally, the CTA is related to emesis in that both responses serve to limit the intake and/or absorption of toxic or potentially toxic foods (Rabin & Hunt, 1986). When a CTA follows treatment with a toxic UCS that is capable of producing vomiting, a general assumption is that an emesis-related gastrointestinal distress produced by the UCS is the proximal stimulus for the acquisition of the CTA (e.g., Garcia, Hankins, & Rusiniak, 1974; Garcia, Lasiter, Bermudez-Rattoni, & Deems, 1985; Nachman & Hartley, 1975). The evidence supporting this hypothesis, however, is indirect, relying on the observations that lower dose treatment with toxic stimuli that produce emesis at higher doses will also produce CTA learning (cf. Grant (1987) for a recent review), and that manipulations, such as lesions of the area postrema, which disrupt CTA acquisition will disrupt emesis as well (Rabin, Hunt, Chedester

& Lee; 1986a). More direct evidence for the involvement of the gastrointestinal system is provided by the observation that it is difficult to establish a CTA by pairing a novel food with external stimuli such as electric shock (Garcia & Koelling, 1966) or with compounds such as gallamine which, in contrast to LiCl, do not produce gastric distress (Lett, 1985).

Although most research on CTA learning has utilized the rat which cannot vomit, comparative studies have shown that taste aversions can be obtained from many species, including those that are capable of vomiting (Collier, 1985; Shettleworth, 1985). Using cats, Rabin et al. (1986a) reported that reliable taste aversions could be obtained with doses of γ rays (^{60}Co) as low as 100 and 300 cGy, whereas exposures of 4500 cGy were needed to reliably elicit vomiting. Similarly, rotation-induced motion sickness in squirrel monkeys (Fox, Corcoran, & Brizzee, 1990; Roy & Brizzee, 1979) and cats (Fox et al., 1990) produces both CTA learning and emesis. Rusiniak, Gustavson, Hankins, & Garcia (1976) reported both responses following systemic or oral administration of LiCl in ferrets. Also, human cancer patients undergoing a course of therapy with emesis-producing cytotoxic drugs (Andrykowski & Otis, 1990; Bernstein, 1978) or ionizing radiation (Smith, Blumsack, Bilek, Spector, Hollander, & Baker, 1984) may acquire a CTA when a novel food is presented just prior to the treatment.

While these results do show that treatment with a toxic UCS can produce both CTA learning and emesis, they do not show that the two responses are related. It is possible that CTA and emesis are related responses, involving similar mechanisms and differentiated only by the dose required to produce the behavioral response. Alternatively, it is possible that CTA and emesis represent independent responses to a single toxic UCS. There are, in fact, some data which would be consistent with the latter hypothesis. Not all toxic compounds (e.g., strychnine and cyanide) produce taste aversions (Ionescu & Burešová, 1977; Nachman & Hartley, 1975). Treatment with antiemetic compounds such as chlorpromazine (Goudie, Stolerman, Demellweek, & D'Mello, 1982; Rabin & Hunt, 1983), antiemetic opioid agonists (Blancquaert & Lefebvre, 1986), or high-dose metachlopramide (Rabin & Hunt, unpublished data) does not prevent the acquisition of a CTA following exposure to ionizing radiation or injections of toxic compounds (LiCl or cisplatin). Also, studies of taste aversion learning in humans indicate that a CTA can develop in the absence of noticeable gastrointestinal upset or reports of nausea

(Bernstein & Webster, 1980; de Silva & Rachman, 1987).

The limitation on the preceding studies is that they have, with a few exceptions (e.g., Fox et al., 1990; Rabin et al., 1986a), used different species to study CTA and emesis. Since both the behavioral endpoint (CTA and emesis) and the species have been varied, it is not clear whether any reported differences result from the different endpoints or whether they result from species-specific differences. The present set of experiments was designed to evaluate further the relationship between CTA and emesis by studying both responses in a single animal following treatment with toxic stimuli. The ferret (Mustela putorius furo) was selected as the subject for these experiments because it is capable of vomiting in response to exposure to low doses of ionizing radiation and to treatment with toxic drugs (Costall, Domeney, Naylor, & Tattersall, 1987; King, 1988) and because previous research has shown that ferrets will acquire a CTA (Rusiniak et al., 1976). As such, the ferret could provide a good animal model for studying the relationships between CTA learning and emesis.

GENERAL METHODS—FERRETS

Subjects

The subjects were adult male ferrets weighing between 0.9 and 1.4 kg which were obtained from Marshall Farms (North Rose, NY). The animals were castrated and descented by the supplier. They were maintained in an AAALAC-accredited facility in stainless steel cages. Except as required by the experimental protocol, a commercial dry cat chow and water were available ad lib. The animal holding rooms were maintained at 21 ± 1°C with 50 ± 10% relative humidity and with a 12-h light:dark light cycle.

Procedures

For CTA acquisition, the ferrets were put on 23-h deprivation schedule for 3 days. On the conditioning day (Day 4), they were presented with the conditioned stimulus (CS) for 1 h, immediately followed by the UCS. The animals were then observed for 1–2 h to monitor emetic responses (vomiting or retching). For the next 1 or 2 days the ferrets were given their regular food or water for 1 h. On the test day (Day 6/7) they were again presented with the CS for 1 h.

Unconditioned Stimuli

Three types of unconditioned stimuli were used. (1) Ionizing radiation (50, 100, or 200 cGy) was provided by either a ^{60}Co source or a linear accelerator (18.5 MeV electrons, 1 μs pulses, 0.47 pulses/s) at a nominal dose rate of 65–100 cGy/min. Dosimetry was performed using a standard protocol (Task Group 21, 1983). Previous research (Rabin, Hunt, & Joseph, 1989) has shown that these sources produce equivalent taste aversions in rats. For irradiation, the ferrets were placed in well-ventilated clear plastic tubes which were placed in the center of the field perpendicular to the source and given whole body exposures. Control animals were placed in plastic restraining tubes and were taken to the source, but were not exposed. (2) LiCl (0.3 M) was administered at doses of 1.5, 2.2, or 3.0 mEq/kg, ip. Controls were given equivalent injections of isotonic saline. (3) Amphetamine was given at a dose of 3.0 or 5.0 mg/kg, ip. Control ferrets were administered equivalent injections of isotonic saline. Each experiment used naive subjects.

Statistical Analyses

Analyses of the results were done using one-way repeated or two-way mixed analyses of variance. Comparisons between individual groups within an experiment were made using Tukey's protected-t test.

EXPERIMENT 1

The initial goal of this series of experiments was to evaluate the relationship between CTA acquisition and emesis. As such, these experiments utilized a 10% sucrose solution for the CS and either ionizing radiation or LiCl as the UCS in order to make the data directly comparable to those obtained using rats.

Procedures

The subjects for these experiments were 15 naive ferrets divided into three groups (n = 5/group). The first two groups were exposed to whole body ionizing radiation (^{60}Co, 100 cGy/min) at doses of 50 or 100 cGy immediately following presentation of the CS. The remaining group was given an injection of LiCl (3.0 mEq/kg, ip) following drinking.

Pilot experiments using a different set of ferrets, Fig. 1, indicated that the ferrets were extremely responsive to the sensory qualities of the sucrose CS, drinking nearly three times the amount of sucrose on the sham conditioning day as that of water
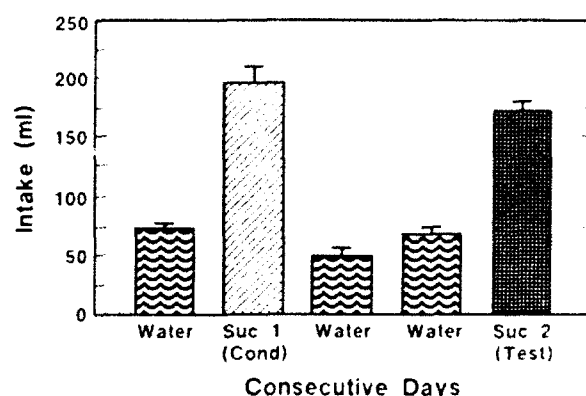

FIG. 1. Water and sucrose intake of control ferrets on consecutive days. The first presentation of the 10% sucrose solution corresponds to the conditioning day and the second presentation corresponds to the test day in the experimental paradigm.

on the preceding day. As a result there was a significant reduction in water intake on the day following the presentation of the 10% sucrose solution compared to the other days during which water was presented, $F(2, 8) = 12.85$, $p < .01$. This unconditioned reduction in fluid intake could result in a reduction in subsequent test day sucrose intake. creating the appearance of a CTA. There was also the possibility that the excessive sucrose intake could make the ferrets sick, independently of the effects produced by the UCS. Therefore, it was decided to limit the amount of the sucrose CS on the conditioning day to approximately the amount of daily water intake (80–85 ml). The amount of CS presented to the animals was increased on the test day to reduce the possibility of a ceiling effect limiting sucrose intake.

Results and Discussion

The results of exposure to ionizing radiation or injection of LiCl on CTA acquisition and emesis are summarized in Fig. 2. The number above each bar gives the average amount of sucrose that was presented to the ferrets. The number in each box is the number of animals that vomited over the number of animals tested. Figure 2 indicates that the doses of radiation (50 and 100 cGy) were below or near the threshold for emesis in ferrets. In contrast. the dose of LiCl (3.0 mEq/kg) was sufficient to cause emesis in all ferrets tested with a latency of 9–12 min. However, treatment with neither UCS produced a CTA. Rather, in each case there was a significant increase in test day sucrose intake (all $ps < .01$).

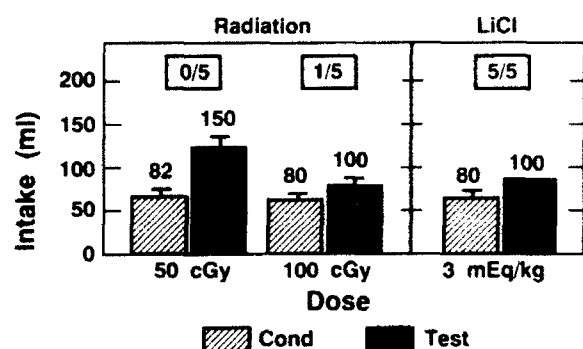The failure to obtain a CTA in the present ex-

FIG. 2. Effects of exposure to ionizing radiation or injection of LiCl on acquisition of a CTA to 10% sucrose. The numbers above each bar give the average amount of sucrose presented to the ferrets. The numbers in the boxes give the number of ferrets vomiting/number of ferrets tested.

periment is in direct contrast to the results reported by Rusiniak et al. (1976). Although the doses of radiation used in the present experiment did not reliably elicit emesis, previous research using rats and cats has shown that a CTA can be elicited at doses well below those required for emesis—doses that produce no observable effects on behavior other than the CTA (Garcia et al., 1974; Rabin et al., 1986a). As such, Garcia (Coil, Rogers, Garcia, & Novin, 1978; Garcia et al., 1985) has proposed that the CTA is the most sensitive indicator of a toxic stimulus that has effects on the gustatory–visceral system. As previously reported (Rusiniak et al., 1976), the dose of LiCl used in this experiment caused repeated short-latency bouts of vomiting. Despite this, the ferrets did not acquire a CTA to the sucrose CS, suggesting that emesis may not be a sufficient condition for CTA learning under these experimental conditions.

EXPERIMENT 2

The failure to obtain the expected CTA to a sucrose CS following treatment with these stimuli may have resulted from the specific nature of the sucrose CS. The extreme responsiveness of the ferrets to the sweet taste of the CS, which resulted in a threefold increase in the intake of sucrose solution compared to their regular daily water intake, may have acted to override the avoidance behavior that would normally be induced by the CS–UCS pairing. To evaluate these possibilities, a second experiment was run using 0.1% sodium saccharin solution as the CS. Saccharin, which has no caloric value, may have a bitter taste component (Stewart & Krafczek, 1988). As such, the responsiveness of the ferrets to the hedonic characteristics of the saccharin solution

may be somewhat reduced compared to sucrose, thereby increasing the possibility of CTA learning following treatment with a toxic UCS.

Procedures

The subjects were five naive ferrets. On the conditioning day they were presented with a 0.1% sodium saccharin solution for the 1-h drinking period, followed immediately by injection of LiCl (3.0 mEq/kg, ip).

Results and Discussion

All ferrets retched or vomited in response to the LiCl injections. The effects of LiCl on saccharin intake are presented in Fig. 3. Injection of LiCl had no effect on saccharin consumption (conditioning intake: 70.00 $\pm$ 1.58 ml; test day intake: 71.80 $\pm$ 4.27 ml; $F(1, 4) = 0.238, p > .10$).

Because there was no reduction in actual test day saccharin intake following injection of LiCl, it cannot be argued that the LiCl UCS produces a CTA to a 0.1% saccharin CS. In this regard, the saccharin CS is similar to the sucrose CS. However, the pattern of responding between sucrose and saccharin was different. With the sucrose CS, unlike the saccharin CS, there was a significant increase in test day sucrose intake. This observation suggests that the sensory qualities of the CS may play an important role in determining the conditionability of an avoidance response to a specific food following gastrointestinal distress and vomiting. For the ferret, at least, the hedonic value of the particular CS may be more important in determining the response to a CS than the consequences resulting from ingestion of the CS.
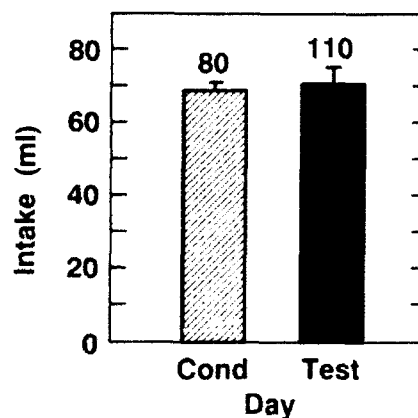

FIG. 3. Acquisition of a taste aversion to 0.1% saccharin following injection of LiCl (3.0 mEq/kg, ip). The numbers above the bars indicate the amount of sucrose that was given to the ferrets.

EXPERIMENT 3

The results of the first two experiments using hedonic stimuli indicated that a CTA could not be induced to either sucrose or saccharin conditioned stimuli in the ferret by either exposure to γ radiation (^{60}Co) or by injection of LiCl. However, Rusiniak et al. (1976) reported that ferrets will acquire a CTA when canned dog or cat food is paired with LiCl. The differences in results between the present experiments and those of Rusiniak et al. (1976) may be due to the specific CS utilized in these experiments. The canned food used by Rusiniak et al. may have a lower hedonic value to the ferret than a sucrose or saccharin CS, resulting in a greater conditionability of the avoidance response to the toxic UCS. Alternatively, it may be that the canned food is a more "natural" CS, thereby increasing the likelihood that an association between ingestion of a food and the gastrointestinal consequences of ingestion would occur.

In either case, it would be expected that the use of canned pet food would increase the probability of CTA learning when paired with a toxic UCS. The present experiment was designed to evaluate this hypothesis.

Procedure

The subjects for this experiment were 34 naive ferrets. The CS was a commercially available canned cat food. Food was not limited and more food was presented than was eaten on either the conditioning or test day. Immediately following the presentation of the CS, 18 ferrets were given an injection of one of three doses of LiCl: 1.5(n = 8), 2.2(n = 6), or 3.0(n = 4) mEq/kg, ip. Six control ferrets were given equivalent injections of isotonic saline. Eight ferrets were exposed to either 100 or 200 cGy of ionizing radiation (n = 4/dose). Two ferrets served as controls in which they were transported to the radiation source and put in a restraining tube, but were not irradiated.

Results and Discussion

The effects of LiCl injections on emesis and CTA acquisition are presented in Fig. 4. Injection of LiCl produced dose-dependent vomiting in the ferrets such that there was an increase in the frequency of emesis as the dose of LiCl was increased. There also were dose-dependent effects on CTA learning. Following saline injections on the conditioning day, there was a significant increase in test day CS intake ($t(5)$ = −3.11, p < .01). This indicates that
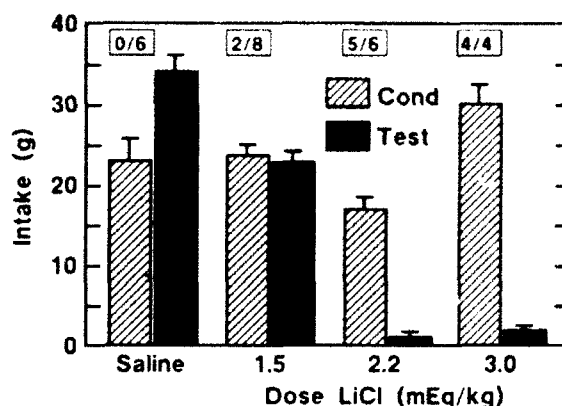

FIG. 4. Effects of injection of LiCl on the intake of canned cat food. The numbers in the boxes give the number of ferrets vomiting/number of ferrets tested.

ferrets are neophobic, showing a reduced intake of a novel food on its first presentation. Injection of 1.5 mEq/kg LiCl did not cause a CTA but rather eliminated the recovery from neophobia that was observed following saline injections. Treatment with the two higher doses of LiCl, 2.2 and 3.0 mEq/kg of LiCl produced maximal avoidance of the cat-food CS.

These results support those of Rusiniak et al. (1976) showing that a CTA learning can occur in ferrets following emesis-producing LiCl injections. While the effects of LiCl injection on CTA learning appear to parallel LiCl-induced emesis, these two effects of LiCl injection may not be related phenomena. Of the two animals that vomited in response to injection of 1.5 mEq/kg LiCl, one showed no change in test day CS intake (20 g on both days) while the other showed an increase in intake from 26 g on the conditioning day to 42 g on the test day. Of the remaining six ferrets which did not vomit following LiCl injection, four showed decreased test day intake, while one showed no change and one showed increased test day intake.

The effects of exposure to ionizing radiation are summarized in Fig. 5. As with LiCl injection, there was a dose-dependent increase in the frequency of vomiting as the dose of radiation was increased. However, in contrast to the results with LiCl, the ferrets did not acquire a CTA following exposure to ionizing radiation. The ferrets given either sham ($t(3)$ = 4.33, p < .05) or 100 cGy ($t(3)$ = 4.81, p < .05) exposures showed significant increases in CS intake on the test day, indicating a recovery from the conditioning day neophobia to the novel CS. Exposing the ferrets to 200 cGy eliminated the recovery from neophobia, but did not produce a CTA.
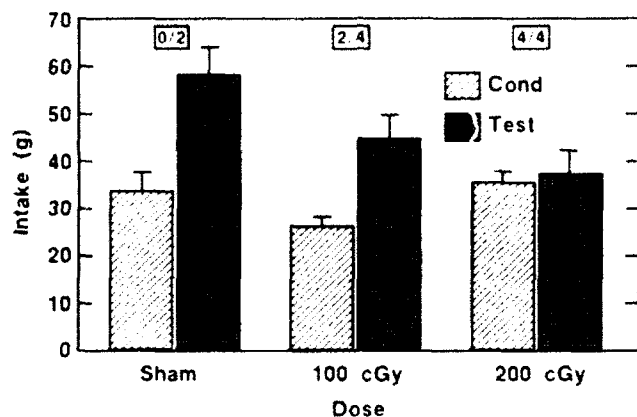
FIG. 5. Effects of exposure to ionizing radiation on the intake of canned cat food. The numbers in the boxes give the number of ferrets vomiting/number of ferrets tested.

In contrast to the results obtained with LiCl injections, there is not even an apparent relationship between emesis and CTA learning following exposure to ionizing radiation. Both of the ferrets that vomited in response to exposure to 100 cGy showed increased test day CS intake compared to their conditioning day intake. Although all ferrets vomited following exposure to 200 cGy, only one showed a decrease in test day CS intake. Of the remaining ferrets, two showed no change in test day CS intake following irradiation and one showed increased CS intake. The observation of a loss of recovery from neophobia at the highest dose of radiation may suggest that a further increase in radiation dose would produce a CTA. However, several ferrets run at a dose of 400 cGy (data not shown) developed an unconditioned decrease in the intake of a novel cat food when it was first presented 24 h following irradiation, possibly as the side effect of a severe radiation-induced illness.

EXPERIMENT 4

The results of the preceding experiment indicate that, for the ferret at least, the nature of the UCS is a critical factor in determining whether or not a CTA will be acquired following the pairing of a toxic stimulus with a novel food. The observation that a CTA could be produced by injection of LiCl, but not by exposure to ionizing radiation, cannot be accounted for by differences in the frequency by which the two stimuli produced emesis because all ferrets vomited to the highest doses of both stimuli. Nonetheless, in contrast to the results with LiCl, no ferret acquired a CTA following exposure to ionizing radiation. It is possible, however, that differences in

latency for emesis following treatment with the toxic UCS (7–15 min for LiCl compared to 20–60 min for radiation) may have affected the conditionability of the avoidance response in the ferret.

While CTA learning is typically considered to be "long-delay" learning (Domjan, 1985; Garcia et al., 1974), this may not be the case for the ferret which shows a rapid gastrointestinal transit time. As a result, the difference in the latency for the gastrointestinal effects produced by the UCS may account for the failure of the ferrets to acquire a CTA. To evaluate this possibility, ferrets were run in an experiment in which LiCl was administered at varying intervals following the 1-h eating period. If the latency of the gastrointestinal consequences of ingestion is a factor affecting CTA learning in the ferret, then increasing the interval between ingestion and treatment with the toxic UCS should result in a decreased frequency of CTA acquisition.

Procedure

The subjects were 18 naive ferrets. On the conditioning day they were given a novel canned cat food CS for 1 h. At delay intervals of 30 (n = 5), 60 (n = 7), or 90 (n = 6) min following the removal of the CS, the ferrets were injected with LiCl (3.0 mEq/kg, ip).

Results and Discussion

The results are summarized in Fig. 6. The data for the 0-min delay interval have been regraphed from Experiment 3. All ferrets vomited in response to the LiCl injection with latencies ranging between 9 and 15 min from the time of injection. Similarly, all ferrets developed equivalent taste aversions to
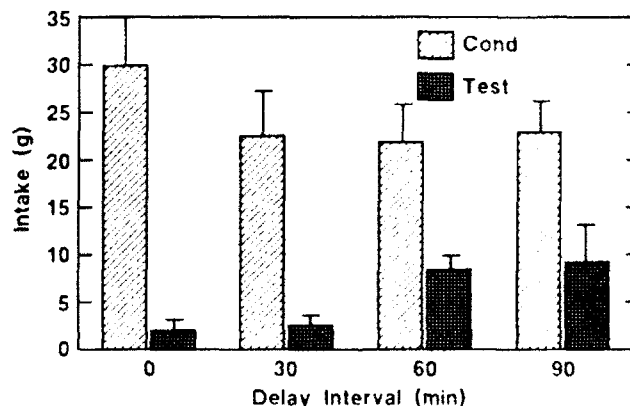

FIG. 6. Effects of increasing the interval (min) between removal of the food and the injection of LiCl (3.0 mEq/kg, ip) on intake of canned cat food. All ferrets vomited in response to the injection.

the CS. A two-way mixed ANOVA indicated that the main effect for the comparison between conditioning and test days was significant, $F(1, 24) = 100.58, p < .001$, but the comparison across the four delay intervals was not significant, $F(3, 24) = 0.49, p > .10$. The interaction was significant, $F(3, 24) = 3.17, p < .05$, suggesting that the pattern of responding across delay intervals was different. However, none of the individual comparisons of test day CS intake across the four delay intervals using Tukey's Protected t test was significant (all $ps > .05$).

These results, therefore, indicate that ferrets are capable of showing the long-delay learning that is characteristic of CTA acquisition in other species. As such, they indicate that the differences in CTA acquisition following injection of LiCl and following exposure to ionizing radiation cannot be due to differences in the time course of the gastrointestinal consequences of treatment with the specific UCS. Rather, the differences in CTA acquisition between LiCl and radiation observed in Experiment 3 must be considered a primary effect of the specific nature of the UCS. The present results also suggest that partially different mechanisms may underlie the acquisition of a CTA following treatment with a specific toxic UCS.

Although the CTA responses to both LiCl and ionizing radiation in the rat are mediated by the area postrema (Ossenkopp, 1983a; Rabin, Hunt, & Lee, 1983), Rabin, Hunt, and Lee (1988) reported that preexposing rats to LiCl could attenuate the acquisition of a radiation-induced CTA, whereas preexposure to radiation did not affect the acquisition of a LiCl-induced CTA. This observation of an asymmetrical generalization gradient between ionizing radiation and LiCl was interpreted as suggesting that the stimulus effects of irradiation were not identical to those of LiCl injection. If the stimulus effects of both unconditioned stimuli were identical, then a symmetrical cross-attenuation of CTA learning following preexposure to either UCS should have been observed. The present observation in ferrets that treatment with LiCl produces a CTA while exposure to radiation does not is consistent with the hypothesis that the stimulus complex following exposure to ionizing radiation is not identical to, nor as extensive as, that obtained following injection of LiCl (Rabin et al., 1988).

EXPERIMENT 5

The preceding series of experiments indicates that the acquisition of a CTA by ferrets, in contrast to rats, following treatment with LiCl or ionizing ra-

diation is dependent upon the characteristics of the specific UCS as well as the CS. This result is surprising because, in the rat, the acquisition of both LiCl- and radiation-induced taste aversions is mediated by the area postrema (Rabin et al., 1983; Ossenkopp, 1983a). Similarly in cats radiation produces an area postrema-dependent CTA at doses significantly lower than those required to produce emesis (Rabin et al., 1986a). These observations raise the question as to whether the differential effectiveness of LiCl and radiation in producing a CTA in the ferret is restricted to these unconditioned stimuli or whether the ferret shows a general pattern of CTA learning which may differ from that observed in other species, perhaps related to the relatively low doses required for emesis (Costall et al., 1987).

In contrast to the toxic stimuli tested above, amphetamine does not require the mediation of the area postrema for CTA learning (Rabin & Hunt, 1989; Ritter, McGlone, & Kelly, 1980) and may, in fact, produce a qualitatively different CTA than that observed following treatment with LiCl (Parker, 1982, 1988). As such, using amphetamine as the UCS for CTA acquisition might provide a means for determining whether the failure to obtain a CTA in ferrets following exposure to ionizing radiation was unique to that UCS or whether ferrets may respond differently to a variety of toxic and nontoxic stimuli than do other species.

Subjects

The subjects for the experiment were ferrets ($n = 18$), cats ($n = 14$), and rats ($n = 16$). The data for the cats were obtained during another series of experiments (Rabin, Hunt, Bakarich, Chedester, & Lee, 1986b). On the conditioning day, half the rats and cats were administered an injection of amphetamine (3 mg/kg, ip) following the drinking period and half were given an equivalent injection of isotonic saline. For the ferrets, 14 were injected with amphetamine and 4 were given a saline injection.

Procedures

(1) Ferrets. The procedures for the ferrets were identical to those detailed previously. Briefly, the ferrets were placed on a 23-h food deprivation schedule for 3 days. On the conditioning day the ferrets were presented with a commercially available cat food for 1 h. Immediately following the eating period, the ferrets were injected with amphetamine or an equivalent volume of isotonic saline. Five ferrets were given an amphetamine injection of 3 mg/kg,
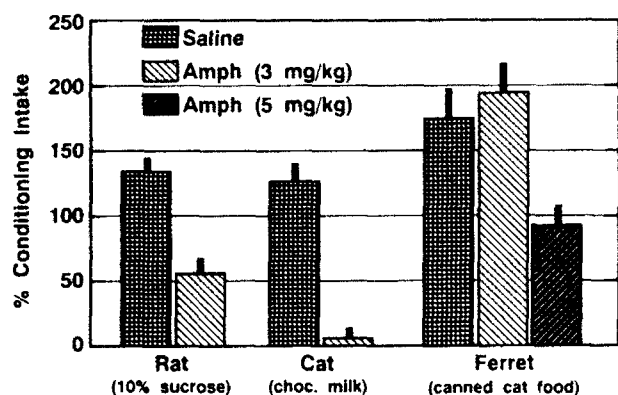
FIG. 7. Effects injection of amphetamine on the acquisition of a CTA in rats, cats, and ferrets. The CS for each species is given in the parentheses.

ip, and nine were injected with 5 mg/kg, ip. The test day was 48 h following conditioning.

(2) Cats. The procedures have been detailed previously (Rabin et al., 1986b). Briefly, all cats were deprived of food and water for 20-h prior to conditioning. On the conditioning day, the cats were given a commercially available chocolate milk for 1 h, after which they were given injection of amphetamine (3 mg/kg, ip) or an equivalent injection of isotonic saline. Four hours following the injection, food and water were returned for 24 h. The cats were then deprived of food and water for 20 h before again presenting them with the chocolate milk on the test day.

(3) Rats. The rats were placed on a 23.5-h water deprivation schedule for 5 days. On the conditioning day (Day 5), the rats were given a single bottle containing a 10% sucrose solution in place of the water for 30 min. Immediately following the drinking period, the rats were given an injection of amphetamine (3 mg/kg, ip) or an equivalent injection on isotonic saline. On the test day (24 h later), all rats were again presented with a single bottle of 10% sucrose solution.

Results and Discussion

In order to make the results presented in Fig. 7 directly comparable for all species, test day intake is presented as the percentage of conditioning day intake. Figure 7 shows that the control rats and cats which were given injections of isotonic saline showed increased CS intake on the test day compared to the conditioning day. In contrast, both rats ($t(16)$ = 7.32, $p < .001$) and cats ($t(12)$ = 10.71, $p < .001$) given injections of amphetamine showed significant reductions in test day CS intake com-

pared to their saline-injected controls. For the ferrets, both saline-injected and amphetamine-injected subjects given 3 mg/kg showed increased CS intake on the test day compared to the conditioning day. The differences in CS intake between these two groups were not significant ($t(7)$ = 0.44, $p > .10$). The ferrets given the higher dose of amphetamine (5 mg/kg) showed a slight, although nonsignificant ($t(8)$ = 1.30, $p > .10$), decrease in test day CS intake.

These results show that cats will acquire a CTA following injection of 3 mg/kg amphetamine, as has been previously established for rats (e.g., Hunt & Amit, 1987; Rabin & Hunt, 1986). Ferrets, in contrast, fail to show CTA learning following injection of this dose of amphetamine despite the fact that this dose was sufficient to cause observable changes in the unrestrained behavior of all animals, in addition to causing a CTA in both cats and rats. The observation that the higher dose of amphetamine (5 mg/kg) eliminated the test day recovery from neophobia suggests that the use of even higher doses of amphetamine may produce CTA. The effects observed with amphetamine thus parallel those seen with ionizing radiation. With the radiation UCS, increasing the dose also eliminated the recovery from neophobia, although the extreme toxicity of the higher doses of this UCS produced unconditioned decreases in CS intake.

The observation that ferrets require significantly higher doses of amphetamine and radiation for CTA learning to occur suggests that ferrets apparently respond differently to a variety of toxic and nontoxic unconditioned stimuli than do other species. In this regard, it may be noted that ferrets, in contrast to monkeys (Fox et al., 1990), cats (Fox et al., 1990; Lucot & Crampton, 1987), and humans (Kohl, 1987), do not vomit in response to rotational stimulation (R. A. Fox, personal communication).

GENERAL DISCUSSION

The present results indicate that the acquisition of a CTA by ferrets depends upon the specific characteristics of both the CS and the UCS. Ferrets failed to show CTA learning when a 10% sucrose solution or a 0.1% saccharin solution was used as the CS. They did acquire a CTA when canned cat food was followed by LiCl injection, but not when the CS was followed by exposure to ionizing radiation or by injection of a standard dose of amphetamine (3 mg/kg).

The ferret seems to differ somewhat from other mammalian species that have been studied in terms of its sensitivity to the characteristics of the CS and UCS. Although not all toxins will produce a CTA

(Ionescu & Burešová, 1977; Nachman & Hartley, 1975), treatment with toxins such as LiCl or ionizing radiation which produce rapid effects on the gastrointestinal system are standard stimuli used in the study of CTA learning because of the reliability with which they produce a CTA. The failure of these toxins to produce a CTA has not been reported previously, although there has not been a systematic study of the effectiveness of various toxins in a single species other than rats. Species differences in the effectiveness of a single UCS have been previously reported by Rabin et al. (1986b), who showed that injection of angiotensin II produced a CTA in cats but not in rats.

Similarly, the ferret apparently differs from other species that have been studied in the capacity of an hedonic CS, sucrose or saccharin, to override the aversive effects of injection of LiCl or exposure to ionizing radiation. The CTA is generally considered to be an evolutionarily important response which functions to protect the organism against the ingestion of potentially toxic foods (Garcia et al., 1974; Rabin & Hunt, 1986) by producing a conditioned avoidance response following intake of small, nonlethal, amounts of the food. The present results do not support this interpretation of the role of the CTA, at least for the ferret, because exposure to lethal levels of ionizing radiation ($LD_{100/15}$ [the dose that produces the death of 100% of the subjects within 15 days] = 200 cGy; Rabin & Hunt, unpublished observations) did not produce a CTA to either CS. In this regard, the failure to observe a CTA cannot be due to a failure of ferrets to show neophobia upon the first presentation of a novel CS. Although the ferrets did not show a neophobic response to the first presentation of the 10% sucrose solution (Fig. 1), they do make such a response to the first presentation of a canned cat food CS (Figs. 4 and 5). Despite this, exposure to ionizing radiation failed to produce CTA learning.

The present results indicated that a treatment-induced loss of recovery from neophobia was followed, with the LiCl UCS, by the acquisition of a CTA produced by injection of a higher dose. While this may suggest that neophobia is related to CTA learning, such an interpretation is not consistent with the observation that exposure to higher dose radiation failed to produce a CTA. Also, several other investigators have reported that it is possible to produce a dissociation between neophobia and CTA learning (e.g., Braveman & Jarvis, 1976; Franchina & Gilley, 1986; Royet & Pager, 1982). The present observation of neophobia in ferrets suggests that neophobia in the rat is not an evolutionary mechanism related to protection against toxicosis

and to the inability of rats to vomit because the ferret vomits readily to a variety of stimuli (Costall et al., 1987). This interpretation is consistent with that of Miller and Holzman (1981) who reported that gerbils fail to show neophobia to a variety of tastes despite the fact that taste aversions can be readily produced to these stimuli.

The present results also have implications concerning the hypothesis that "sickness" is the proximal UCS for CTA learning. As indicated above, there are data that are consistent with this hypothesis (Garcia et al., 1974, 1975). These data are, for the most part, indirect because, with few exceptions (e.g., Fox et al., 1990; Rabin et al., 1986a), emesis and CTA learning in response to treatment with a variety of toxins have not been studied in the same animals. However, the present results which show that it is possible to produce vomiting in the ferret following exposure to ionizing radiation or injection of LiCl without producing a CTA do not support the hypothesis that a treatment-induced sickness is the proximal UCS leading to the acquisition of a CTA. The observation that ferrets will vomit in response to exposure to ionizing radiation, but will not acquire a radiation-induced CTA, indicates that gastrointestinal distress is not a sufficient condition for CTA learning in these animals.

This conclusion is consistent with previous observations that rats will self-administer compounds (e.g., amphetamine) that will produce a CTA when administered following the ingestion of a novel food (Hunt & Amit, 1987) and that cats will also acquire a CTA following injection of amphetamine (Experiment 5, above). Similarly, treatment with a variety of antiemetics does not prevent the acquisition of a CTA (Blancquaert & Lefebvre, 1986; Goudie et al., 1982; Rabin & Hunt, 1983). In addition Rabin and Rabin (1984) and Burešová and Bureš (1977) have shown that rats will acquire radiation- and toxin-induced taste aversions when the UCS is administered to an animal maintained under surgical levels of anesthesia for up to 4 h. Under these conditions, it is doubtful that the rats could have experienced the UCS-induced sickness. These findings may further suggest that gastrointestinal distress is not a necessary condition for the acquisition of a CTA.

The present results, therefore, are consistent with the hypothesis that a toxin-induced gastrointestinal distress is neither a necessary nor a sufficient condition for CTA learning. Nonetheless, for the most part, stimuli that are capable of producing emesis do produce CTA learning. This suggests that the two responses are related in some way, although based upon the currently available research, the

nature of this relationship is not certain. It is possible that emesis and CTA learning represent independent responses to a variety of toxic and nontoxic stimuli. To the extent that any given UCS affects the neural substrates underlying these responses, then one or the other or both responses will occur (Rabin & Rabin, 1984; Rabin & Hunt, 1986).

This hypothesis requires several assumptions. First, there is some degree of overlap in the neural mechanisms subserving emesis and CTA learning in response to treatment with a variety of toxic and nontoxic stimuli. This assumption is supported by the observation that lesions of the area postrema can disrupt CTA learning in response to treatment with a wide range of toxic stimuli (e.g., Ossenkopp, 1983a; Rabin et al., 1983; Rabin & Hunt, 1986). In addition, Rabin and Hunt (1989) have reported that lesions of the area postrema combined with pretreatment with haloperidol will prevent the acquisition of an amphetamine-induced CTA, whereas the use of either procedure alone will attenuate but not prevent its acquisition.

Second, there are mulitple afferent mechanisms, depending upon the specific nature of the UCS, which can trigger emesis or CTA acquisition. Evidence consistent with this assumption has been provided by studies comparing the neural mechanisms leading to motion-induced emesis and CTA learning with those following the use of a variety of toxic treatments. Thus, the area postrema is a critical structure for the acquisition of a CTA following exposure to ionizing radiation or injection of toxic compounds (Ossenkopp, 1983a; Rabin et al., 1983; Ritter et al., 1980). Similarly destruction of the area postrema disrupts radiation- and drug-induced emesis following these treatments (Borison & Borison, 1986; Fox et al., 1990; Rabin et al., 1986a). Area postrema lesions do not attenuate either rotation-induced CTA learning or emesis (Fox et al., 1990; Ossenkopp, 1983b; Sutton, Fox, & Daunton, 1988). Conversely, vagotomy does not prevent the acquisition of a radiation- or LiCl-induced CTA in rats (Rabin, Hunt, & Lee, 1985), but does prevent rotation-induced CTA learning (Fox & McKenna, 1988).

In summary, the results of the present series of experiments with ferrets show that gastrointestinal illness is not a sufficient condition for the acquisition of a CTA. These results combined with previous research would be consistent with the hypothesis that the proximal UCS for CTA learning involves the activation of the underlying neural circuits which may, for some species and under some conditions, overlap the neural circuits that mediate emesis. More research with a variety of species and a variety of conditioned and unconditioned stimuli is needed to fully determine the relationships between gastrointestinal distress, CTA learning, and emesis.

REFERENCES

Andrykowski, M. A., & Otis, M. L. (1990). Development of learned food aversions in humans. Investigation in a "natural laboratory" of cancer chemotherapy. Appetite, 14, 145–158.

Bernstein, I. L. (1978). Learned taste aversions in children receiving chemotherapy. Science, 200, 1302–1303.

Bernstein, I. L., & Webster, M. M. (1980). Learned taste aversions in humans. Physiology & Behavior, 25, 363–366.

Blancquaert, J.-P., & Lefebvre, R. A. (1986). Different effects of opioid agonists on emesis in the dog and conditioned taste aversion in the rat: A comparative study. Biologisch Jaarboek Dodonaea, 54, 46–57.

Borison, H. L., & Borison, R. (1986). Motion sickness reflex arc bypasses the area postrema in cats. Experimental Neurology, 92, 723–737.

Braveman, N. S., & Jarvis, P. S. (1978). Independence of neophobia and taste aversion learning. Animal Learning and Behavior, 6, 406–412.

Burešová, O., & Bureš, J. (1977). The effect of anesthesia on acquisition and extinction of conditioned taste aversion. Behavioral Biology, 20, 41–50.

Coil, J. D., Rogers, R. C., Garcia, J., & Novin, D. (1978). Vagal and circulatory mediation of the toxic unconditioned stimulus. Behavioral Biology, 24, 509–519.

Collier, G. H. (1985). Conditioned taste aversion—Function and mechanism. Annals of the New York Academy of Sciences, 443, 152–157.

Costall, B., Domeney, A. M., Naylor, R. J., & Tattersall, F. D. (1987). Emesis induced by cisplatin in the ferret as a model for the detection of anti-emetic drugs. Neuropharmacology, 26, 1321–1326.

de Silva, P., & Rachman, S. (1987). Human food aversions: Nature and acquisition. Behavior Research and Therapy, 25, 457–468.

Domjan, M. (1985). Cue-consequence specificity and long-delay learning revisited. Annals of the New York Academy of Sciences, 443, 54–66.

Fox, R. A., & McKenna, S. (1988). Conditioned taste aversion induced by motion is prevented by selective vagotomy in the rat. Behavioral and Neural Biology, 50, 275–284.

Fox, R. A., Corcoran, M., & Brizzee, K. R. (1990). Conditioned taste aversion and motion sickness in cats and squirrel monkeys. Canadian Journal of Physiology and Pharmacology, 68, 269–278.

Franchina, J. J., & Gilley, D. W. (1986). Effects of pretraining on conditioning-enhanced neophobia: Evidence for separable mechanisms of neophobia and aversion conditioning. Animal Learning and Behavior, 14, 153–162.

Garcia, J., & Koelling, R. A. (1966). Relation of cue to consequence in avoidance learning. Psychonomic Science, 4, 123–124.

Garcia, J., Hankins, W. G., & Rusiniak, K. W. (1974). Behavioral regulation of the milieu interne in man and rat. Science, 185, 824–831.

Garcia, J., Lasiter, P. A., Bermudez-Ratoni, F. & Deems, D. A. (1985). A general theory of aversion learning. *Annals of the New York Academy of Sciences*, **443**, 8–21.

Goudie, A. J., Stolerman, I. P., Demellweek, C., & D'Mello, G. D. (1982). Does conditioned nausea mediate drug-induced conditioned taste aversion? *Psychopharmacology*, **78**, 277–281.

Grant, V. L. (1987). Do conditioned taste aversions result from activation of emetic mechanisms? *Psychopharmacology*, **93**, 405–415.

Hunt, T., & Amit, Z. (1987). Conditioned taste aversion induced by self-administered drugs: Paradox revisited. *Neuroscience and Biobehavioral Reviews*, **11**, 107–130.

Ionescu, E., & Burešova, O. (1977). Failure to elicit conditioned taste aversion by severe poisoning. *Pharmacology, Biochemistry and Behavior*, **6**, 251–254.

King, G. L. (1988). Characterization of radiation-induced emesis in the ferret. *Radiation Research*, **114**, 599–612.

Kohl, R. L. (1987). Failure of metachlopramide to control emesis or nausea due to stressful angular or linear acceleration. *Aviation, Space, and Environmental Medicine*, **58**, 125–131.

Lett, B. T. (1985). The painlike effect of gallamine and naloxone differs from sickness induced by lithium chloride. *Behavioral Neuroscience*, **99**, 145–150.

Lucot, J. B., & Crampton, G. H. (1987). Busiprone blocks motion sickness and xylazine-induced emesis in the cat. *Aviation, Space and Environmental Medicine*, **58**, 989–991.

Miller, R. R., & Holzman, A. D. (1981). Neophobia: Generality and function. *Behavioral and Neural Biology*, **33**, 14–44.

Nachman, M., & Hartley, P. L. (1975). Role of illness in producing learned taste aversion in rats: A comparison of several rodenticides. *Journal of Comparative and Physiological Psychology*, **189**, 1010–1018.

Ossenkopp, K.-P. (1983a). Taste aversions conditioned with gamma radiation. Attenuation by area postrema lesions in rats. *Behavioural Brain Research*, **7**, 295–305.

Ossenkopp, K.-P. (1983b). Area postrema lesions in rats enhance the magnitude of body rotation-induced conditioned taste aversions. *Behavioral and Neural Biology*, **38**, 82–96.

Parker, L. A. (1982). Nonconsummatory and consummatory behavioral CRs elicited by lithium- and amphetamine-paired flavors. *Learning and Motivation*, **13**, 281–303.

Parker, L. A. (1988). Positively reinforcing drugs may produce a different kind of CTA than drugs which are not positively reinforcing. *Learning and Motivation*, **19**, 207–220.

Rabin, B. M., & Hunt, W. A. (1983). Effects of antiemetics on the acquisition and recall of radiation- and lithium chloride-induced conditioned taste aversions. *Pharmacology, Biochemistry and Behavior*, **18**, 629–635.

Rabin, B. M., & Hunt, W. A. (1986). Mechanisms of radiation-induced conditioned taste aversion learning. *Neuroscience and Biobehavioral Reviews*, **10**, 55–65.

Rabin, B. M., & Hunt, W. A. (1989). Interaction of haloperidol and area postrema lesions in the disruption of amphetamine-induced conditioned taste aversion learning in rats. *Pharmacology, Biochemistry and Behavior*, **33**, 847–851.

Rabin, B. M., & Rabin, J. S. (1984). Acquisition of radiation- and lithium chloride-induced conditioned taste aversions in anesthetized rats. *Animal Learning and Behavior*, **12**, 439–441.

Rabin, B. M., Hunt, W. A. & Joseph, J. A. (1989). An assessment of the behavioral toxicity of high-energy iron particles compared to other qualities of radiation. *Radiation Research*, **119**, 113–122.

Rabin, B. M., Hunt, W. A., & Lee, J. (1983). Attenuation of radiation- and drug-induced conditioned taste aversions following area postrema lesions in the rat. *Radiation Research*, **93**, 388–394.

Rabin, B. M., Hunt, W. A., & Lee, J. (1985). Intragastric copper sulfate produces a more reliable conditioned taste aversion in vagotomized rats than in intact rats. *Behavioral and Neural Biology*, **44**, 364–373.

Rabin, B. M., Hunt, W. A., & Lee, J. (1987). Interactions between radiation and amphetamine in taste aversion learning and the role of the area postrema in amphetamine-induced conditioned taste aversions. *Pharmacology, Biochemistry, and Behavior*, **26**, 677–683.

Rabin, B. M., Hunt, W. A., & Lee, J. (1988). Attenuation and cross-attenuation in taste aversion learning in the rat. Studies with ionizing radiation, lithium chloride, and ethanol. *Pharmacology, Biochemistry and Behavior*, **31**, 909–918.

Rabin, B. M., Hunt, W. A., Chedester, A. L., & Lee, J. (1986a). Role of the area postrema in radiation-induced taste aversion learning and emesis in cats. *Physiology and Behavior*, **37**, 815–818.

Rabin, B. M., Hunt, W. A., Bakarich, A. C. Chedester, A. L., & Lee, J. (1986b). Angiotensin II-induced taste aversion learning in cats and rats and the role of the area postrema. *Physiology and Behavior*, **36**, 1173–1178.

Ritter, S., McGlone, J. L., & Kelly, K. W. (1980). Absence of lithium-induced taste aversion after area postrema lesion. *Brain Research*, **201**, 501–506.

Roy, M. A., & Brizzee, K. R. (1979). Motion sickness-induced food aversions in the squirrel monkey. *Physiology and Behavior*, **23**, 39–41.

Rovet, J.-P., & Pager, P. (1982). Lesions of the olfactory pathways affecting neophobia and learned aversions differently. *Behavioural Brain Research*, **4**, 251–262.

Rusiniak, K. W., Gustavson, C. R., Hankins, W. G., & Garcia, J. (1976). Prey-lithium aversions II: Laboratory rats and ferrets. *Behavioral Biology*, **17**, 73–85.

Shettleworth, S. J. (1985). Foraging, memory, and constraints on learning. *Annals of the New York Academy of Sciences*, **443**, 216–226.

Smith, J. C., Blumsack, J. T., Bilek, F. S., Spector, A. C., Hollander, G. R., & Baker, D. L. (1984). Radiation-induced taste aversion as a factor in cancer therapy. *Cancer Treatment Reports*, **68**, 1219–1227.

Stewart, C. N., & Krafczek, S. A. (1988). The taste characteristics of sodium saccharin in the rat: A re-examination of the dual taste hypothesis. *Chemical Senses*, **13**, 205–212.

Sutton, R. L., Fox, R. A., & Daunton, N. G. (1988). Role of the area postrema in three putative measures of motion sickness in the rat. *Behavioral and Neural Biology*, **50**, 133–152.

Task Group 21, Radiation Therapy Committee, American Association of Physicists in Medicine (1983). A protocol for the determination of absorbed dose from high-energy photon and electron beams. *Medical Physics*, **10**, 741–771.

Prostaglandin E$_2$ localization in the rat ileum

ELSA A. SCHMAUDER-CHOCK and STEPHEN P. CHOCK

Department of Experimental Hematology, Armed Forces Radiobiology Research Institute, Bethesda, MD 20814-5145, USA

Summary

The application of anti-prostaglandin E$_2$ immunoglobulin to plastic-embedded thin sections of the rat ileum has permitted the localization of prostaglandin E$_2$ in this tissue. In agreement with the published data (Chock & Schmauder-Chock 1988, Schmauder-Chock & Chock (1989)), the results also suggest the presence of an arachidonic acid cascade in the granules of various secretory cells of the gut. Since antibody labelling was found within the secretory granules of connective tissue mast cells, goblet cells, and Paneth cells, the presence of the arachidonic acid cascade in these granules is implied. The appearance of prostaglandin E$_2$ over the non-cellular internal elastic lamina of arterioles suggests that it may have been secreted along with the elastin. The even distribution of prostaglandin throughout the cytoplasm of the erythrocyte is consistent with the concept that this cell scavenges the eicosanoid from the circulation. These data further link the secretory granule to the production of eicosanoids and therefore illustrate the potential sources of prostaglandins in the rat ileum.

Introduction

The tissue concentration of prostaglandins and other eicosanoids is known to increase in various inflammatory conditions. In the intestine, their elevation is frequently associated with inflammatory bowel diseases, anaphylactic enteropathy, and radiation-induced gastrointestinal syndrome (Trier & Browning, 1966; Bach, 1982; Boughton-Smith *et al.*, 1983; Hahn *et al.*, 1983; Lake *et al.*, 1984; Lobos *et al.*, 1987; Heavey *et al.*, 1988; Perdue *et al.*, 1989; Buell & Harding, 1989). Although the lipid mediators are known to play crucial roles in the mechanism of inflammation, little is known about their sites of synthesis.

The eicosanoids, which are products of the arachidonic acid cascade, exert a wide range of potent biological effects. Prostaglandin E$_2$ (PGE$_2$) is generally considered to have immunosuppressive activity. Prostaglandin E (PGE) is also responsible for mediating cellular responses such as inhibition of mononuclear phagocyte proliferation (Kurland *et al.*, 1978), inhibition of phagocytosis (Hutchison & Myers, 1987), inhibition of macrophage interleukin 1 production (Kunkel *et al.*, 1986, 1988), and inhibition of natural killer cell activity (Brunda *et al.*, 1980). Since they are potent mediators, and since most cells can produce prostaglandins, it is important to recognize the potential sources of these messenger molecules.

Recently, we have shown that the secretory granule also contains the enzymes and other ingredients of the arachidonic acid cascade. This means that the secretory granule, besides being a mediator storage organelle, can also serve as the site of eicosanoid production. Since the formation of eicosanoids is often tied to the process of exocytosis, our localization of the arachidonic acid cascade in the secretory granule has provided the physical basis for the linking of these two events (Chock & Schmauder-Chock, 1988, 1989, 1990; Schmauder-Chock & Chock, 1989). In an effort to extend our understanding of this topic, we have extended our investigation to include the granule-bearing cells of the intestine where the release of prostaglandins may also have a cytoprotective function (Robert, 1979).

Since there is currently no available technique for the large-scale purification of various intestinal cell populations and their secretory granules, we have resorted to using ultrastructural immunocytochemical techniques to localize the presence of the arachidonic acid cascade by means of anti-PGE$_2$ labelling. Our results suggest that, like the mast cell, the secretory granules of the goblet cell and the Paneth cell of the ileum, also contain the machinery for eicosanoid synthesis.

Materials and methods

Male Sprague-Dawley rats weighing 300 to 400 g were euthanized with carbon dioxide inhalation prior to any

procedure. Segments of ileum were immersion-fixed for 2 h in 2% paraformaldehyde, 2.5% glutaraldehyde, 4 mM MgCl, in 100 mM cacodylate buffer at pH 7.3. Specimens were postfixed in 1% osmium tetroxide and dehydrated in an ethanol series. Embedding was done in Epon 812 Semi-thin sections of approximately 150 nm in thickness were placed on nickel grids.

The grids were immersed in 7.5% hydrogen peroxide for 15 min and rinsed briefly in distilled water. They were then submerged in a 1:30 dilution of goat serum (Cappel, Cochranville, PA) in antibody diluent (Ab-D) for 60 min at room temperature. The antibody diluent was made from a normal saline to which 10 mM EGTA and 20 mM HEPES were added. The pH was adjusted to 7.3 with NaOH. The grids were then well washed in Ab-D and incubated overnight at 4°C in a polyclonal rabbit PGE, anti-serum (Caymen Chemical Co., Ann Arbor, MI; catalogue No. 114010). This antibody may

cross-react with PGE and PGE, but their occurrence is insignificant compared to that of PGE. The same antibody has been used with a radioimmunoassay kit for the quantification of PGE in biological samples. Control grids were incubated overnight at 4°C in 50 µg/ml of pre-immune normal rabbit serum in Ab-D. The next day, all grids were well washed in Ab-D and then incubated for 2 h in 10 nm gold conjugated anti-rabbit IgG raised in goat (Sigma Chemical Co., St Louis, MO). Grids were washed in distilled water and photographed without staining in a Philips 400 electron microscope at 60 kv.

Results

The localization of PGE to the secretory granules of the connective tissue mast cells (CTMC) can be seen in Figs 1 A

Fig. 1. (A and B) Connective tissue mast cell secretory granules (arrows) are labelled with immunogold for the presence of PGE. These cells are surrounded with bundles of collagen fibres (c) in the ileal serosa. × 16 560. Inserts represent selected areas × 29 375. Bar = 0.5 µm.

and B) and 2A. These cells were located beneath the villus crypts within the collagen fibrils of the connective tissue. In agreement with the published results (Chock & Schmauder-Chock, 1988; Schmauder-Chock & Chock, 1989), all of the granules of the CTMC observed were well-labelled for the presence of PGE₂. A control CTMC can be seen in Fig. 2B.

In Fig. 3, different sections of a single goblet cell are shown. Like the mast cell, the secreting goblet cell granules are also heavily labelled with PGE₂ activity

Fig. 2. (A) Connective tissue mast cell secretory granules in the ileal serosa are labelled for the presence of prostaglandin E₂ (arrow). A small amount of label can be seen over the nucleus (n₁) of the cell and over the nucleus (n₂) of a second CTMC which is partially shown. (B) Control CTMC in the ileal serosa surrounded by collagen fibres (c). The secretory granules (arrows) have little or no label. A and B × 16 560. Inserts represent selected areas. × 29 375. Bar = 0.5 μm.

Besides the mucus-containing granules, PGE_2 label is frequently seen on the microvilli of the epithelial cells adjacent to the secreting goblet cell (Fig. 3A). The label always appeared tightly bound to the secretory granule components. The presence of label in association with the microvilli may be expected since the mucosa is constantly bathed with mucus which is a primary secretory product of the goblet cell. All goblet cells which had been exposed to the PGE_2 antibody exhibited strong labelling in their granules. When pre-immune serum was used in place of the anti-PGE_2 immunoglobulin, only a very small amount of non-specific labelling was observed (Fig. 3B).

Fig. 3. (A) Secreting goblet cell granules labelled for the presence of prostaglandin E_2 (arrow) Some label can also be observed in association with the microvilli of the adjacent epithelial cells (*). (B) Another section of the same cell treated as control The secreting granules show little or no label (arrow). The microvilli of adjacent epithelial cells are also unlabelled (*) A and B × 16 560 Enlarged selected areas × 29 375 Bar 0.5 μm.

Paneth cells are secretory cells which reside in the fundus of the crypts of Lieberkuhn in some species. As seen in Figs 4 (A and B), the granules of these cells are also heavily labelled with PGE₂ activity. All Paneth cells, which normally occur in groups, contained labelled granules. A Paneth cell under control conditions is shown in Fig. 4C.

The PGE₂ activity was consistently observed in association with the internal elastic lamina (IEL) of arterioles in the ileum (Figs 5, A–C). The source of this PGE₂ was not defined. Occasionally, label was seen in low levels over adjacent smooth muscle cells or endothelial cells, but not in a significant accumulation. An arteriole under control conditions can be seen in Fig. 5D.

The PGE₂ activity was also observed in erythrocytes. Figure 6 (A and B) show different images of the same cell which is located in the lumen of the gut. This erythrocyte was probably dislodged from a blood vessel during surgical excision of the tissue prior to fixation. Though it is distorted in shape due to the adverse environment of the gut, it is evenly labelled for PGE₂ activity. Adjacent to this erythrocyte are microvilli of an intestinal epithelial cell which are also labelled for PGE₂ activity, as has been seen previously in Fig. 3. In Fig. 6C, an erythrocyte in a small arteriole is also labeled for PGE₂ activity. Figure 6D is an image of an erythrocyte in an arteriole which has been treated under control conditions. As expected, only a small amount of non-specific label is seen in the control sample.

Discussion

The presence of an arachidonic acid cascade in the secretory granule of the rat peritoneal mast cell, a CTMC, has been previously established. The secretory granule contains a non-bilayer phospholipid store which can serve as the source of arachidonic acid for the cascade (Chock & Schmauder-Chock, 1987, 1989); a phospholipase A₂ to render the arachidonic acid available as substrate to the enzymes of the cascade (Chock et al., 1991); and a prostaglandin H synthase (cyclooxygenase) along with other enzymes of the cascade to convert archidonic acid to various eicosanoids, including PGE₂ (Chock & Schmauder-Chock, 1988; Schmauder-Chock & Chock, 1989). It has been implied that the stimulation of cell surface receptors can result in an influx of water across the perigranular membrane into the granule proper. This water influx triggers a series of simultaneous intra-granular events which, together, comprise the granule activation process. The events of granule activation include: de novo membrane generation (Chock & Schmauder-Chock, 1985; Schmauder-Chock & Chock, 1987a, b, 1990), initiatior. of the arachidonic acid cascade, and the rapid turnover of granule phospholipid (Chock & Schmauder-Chock, 1988; Schmauder-Chock & Chock, 1989; Chock et al., 1991). The role that the granule plays in the mechanism of stimulus-secretion coupling, has

recently been reviewed (Chock & Schmauder-Chock, 1990, 1992).

Since eicosanoids are not stored pre-formed mediators, but are synthesized from phospholipid-derived arachidonic acid at the onset of granule activation, the presence of PGE₂ within a membrane-bound secretory granule suggests the presence of an arachidonic acid cascade within the granule. The consistent appearance of a high level of PGE₂ activity within the secretory granules of the various cell types in the gut (Figs 1–4) further supports the conclusion that the secretory granule is the site of PGE₂ synthesis during secretion. A low level of PGE₂ labelling could also be found in the cytoplasm surrounding the intensely labelled granules, such as those shown in Fig. 4B. The appearance of secretory components outside the secretory granule has also been observed before (Bendayan et al., 1980). This may be a consequence of de novo membrane generation which results in the extrusion of granule components into the cytosol (Chock & Schmauder-Chock, 1990).

The technique of using embedded plastic sections for ultrastructural immunocytochemical localization of subcellular components has been well established (Bendayan et al., 1980; Probert et al., 1981). The use of rabbit polyclonal anti-PGE₂ immunoglobulin for the quantification of PGE₂ in biological specimens is also routine (Jaffe et al., 1973; Levine, 1973; Dray et al., 1975; Maclouf et al., 1976). Although the antibodies used in this experiment may cross-react with other E-series prostaglandins, these prostaglandins, if present, also confirm the presence of the arachidonic acid cascade.

The presence of the arachidonic acid cascade in the mast cell granule has been confirmed biochemically by using purified mast cell granules, and has been supported by the localization of prostaglandin H synthase (cyclooxygenase, the key enzyme of the cascade) in secreting mast cells. The synthesis of PGE₂ by the granules has also been verified immunocytochemically by using anti-PGE₂ immunoglobulin (Chock & Schmauder-Chock, 1988; Schmauder-Chock & Chock, 1989). In the current method, the presence of the arachidonic acid cascade in the mast cell granule is also confirmed by the antibody binding (Figs 1 and 2).

The localization of PGE₂ to the secretory granules of the goblet cells (Fig. 3) and the Paneth cells (Fig. 4) supports the concept that lipid-mediators, in general, originate from receptor-mediated exocytosis of granule-bearing cells. A low level of continuous secretion of PGE₂ via the mucus granules of the goblet cell is consistent with the belief that prostaglandins, at low levels, are cytoprotective to the gastric mucosa (Jacobson et al., 1976; Robert, 1979). However, the excessive mucus secretion that is observed during intestinal enteropathy, whether induced by radiation or anaphylaxis, may be very destructive in terms of fluid and electrolyte loss. More importantly, the excess PGE₂ secreted may be inhibitory to the normal epithelial cell proliferation.

Fig. 4. (A and B) Paneth cell granules labelled for the presence of prostaglandin E, arrows. (C) (control) Paneth cell granules with little or no label (arrow) A–C ×16 560 Inserts ×29 375 Bar = 0.5 μm

Similarly, the secretion of PGE₂ by the antibacterial Paneth cell may also occur for similar reasons. Its oversecretion may also be detrimental to epithelial cell proliferation. This detrimental effect may be easily realized especially since both the Paneth cell and the dividing epithelial cell reside together in the intestinal crypt

The presence of label for PGE₂ over the IEL of arterioles (Fig. 5) in the ileum was not anticipated

Fig. 5. (A–C) Internal elastic lamina of a small arteriole labelled for the presence of prostaglandin E₂ (arrows) The endothelial cells (e) and the surrounding smooth muscle cells (m) were occasionally lightly labelled. (D) (control) Internal elastic lamina of a small arteriole with little or no label for prostaglandin E₂ (arrow). A–D ×16 560. Inserts ×29 375. Bar = 0.5 μm.

Fig. 6. (A–C) Prostaglandin E₂ label associated with erythrocyte cytoplasm (arrows) and with the microvilli of an adjacent epithelial cell (*). A and B are adjacent sections of the same erythrocyte which was dislodged during dissection to a location in the ileal lumen. C is an erythrocyte which was located in an arteriole. (D) (control) Erythrocytes with little or no label for prostaglandin E₂ (arrow) are surrounded with endothelial cells (e) in an ileal arteriole. A–D × 16,560. Inserts × 29,375. Bar 0.5 μm.

Endogenous prostaglandin has been strongly implicated in the regulation of vascular reactivity (McGiff et al., 1976; Messina et al., 1976). The administration of prostaglandin E_1 was effective in inhibiting vascular permeability by blocking neutrophil adherence to endothelial cells (Gee et al., 1987). Endothelial cell integrity is disrupted as a result of radiation, and delayed regeneration of endothelial cells may lead to fibroblast overgrowth of the damaged vasculature (Adamson & Bowden, 1983). This poses the question that, with endothelial cell loss, does PGE_2 in the IEL provide temporary vascular protection from excessive neutrophil adherence or fibroblast overgrowth? This collar of IEL-containing PGE_2 may also protect the vessel lumen from smooth muscle cell overgrowth with subsequent occlusion.

Localization of PGE_2 in the erythrocyte (Fig. 6) is in agreement with the results previously observed with prostacyclin (PGI_2). Prostacyclin is rapidly taken up by erythrocytes in a time-dependent fashion. This may represent a means by which tissue can be protected from the ill effects of excess exposure to prostacyclin and other eicosanoids (Willems et al., 1983). The red blood cell thus can serve as a scavenger of some eicosanoids.

The identification of the potential sources of PGE_2 in the rat ileum may aid our understanding of the role of this lipid mediator in the mechanism of intestinal enteropathy. The clinical features of radiation-induced damage to intestinal mucosa largely duplicate those seen in the well-studied syndrome of human anaphylactic enteropathy. In both these syndromes, the damaging potential for harm becomes apparent when cells are activated to secrete in an excessive fashion. Initially, an overwhelming event such as tissue injury, antigen stimulation or radiation can initiate secretory cells to activate one another in a cascading fashion. Activator and suppressor mediators are released which may have feedback mechanisms which respectively suppress and activate other cells. These mechanisms function efficiently in the micro-environments of the intestine, and only during excessive activation do they become detrimental to the host.

References

ADAMSON, I. Y. R. & BOWDEN, D. H. (1983) Endothelial injury and repair in radiation-induced pulmonary fibrosis. Am. J. Pathol. 112, 224–30.

BACH, M. K. (1982) Mediators of anaphylaxis and inflammation. Ann. Rev. Microbiol. 36, 371–413.

BENDAYAN, M., ROTH, J., PERRELET, A. & ORCI, L. (1980) Quantitative immunocytochemical localization of pancreatic secretory proteins in subcellular compartments of the rat acinar cell. J. Histochem. Cytochem. 28, 149–60.

BOUGHTON-SMITH, N. K., HAWKEY, C. J. & WHITTLE, B. J. R. (1983) Biosynthesis of lipoxygenase and cyclo-oxygenase products from [¹⁴C]-arachidonic acid by human colonic mucosa. Gut 24, 1176–82.

BRUNDA, M. J., HERBERMAN, R. B. & HOLDEN, H. T. (1980) Inhibition of murine natural killer cell activity by prostaglandins. J. Immunol. 124, 2682–7.

BUELL, G. B. & HARDING, R. K. (1989) Proinflammatory effects of local abdominal irradiation on rat gastrointestinal tract. Dig. Dis. Sci. 34, 390–9.

CHOCK, S. P. & SCHMAUDER-CHOCK, E. A. (1985) Evidence of de novo membrane generation in the mechanism of mast cell secretory granule activation. Biochem. Biophys. Res. Commun. 132, 134–9.

CHOCK, S. P. & SCHMAUDER-CHOCK, E. A. (1987) The mast cell granules: a phospholipid source for prostaglandins synthesis. In Prostaglandins and Lipid Metabolism in Radiation Injury (edited by WALDEN, T. L. & HUGHES, H. N.) pp. 127–32. New York: Plenum Press.

CHOCK, S. P. & SCHMAUDER-CHOCK, E. A. (1988) Synthesis of prostaglandins and eicosanoids by the mast cell secretory granule. Biochem. Biophys. Res. Commun. 156, 1308–15.

CHOCK, S. P. & SCHMAUDER-CHOCK, E. A. (1989) Phospholipid storage in the secretory granule of the mast cell. J. Biol. Chem. 264, 2862–8.

CHOCK, S. P. & SCHMAUDER-CHOCK, E. A. (1990) Review: A new model for the mechanism of stimulus-secretion coupling. Biofactors 2, 133–46.

CHOCK, S. P. & SCHMAUDER-CHOCK, E. A. (1992) The secretory granule and the mechanism of stimulus-secretion coupling. Cur. Top. Cell. Regul. 32, 183–208.

CHOCK, S. P., RHEE, S. G., TANG, L. C. & SCHMAUDER CHOCK, E. A. (1991) Linking phospholipase A₂ to phospholipid turnover and prostaglandin synthesis in mast cell granules. Eur. J. Biochem. 195, 707–13.

DRAY, F., CHARBONNEL, B. & MACLOUF, J. (1975) Radioimmunoassay of prostaglandins F, E₁ and E₂ in human plasma. Eur. J. Clin. Invest. 5, 311–8.

GEE, M. H., TAHAMONT, M. V., FLYNN, J. T., COX, J. W., PULLEN, R. H. & ANDREADIS, N. A. (1987) Prostaglandin E₁ prevents increased lung microvascular permeability during intravascular complement activation in sheep. Cir. Res. 61, 420–8.

HAHN, G. L., MENCONI, J., CAHILL, M. & POLGAR, P. (1983) The influence of gamma radiation on arachidonic acid release and prostacyclin synthesis. Prostaglandin 25, 783–91.

HEAVEY, D. J., ERNST, P. B., STEVENS, R. C., BEFUS, A. D., BIENENSTOCK, J. & AUSTEN, F. (1988) Generation of leukotriene C₄, leukotriene B₄, and prostaglandin D₂ by immunologically activated rat intestinal mucosa mast cells. J. Immunol. 140, 1953–7.

HUTCHISON, D. L. & MYERS, R. L. (1987) Prostaglandin-mediated suppression of macrophage phagocytosis of Listeria monocytogenes. Cell Immunol. 110, 68–76.

JACOBSON, E. D., CHAUDHURY, T. K. & THOMPSON, W. J. (1976) Mechanism of gastric mucosal cytoprotection by prostaglandins. Gastroenterology 70, 897.

JAFFE, B. M., BEHRMAN, H. R. & PARKER, C. W. (1973) Radioimmunoassay measurement of prostaglandins E, A, and F in human plasma. J. Clin. Invest. 52, 398–405.

KUNKEL, S. L., CHENSUE, S. W. & PHAN, S. H. (1986) Prostaglandins as endogenous mediators of interleukin production. J. Immunol. 136, 186–92.

KUNKEL, S. L., SPENGLER, M., MAY, M. A., SPENGLER, R., LARRICK, J. & REMICK, D. (1988) Prostaglandin E₂ regulates macrophage-derived tumor necrosis factor gene expression. J. Biol. Chem. 263, 5380–4.

KURLAND, J. I., BOCKMAN, R. S., BROXMEYER, H. E. & MOORE, M. A. S. (1978) Limitation of excessive myelopoiesis by the intrinsic modulation of macrophage-derived prostaglandin E. *Science* **199**, 552–5.

LAKE, A. M., KAGEY-SOBOTA, A., JAKUBOWICZ, T. & LICHTENSTEIN, L. M. (1984) Histamine release in acute anaphylactic enteropathy of the rat. *J. Immunol.* **133**, 1529–34.

LEVINE, L. (1973) Antibodies to pharmacologically active molecules: specificities and some applications of anti-prostaglandins. *Pharmacol. Rev.* **25**, 293–307.

LOBOS, E. A., SHARON, P. & STENSON, W. F. (1987) Chemotactic activity in inflammatory bowel disease. Role of leukotriene B₄. *Dig. Dis. Sci.* **32**, 1380–8.

MCLOUF, J., PRADEL, M., PRADELLES, P. & DRAY, F. (1976) ¹²⁵I derivatives of prostaglandin analysis by radioimmunoassay. *Biochim. Biophys. Acta* **431**, 139–46.

MCGIFF, J. C., MALIK, K. U. & TERRAGNO, N. A. (1976) Prostaglandins as determinants of vascular reactivity. *Fed. Proc.* **35**, 2382–7.

MESSINA, E. J., WEINER, R. & KALEY, G. (1976) Prostaglandins and local circulatory control. *Fed. Proc.* **35**, 2367–75.

PERDUE, M. H., RAMAGE, J. K., BURGET, D., MARSHALL, J. & MASSON, S. (1989) Intestinal mucosal injury is associated with mast cell activation and leukotriene generation during *nip-postrongylus*-induced inflammation in the rat. *Dig. Dis. Sci.* **34**, 724–31.

PROBERT, L., DE MEY, J. & POLAK, J. M. (1981) Distinct subpopulations of enteric p-type neurons contain substance P and vasoactive intestinal polypeptide. *Nature* **294**, 470–1

ROBERT, A. (1979) Cytoprotection by prostaglandins *Gastroenterology* **77**, 761–7.

SCHMAUDER-CHOCK, E. A. & CHOCK, S. P. (1987a) Mechanism of secretory granule exocytosis: can granule enlargement precede pore formation? *Histochemical J.* **19**, 413–8.

SCHMAUDER-CHOCK, E. A. & CHOCK, S. P. (1987b) New membrane assembly during exocytosis. In *Proceedings of the 45th Annual Meeting of the Electron Microscopy Society of America* (edited by BAILEY G. W.) pp. 782–3. San Francisco: San Francisco Press.

SCHMAUDER-CHOCK, E. A. & CHOCK, S. P. (1989) Localization of cyclo-oxygenase and prostaglandin E₂ in the secretory granule of the mast cell. *J. Histochem. Cytochem.* **37**, 1319–28.

SCHMAUDER-CHOCK, E. A. & CHOCK, S. P. (1990) New membrane assembly in IgE receptor-mediated exocytosis. *Histochemical J.* **22**, 215–26.

TRIER, J. S. & BROWNING, T. H. (1966) Morphologic response of the mucosa of human small intestine to X-ray exposure *J. Clin. Invest.* **45**, 194–204.

WILLEMS, C., STEL, H. V., VAN AKEN, W. G. & VAN MOURIK, J. A. (1983) Binding and inactivation of prostacyclin (PGI₂) by human erythrocytes. *Brit. J. Haemat.* **54**, 43–52.

Estimation of open dwell time and problems of identifiability in channel experiments

Grace L. Yang[*]

Department of Mathematics, University of Maryland, College Park, MD, USA

Charles E. Swenberg

Armed Forces Radiobiology Research Institute, Bethesda, MD, USA

Abstract. Membrane channels can open or close in response to a change in membrane voltage. An important neurophysiological problem is the estimation of the duration of a channel opening, called the open dwell time. In many experiments, however, the recorded measurement is often a summation of several open dwell times from multi-channels. Under a standard kinetic model, this would give rise to a distribution of the total open dwell time which is a mixture of gamma distributions with binomial weights. For such a mixture the maximum likelihood estimates are difficult to compute. We illustrate an easily implementable estimation method introduced by Le Cam. The method produces asymptotically optimal estimates. We also discuss problems of parameter identification and the potential bias associated with using a continuous-time model to analyze discrete-time data.

Key words and phrases: Markov process; open dwell time; loglikelihood ratio.

1. Introduction

Cell membranes are known to contain several types of ion channels that allow for the selective passage of ions between the extracellular and intracellular medium. A single ion channel can exist in several different kinetic states, and, depending on the particular state, transports specific amounts of ionic current. When a channel allows for the transport of ions the channel is said to be in an open state; otherwise, it is in a closed state. A given channel can have several kinetically distinct open states and closed states. The channel may change from one state to another spontaneously or in response to incoming signals. A closed state having an extremely low transition rate into other states is called an inactivated state. In addition, ion channels are

Correspondence to: Prof. Grace L. Yang, Dept. of Mathematics, University of Maryland, College Park, MD 20742, USA.

divided into two broad classes depending on whether the channel opening is in response to a change in membrane voltage or is chemically activated. Typical examples of these two types are the sodium and potassium channels on neuronal axons, and the acetylcholine activated channels at postsynaptic membranes of many neurons. Transitions between these kinetic states are usually modelled either as a finite state stationary or nonstationary Markov process. In this paper we address a problem of estimation of the distribution of the total open dwell time for channels activated by membrane voltage depolarization, and also, through this estimation problem, we address some general questions of model identifiability.

In channel studies, the method of maximum likelihood is routinely used for the estimation of parameters. There are, however, problems since the likelihood function can be of a complicated analytical form. It requires heavy numerical computation and it is also difficult to investigate theoretically the properties of the computed estimates (e.g. Horn, 1984). The likelihood functions derived in this paper are mixtures of probability distributions which make the method of the maximum likelihood hard to apply. Here we illustrate an estimation method introduced by Le Cam (1960, 1986). This method produces asymptotically optimal estimates, and was applied successfully in the statistical analysis of ion channels (Yang, 1992).

2. Formulation of problem

Consider a specific channel and let X_t denote the kinetic state of this channel at time t, for $t \geq 0$, where 0 is the starting time of the experiment. Following the practice in the neurophysiology literature, we label the collection of all possible kinetic states by

$$\{o_1, \ldots, o_a, C_1, \ldots, C_b\},$$

where $o_1, \ldots, o_a$ denote open kinetic states and the rest are closed states.

At any time t, the channel is in one and only one of these kinetically distinct states. Experimentally, the changes in channel states are manifested in current recordings obtained from a patch-clamp technique which involves forming a high resistance seal between a glass pipette and a small patch of a cell membrane. The high resistance seal insures that current flowing through the pipette is identical to the current flowing through the membrane covered by the pipette (Sakmann and Neher, 1984).

We restrict our investigation to current records having only two levels of conductance corresponding to whether X_t is in the class of open states or in the class of closed states. The current record cannot identify which specific state that X_t is in. In other words, X_t is only partially observable. These two levels of conductance can be described by

$$U(t) = \begin{cases} 1 & \text{if } X_t \in \{o_1, \ldots, o_a\}, \\ 0 & \text{if } X_t \in \{C_1, \ldots, C_b\}. \end{cases} \tag{1}$$

The general problem is to study kinetic transitions of channels through the current record U. However, there is an additional complication in data collection. Since it is not always possible to isolate within a membrane patch a single ion channel, the observed current record $B(t)$ is a collective fluctuation of currents from several individual channels. Suppose there are m channels present in the membrane patch and that the currents are additive; we then have

$$B(t) = \sum_{r=1}^{m} U_r(t),$$ (2)

where $U_r(t)$, for $r = 1, \ldots, m$, is the current from the r-th channel.

Under this circumstance, the observed quantity is B not the individual U's. Thus data on kinetic transitions are doubly aggregated in U and in B. This is illustrated in Figure 1. Each aggregation results in a loss of information about X.

A Markov model is usually assumed for X in the analysis of the data of U and B. The literature contains many studies on the identification of models, estimation of kinetic transition rates and determination of pathways connecting different states. See for instance Neher and Stevens (1977), Horn and Vandenberg (1984), Colquhoun and Hawkes (1977, 1983), Jackson (1985), Fredkin et al. (1985), Aldrich et al. (1983), Vandenberg and Horn (1984).

3. Markov model for X and distributions for many-channel current record

For statistical analysis, we need to clarify the time factor involved in the experiments and its connection to the time parameter in the Markov process, since it determines the selection of using either stationary or non-stationary Markov models. We will discuss two types of such experiments. Examples of the first kind are those of Aldrich et al. (1983) and of Horn and Vandenberg (1984). In this case,
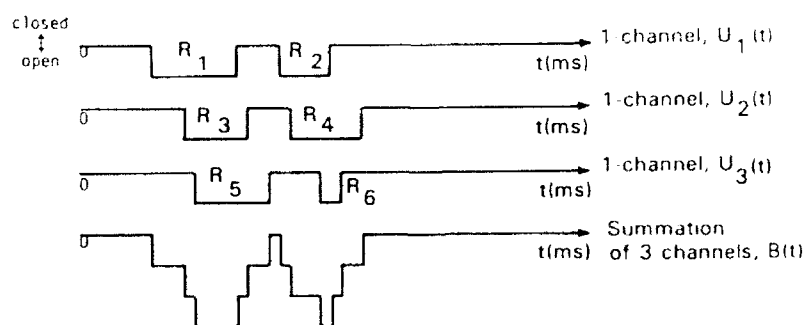

Fig. 1. Idealized current records of individual ion channels and their summed current for three channels in a membrane patch. Each channel is assumed to have only two conductance levels, R_i denotes the open dwell times and the downward direction denotes the open state.

the response of voltage regulated sodium channels were studied. The experimental protocol involved a repetitive application of a fixed voltage to the membrane patch for a predetermined length of time T, termed a voltage pulse. The interpulse waiting time was selected sufficiently long to ensure that the channels return to the initial condition of the experiment, where initially the channels were experimentally controlled to be in one of the resting closed states. The selection of T varies with the experimental protocol; particularly it depends on the type of cells used. For neuroblastoma cells, T was selected to be 15 ms (Aldrich et al. 1983). For tissue cultured GH3 cells (a rat pituitary cell line), Horn and Vandenberg (1984) set T equal to 44 ms. The value of T was selected to be long enough for a channel to produce all its expected responses to a given voltage pulse. At the termination of the voltage pulse T, the channel is taken to be in its inactivation state. The channel need not open to voltage pulse and may pass directly from a resting closed state to inactivation.

In contrast, the second type of experiments involves an application of chemicals to evoke responses (channel openings). In this case there are no interpulse waiting times and the data collection is continuous in time over periods measured in minutes (or hours) as opposed to milli-seconds for voltage pulse and seconds for interpulse time. In this case a stationary Markov model is utilized whereas in the experiments of the first kind a non-stationary Markov process is used in which the inactivated state is approximated by an absorbing state of the Markov process. The likelihood function for the statistical analysis of the channel kinetics is naturally affected by the experimental protocol.

In the subsequent discussion we will restrict ourselves to the experiments of the first kind. Specifically, we consider the class of kinetic models with state space

$$\mathscr{S} = \{o_1, C_1, \ldots, C_b\}, \tag{3}$$

which consists of one open state and an arbitrary number of closed states, one of which is an inactivation state, say C_b. Figure 2(a) illustrates a model having four kinetic states with possible transitions indicated by arrows. This particular scheme
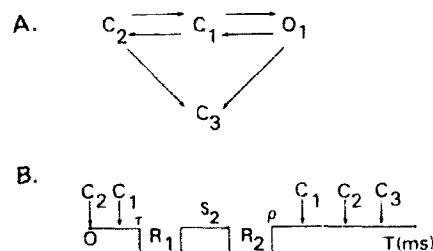

Fig. 2. (a) Kinetic pathway for a four state model of a sodium channel. C_1 and C_2 are closed states, o_1 denotes the open state and C_3 an inactivated state. (b) Typical single channel current record of duration T. R_1 and R_2 denote open dwell times, S_2 closed time, τ the first latency and ρ the last exit time from an open state.

It is well known that with a specific initial condition, $X_0 = C_i$, the random variable N has a truncated geometric distribution with

$$P\{N = k \mid X_0 = C_i\} = \begin{cases} p_i \theta^{k-1}(1 - \theta) & \text{for } k \geqslant 1, \\ 1 - p_i & \text{for } k = 0, \end{cases} \tag{5}$$

where

$$p_i = P\{\tau < \infty \mid X_0 = C_i\}, \tag{6}$$

$$\theta = P\{X \text{ ever returns to the open state } o_1 \text{ in finite time} \mid X_0 = o_1\}. \tag{7}$$

The parameters p_i and θ are functions of the transition rate ($q_{i,i}$'s) of the Markov process X. The distribution of the total open dwell time W has an atom at zero,

$$P[W = 0] = P[W = 0 \mid X_0 = C_i] = 1 - p_i, \tag{8}$$

and an absolute continuous part with an exponential density function,

$$p_i \mu (1 - \theta) \exp(-\mu(1 - \theta)w), \quad \text{for } w > 0, \tag{9}$$

where $\mu = -q_{o_1 o_1} = \sum_{j \neq o_1} q_{o_1 j}$ is the sum of the transition rates leading from the open state o_1. Note that if the initial distribution of X_0 is not concentrated at C_i but is over a subset H of the closed states, then the distribution of N and hence W need to be weighted by a known initial distribution $P\{X_0 = C_i\}$, $C_i \in H$. The total open time W will have a compounded distribution of gamma and weighted geometric distributions, namely,

$$P\{W = 0\} = \sum_{C_i \in H} (1 - p_i) P[X_0 = C_i], \tag{10}$$

and a density on $W > 0$,

$$\sum_{k=1}^{\infty} g_k(t) \sum_{C_i \in H} P[(N = k) \cap (X_0 = C_i)],$$

where g_k is given in (12) below.

Without loss of generality, we shall assume $P\{X_0 = C_i\} = 1$ since the statistical method discussed below applies equally to the case when the initial condition is $X_0 \in H$. Thus for simplicity we shall delete i in the parameter p_i.

Note that in the literature the exponential density $\mu \exp(-\mu x)$ instead of (9) is used to fit the histogram of open dwell times R_j. This will affect the estimation of the mean duration of the open dwell time '$1/\mu$', since the random variable N is not accounted for in fitting the data. A similar problem may occur in fitting exponential density to the open dwell time on the basis of a stationary Markov model as well. The number of channel openings n_L during the experiment, $[0, L]$, needs to be derived from an alternating renewal process, U.

Next we consider a membrane patch that contains m channels, and let W_r denote the total open dwell time of the r-th channel, $r = 1, \ldots, m$. The W_r are not ex-

perimentally measurable; the measurable quantity is the sum $V = \sum_j W_j$. It is easy to see that V corresponds to the total area (physically this is proportional to the total current transported by the membrane during time T—see the last graph in Figure 1, the areas below the horizontal line induced by the openings) that is generated by all the open dwell times $R_j^{(m)}$ in the patch. As a generalization from simple channel to many-channel analysis, one should utilize the open dwell times $R_j^{(m)}$. These dwell times correspond to busy periods of $B(t)$ in queueing theory; note that $B(t)$ is generally a non-Markovian process. The distributions of $R_j^{(m)}$, for $m > 1$, are difficult to obtain. We therefore propose alternatively to use the distribution of the total open time, V, for estimation purposes. To derive the distribution of V, we assume that individual channels behave independently and the W_j's are identically distributed. These are widely used assumptions in the literature. However, there were investigations of possible interactions of the channels (e.g. Iwasa et al. (1986)). The distribution of the sum V is derived to be

$$P[V \leqslant t] = \sum_{l=0}^{m} \binom{m}{l} (1-p)^{m-l} p^l G_l(t), \quad t \geqslant 0, \tag{11}$$

where $G_0 = 1$ and $G_l(t)$, for $l = 1, \ldots, m$, is a gamma distribution function with probability density function (pdf)

$$g_l(t) = \lambda(\lambda t)^{l-1} \exp(-\lambda t)/(l-1)!, \tag{12}$$

where $\lambda = \mu(1 - \theta)$.

4. Parameter estimation for total open dwell time

The distribution of the total open dwell time W in (8) and (9) contains two unknown parameters p and λ. Estimation of p and λ will be based on the likelihood
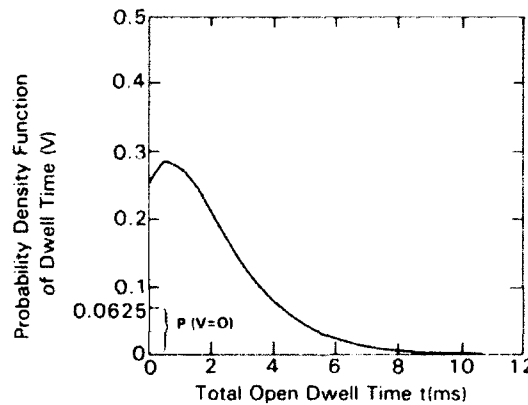

Fig. 3. Probability distribution of total open dwell time V with $m = 4$, $p = 5$ and $\lambda = 1$. The density of V is given in (13) and $P(V = 0) = (1-p)^4 = 0.0625$.

function constructed from the distribution of the total current in the patch, V, which is an observable quantity. It follows from (11) and (12) that the pdf of V is

$$f(v, \delta; p, \lambda) = (1-p)^{m(1-\delta)} \left[\sum_{l=1}^{m} \binom{m}{l} (1-p)^{m-l} p^l g_l(v) \right]^{\delta}, \quad \text{for } v > 0, \quad (13)$$

where δ is an indicator,

$$\delta = I[\tau_r < \infty, \text{ for some } r = 1, \ldots, m],$$

$$\lambda = \mu(1 - \theta),$$

and m is assumed to be known. Figure 3 shows the pdf of V for a specific set of parameter values. Clearly, the pdf in (13) can identify $\mu(1 - \theta)$ as one parameter λ but not as two parameters μ and θ separately. The parameters μ and θ can be estimated separately, if in addition to V we have the data on the number of openings Y (see Le Cam and Yang, 1988). Here the parameter estimation is based on the total current record V only. A more general approach is to utilize the joint distribution of V and Y. This requires simultaneous recording of the data V and Y. While these data can be obtained experimentally, to our knowledge the experimental results are not recorded in this format.

Given a sample of n observations (V_j, δ_j), $j = 1, \ldots, n$, the loglikelihood function of p and λ is

$$\log \prod_{j=1}^{n} f(v_j, \delta_j; p, \lambda)$$

$$= m \log(1-p) \sum_{j=1}^{n} (1 - \delta_j) + \sum_{j=1}^{n} \delta_j \log \left[\sum_{l=1}^{m} \binom{m}{l} (1-p)^{m-l} p^l g_l(v_j) \right], \quad (14)$$

where g is given in (12). This likelihood equation is intractable for providing maximum likelihood estimates for p and λ. Numerical computations are quite time demanding and need not be reliable. Here we will illustrate an estimation method introduced by Le Cam (1960). It is computationally simpler and applicable under weaker mathematical conditions than that of the method of maximum likelihood. The requirement is that the family of probability distributions considered satisfies the LAN conditions. The theoretical justifications for applying this method to partially observed random variables are given in Le Cam and Yang (1988).

Briefly, Le Cam's method is a two-step estimation procedure which consists of constructing appropriate preliminary estimators, say ξ_n^*, for the k-dimensional unknown parameters ξ and then improving upon them to arrive at final estimates. The derived estimates are asymptotically optimal. In the case of i.i.d. observations we can choose for preliminary estimates the method of moments estimators which are $\sqrt{n}$ consistent, i.e., the probability distributions of $\sqrt{n}(\xi_n^* - \xi)$ form a relatively compact sequence. In the present case, the preliminary estimates are

$$p^* = 1 - (1 - \bar{\delta})^{1/m}$$

and

$$\lambda^* = m(1 - (1 - \delta)^{1/m})/\bar{V},$$

where $\delta = \sum_j \delta_j/n$ and $\bar{V} = \sum_j V_j/n$.

Next we compute the differences (instead of derivatives) of the likelihood ratios, for $j = 1, \ldots, n$:

$$Z_{nj1} = \frac{f(v_j, \delta_j; p^* + h_1 n^{-1/2}, \lambda^*)}{f(v_j, \delta_j; p^*, \lambda^*)} - 1,$$

$$Z_{nj2} = \frac{f(v_j, \delta_j; p^*, \lambda^*(1 + h_2 n^{-1/2}))}{f(v_j, \delta_j; p^*, \lambda^*)} - 1, \tag{15}$$

where h_1 and h_2 are arbitrarily selected numbers, say $h_1 = h_2 = 1$. (Note that since λ is a scale parameter, it is more convenient to take the difference in Z_{nj2} in units of λ where λ is estimated by λ^*.) The selection of h's depends on the sample size of n which we will comment on later.

Set

$$Z_n = \begin{bmatrix} \sum_{j=1}^{n} Z_{jn1} \\ \sum_{j=1}^{n} Z_{jn2} \end{bmatrix}.$$

Let M_n be a 2×2 matrix with the (i, l)th component given by

$$\sum_{j=1}^{n} Z_{jni} Z_{jnl}. \tag{16}$$

Then the final estimates for p and λ are given by

$$\begin{bmatrix} \hat{p} \\ \hat{\lambda} \end{bmatrix} = \begin{bmatrix} p^* \\ \lambda^* \end{bmatrix} + \frac{1}{\sqrt{n}} \begin{bmatrix} h_1 & 0 \\ 0 & \lambda^* h_2 \end{bmatrix} M_n^{-1} Z_n. \tag{17}$$

Let $P_{n,(p,\lambda)}$ be the probability measure determined by the joint density $\prod_j f(v_j, \delta_j; p, \lambda)$. Le Cam's theory on LAN families (1960, 1986) gives that as $n \to \infty$, the estimates $\hat{p}$ and $\hat{\lambda}$ converge in law under $P_{n,(p,\lambda)}$ probability to a bivariate normal distribution, i.e.,

$$L\left\{ \begin{bmatrix} \hat{p} - p \\ \hat{\lambda} - \lambda \end{bmatrix} \right\} \to \mathcal{N}(0, \Gamma^{-1}),$$

where Γ is the Fisher information matrix for the density in (13).

Denote the components of the inverse matrix M_n^{-1} by a_{ij}. Then the covariance matrix Γ^{-1} can be estimated by $\hat{\Gamma}^{-1}$ where

$$\hat{\Gamma}^{-1} = \begin{bmatrix} h_1^2 a_{11} & h_1(\lambda^* h_2) a_{12} \\ h_1(\lambda^* h_2) a_{12} & (\lambda^* h_2)^2 a_{22} \end{bmatrix}.$$

The general idea behind this method is that for n sufficiently large, a globally $\sqrt{n}$

consistent estimator ξ_n^* would indicate, with large probability, in which neighborhood Ω_n the true parameter ξ_0 lies. Here we take $\Omega_n = \{\xi : \sqrt{n}\,|\xi - \xi_0| \leq d\}$ to be a subset of k-dimensional Euclidean space. On Ω_n we approximate the loglikelihood ratio by a linear-quadratic form.

Let $s_{0n}, s_{1n}, \ldots, s_{kn}$ be vectors in Ω_n such that $s_{1n} - s_{0n}, \ldots, s_{kn} - s_{0n}$ form a basis in Ω_n. We represent vectors t_n in Ω_n with respect to this basis as

$$t_n - s_{0n} = \sum_{i=1}^{k} \eta_{ni}(s_{in} - s_{0n}).$$

Let $f_j(x_j, \xi)$ be the pdf of the random variable X_j. Define

$$Z_{nji} = \frac{f_j(x_j; s_{in})}{f(x_j; s_{0n})} - 1, \quad \text{for } i = 1, \ldots, k; \; j = 1, \ldots, n,$$

$$Z_n = \begin{bmatrix} \sum_{j=1}^{n} Z_{jn1} \\ \vdots \\ \sum_{j=1}^{n} Z_{jnk} \end{bmatrix}, \qquad \eta_n = \begin{bmatrix} \eta_{n1} \\ \vdots \\ \eta_{nk} \end{bmatrix},$$

and M_n to be a $k \times k$ matrix whose (i,l) component is $\sum_j Z_{jni} Z_{jnl}$. Then the loglikelihood ratio

$$\log \frac{\prod_j f_j(x_j; t_n)}{\prod_j f_j(x_j; s_{0n})}$$

can be approximated by

$$L_n(t_n) \approx \xi_n' Z_n - \tfrac{1}{2}\xi_n' M_n \eta_n, \quad t_n \in \Omega_n. \tag{18}$$

If the inverse M_n^{-1} exists, the maximum of $L_n(t_n)$ is attained at

$$\hat{\eta}_n = M_n^{-1} Z_n,$$

or at

$$\hat{t}_n = s_{0n} + \sum_{i=1}^{k} \hat{\eta}_{ni}(s_{in} - s_{0n}).$$

Both s_{0n} and $s_{in} - s_{0n}$ are unknowns. We estimate s_{0n} by the preliminary estimate ξ_n^* and take a local basis around ξ_n^* as $s_{in} - s_{0n}$. In the example of open dwell times, $k = 2$, $s_{0n}' = (p_0, \lambda_0)$, which is estimated by $s_{0n}'^* = (p^*, \lambda^*)$,

$$s_{1n} - s_{0n} = \begin{bmatrix} h_1/\sqrt{n} \\ 0 \end{bmatrix}, \qquad s_{2n} - s_{0n} = \begin{bmatrix} 0 \\ \lambda_0/\sqrt{n} \end{bmatrix},$$

and $s_{2n} - s_{0n}$ is estimated by $\lambda^* h_2/\sqrt{n}$. From these we obtain (15).

The values h_1 and h_2 should be so chosen that $s_{in} - s_{0n}$ are in Ω_n. In applications, the selection of h_1 and h_2 for computations depends on the value of n. In the data on sodium channels, we have n around 500. We found the final estimates do not

vary much when the h_i's are between -10 and 10 (Yang, 1992). Asymptotically, any choice of h_1 and h_2 is valid. However, in applying the asymptotic method to a finite sample, one needs to be careful in choosing the values for the h's. As a practical guideline, we can compute the final estimates with different values of h's and choose a pair of h_1 and h_2 among those considered that fits the data best.

5. Conclusions

The distribution of total open dwell time for ion channels contained in a membrane patch is derived. Le Cam's estimation method is used to derive estimators for parameters in the distribution. Here we treat the number of channels, m, in a membrane patch as a known constant. The problem of considering m as a random variable will be investigated in the future.

Recording techniques of ion channel data present unique sampling and stochastic modelling problems in kinetic analysis. The estimation method used depends, in turn, on the sampling technique and the stochastic model used. Usually, the methods of least squares and maximum likelihood are utilized for estimation of parameters. In our investigation, we found Le Cam's estimation method easily implementable. It overcomes some of the difficulties of the maximum likelihood estimates encountered in the channel studies.

In applications, one should however be aware of the fact that the data collected from the patch-clamp experiments, like many other automated recordings, are in discrete time units as dictated by the sampling rate. Thus there exists a potential bias in statistical findings when a continuous-time model like ours is used to analyze discrete-time data. It is intuitively clear that a faster sampling rate will yield a smaller bias. For channel experiments considered here, a sampling rate of 10 kHz corresponds to a sampling interval (Δ) one tenth of the unit of measurements (millisecond) of our data R or V. Its effects on the number of channel openings N and on the open dwell times R are different. A finite sampling rate always results in an undercount of N. In the measurements of R, it induces mainly a rather insignificant amount of truncation error. We will give a heuristic explanation of these effects. A rigorous mathematical investigation, which requires considerable amount of effort, will be pursued in the future.

If $R > \Delta$, then clearly there will be no error in counting N. If $R \leqslant \Delta$, then the probability of counting the j-th opening is given by

$$\beta_j = P\{v_j \leqslant k\Delta \leqslant v_j + R_j, \text{ for some } k = 1, 2, \ldots\}, \quad \text{for } j = 1, 2, \ldots,$$

where v_j is the time of the j-th opening of a single channel. The probability of miscounting the j-th opening is therefore $1 - \beta_j$. The explicit formula for β_j in terms of the distributions of v_j and R_j remains to be evaluated. A crude upper bound is readily available, i.e.,

$$0 \leqslant 1 - \beta_j \leqslant P\{R_j \leqslant \Delta\} = 1 - \exp\{-\Delta\mu\},$$

where $1/\mu$ is the average open dwell time.

The effect of sampling rate is clearly seen in the exponent. The smaller the Δ, the smaller the probability of undercounting the N, and Δ should be small as compared with the average open dwell time $1/\mu$. In terms of N, the expected number of miscount is no more than $(1 - \exp(-\Delta\mu))EN$.

The effect on open dwell times R_j could be studied as follows. Each R_j is the difference $v_j^* - v_j$ of the closing and starting times of the j-th opening in a single channel. Both v_j^* and v_j are subject to a measurement error due to sampling truncation. Suppose $\tilde{v}_j$ is the actual measurement and ε_j is the error in measurement due to the finite sampling rate. Then $v_j = \tilde{v}_j + \varepsilon_j$. Similarly, $v_j^* = \tilde{v}_j^* + \varepsilon_j^*$, where

$$0 \leqslant \varepsilon_j, \qquad \varepsilon_j^* \leqslant \Delta, \qquad |\varepsilon_j - \varepsilon_j^*| \leqslant \Delta.$$

Therefore,

$$R_j = \tilde{v}_j^* - \tilde{v}_j = v_j^* - v_j + (\varepsilon_j - \varepsilon_j^*).$$

Conceivably, the average error $E(\varepsilon_j - \varepsilon_j^*)$ is approximately zero. Thus the bias in the total open dwell time W, where $W = \sum_{j=1}^{N} R_j$, is primarily contributed by the undercount of N which results in undermeasuring of W.

Therefore, in the measurement unit we considered the sampling rate does not seem to have a serious effect on the statistical analysis. On the other hand, typical sampling rate ranges from 1 to 10 kHz. For a slow sampling rate of 1 kHz, there could be a nonnegligible bias in the measurements. This problem will be addressed in the future.

References

Aldrich, R.W., D.P. Corey and C.F. Stevens (1983). A reinterpretation of mammalian sodium channel gating based on single channel recording. Nature 306, 436-441.

Colquhoun, D. and A.G. Hawkes (1977). Relaxation and fluctuations of membrane currents that flow through drug-operated ion channels. Proc. Roy. Soc. London Ser. B 199, 231-262.

Colquhoun, D. and A.G. Hawkes (1983). The principles of the stochastic interpretation of ion-channel mechanisms. In: B. Sakmann and E. Neher, Eds., Single Channel Recording. Plenum, New York, 135-175.

Fredkin, D.R., M. Montal and J.A. Rice (1985). Identification of aggregated Markovian models: Application to the nicotinic acetylcholine receptor. In: Proceedings of the Berkeley Conference in Honor of Jerzy Neyman and Jack Kiefer. Wadsworth, Belmont, CA.

Horn, R. and C.A. Vandenberg (1984). Statistical properties of single sodium channels. J. Gen. Physiol. 84, 505-534.

Horn, R. (1984). Gating of channels in nerve and muscle, a stochastic approach. In: W.D. Stein, Ed., Ion Channels: Molecular and Physiological Aspects. Academic Press, New York, 53-97.

Iwasa, K., G. Ehrenstein, N. Moran and M. Jia (1986). Evidence for interactions between batrachotoxin-modified channels in hybrid neuroblastoma cells. Biophys. J. 50, 531-537.

Jackson, M.B. (1985). Stochastic behavior of a many-channel membrane system. *Biophys. J.* **47**, 129-137.

Le Cam, L. (1960). *Locally Asymptotically Normal Families of Distributions*. University of California Publ. Statistics, Berkeley, CA.

Le Cam, L. (1986). *Statistical Methods in Asymptotic Decision Theory*. Springer, Berlin.

Le Cam, L. and G.L. Yang (1988). On the preservation of local asymptotic normality under information loss. *Ann. Statist.* **16** (2), 483-520.

Neher, E. and C.F. Stevens (1977). Conductance fluctuations and ionic proes in membranes. *Ann. Rev. Biophys. Bioeng.* **6**, 345-381.

Sakmann, B. and E. Neher (1984). Patch clamps techniques for studying ionic channels in excitable membranes. *Ann. Rev. Physiol.* **46**, 455-472.

Vandenberg, C.A. and R. Horn (1984). Inactivation viewed through single sodium channels. *J. Gen. Physiol.* **84**, 535-564.

Yang, G.L. (1992). Stochastic modelling of sodium channel gating phenomena and estimation of parameters. In preparation.

DISTRIBUTION LIST

DEPARTMENT OF DEFENSE

ARMED FORCES INSTITUTE OF PATHOLOGY
        ATTN: RADIOLOGIC PATHOLOGY
                    DEPARTMENT

ARMED FORCES RADIOBIOLOGY RESEARCH INSTITUTE
        ATTN: PUBLICATIONS DIVISION
        ATTN: LIBRARY

ARMY/AIR FORCE JOINT MEDICAL LIBRARY
        ATTN: DASG-AAFJML

ASSISTANT TO SECRETARY OF DEFENSE
        ATTN: AE
        ATTN: HA(IA)

DEFENSE NUCLEAR AGENCY
        ATTN: TITL
        ATTN: DDIR
        ATTN: RARP

DEFENSE TECHNICAL INFORMATION CENTER
        ATTN: DTIC-DDAC
        ATTN: DTIC-FDAC

FIELD COMMAND DEFENSE NUCLEAR AGENCY
        ATTN: FCFS

INTERSERVICE NUCLEAR WEAPONS SCHOOL
        ATTN: TCHTS/RH

LAWRENCE LIVERMORE NATIONAL LABORATORY
        ATTN: LIBRARY

UNDER SECRETARY OF DEFENSE (ACQUISITION)
        ATTN: OUSD(A)/R&AT

UNIFORMED SERVICES UNIVERSITY OF THE HEALTH
SCIENCES
        ATTN: LIBRARY

DEPARTMENT OF THE ARMY

HARRY DIAMOND LABORATORIES
        ATTN: SLCHD-NW
        ATTN: SLCSM-SE

LETTERMAN ARMY INSTITUTE OF RESEARCH
        ATTN: SGRD-ULY-OH

SURGEON GENERAL OF THE ARMY
        ATTN: MEDDH-N

U.S. ARMY AEROMEDICAL RESEARCH LABORATORY
        ATTN: SCIENTIFIC INFORMATION CENTER

U.S. ARMY ACADEMY OF HEALTH SCIENCES
        ATTN: HSMC-FCM

U.S. ARMY CHEMICAL RESEARCH, DEVELOPMENT, AND
ENGINEERING CENTER
        ATTN: SMCCR-RST

U.S. ARMY INSTITUTE OF SURGICAL RESEARCH
        ATTN: DIRECTOR OF RESEARCH

U.S. ARMY MEDICAL RESEARCH INSTITUTE OF CHEMICAL
DEFENSE
        ATTN: SGRD-UV-R

U.S. ARMY NUCLEAR AND CHEMICAL AGENCY
        ATTN: MONA-NU

U.S. ARMY RESEARCH INSTITUTE OF ENVIRONMENTAL
MEDICINE
        ATTN: SGRD-UE-RPP

U.S. ARMY RESEARCH OFFICE
        ATTN: BIOLOGICAL SCIENCES PROGRAM

WALTER REED ARMY INSTITUTE OF RESEARCH
        ATTN: DIVISION OF EXPERIMENTAL
                    THERAPEUTICS

DEPARTMENT OF THE NAVY

NAVAL AEROSPACE MEDICAL RESEARCH LABORATORY
        ATTN: COMMANDING OFFICER

NAVAL MEDICAL COMMAND
        ATTN: MEDCOM-21

NAVAL MEDICAL RESEARCH AND DEVELOPMENT COMMAND
        ATTN: CODE 40C

NAVAL MEDICAL RESEARCH INSTITUTE
        ATTN: LIBRARY

NAVAL RESEARCH LABORATORY
        ATTN: LIBRARY

OFFICE OF NAVAL RESEARCH
        ATTN: BIOLOGICAL SCIENCES DIVISION

SURGEON GENERAL OF THE NAVY
        ATTN: MEDICAL RESEARCH AND
                    DEVELOPMENT

DEPARTMENT OF THE AIR FORCE

BOLLING AIR FORCE BASE
        ATTN: AFOSR

BROOKS AIR FORCE BASE
        ATTN: AL/OEBSC
        ATTN: USAFSAM/RZ
        ATTN: AL/DEBL

NUCLEAR CRITERIA GROUP, SECRETARIAT
        ATTN: OAS/XRS

SURGEON GENERAL OF THE AIR FORCE
        ATTN: HQ USAF/SGPT
        ATTN: HQ USAF/SGES

U.S. AIR FORCE ACADEMY
        ATTN: HQ USAFA/DFBL

OTHER FEDERAL GOVERNMENT

ARGONNE NATIONAL LABORATORY
        ATTN: BIOLOGY LIBRARY

BROOKHAVEN NATIONAL LABORATORY
        ATTN: RESEARCH LIBRARY, REPORTS
                    SECTION

CENTER FOR DEVICES AND RADIOLOGICAL HEALTH
        ATTN: HFZ-110

DEPARTMENT OF ENERGY
        ATTN: ER-72 GTN

GOVERNMENT PRINTING OFFICE
        ATTN: DEPOSITORY RECEIVING SECTION
        ATTN: CONSIGNED BRANCH

LIBRARY OF CONGRESS
        ATTN: UNIT X

LOS ALAMOS NATIONAL LABORATORY
        ATTN: REPORT LIBRARY/P364

NATIONAL AERONAUTICS AND SPACE ADMINISTRATION
        ATTN: RADLAB

NATIONAL AERONAUTICS AND SPACE ADMINISTRATION.
GODDARD SPACE FLIGHT CENTER
        ATTN: LIBRARY

NATIONAL CANCER INSTITUTE
        ATTN: RADIATION RESEARCH PROGRAM

NATIONAL DEFENSE UNIVERSITY
        ATTN: LIBRARY

NATIONAL LIBRARY OF MEDICINE
        ATTN: OPI

U.S. ATOMIC ENERGY COMMISSION
        ATTN: BETHESDA TECHNICAL LIBRARY

U.S. FOOD AND DRUG ADMINISTRATION
        ATTN: WINCHESTER ENGINEERING AND
                ANALYTICAL CENTER

U.S. NUCLEAR REGULATORY COMMISSION
        ATTN: LIBRARY

RESEARCH AND OTHER ORGANIZATIONS

BRITISH LIBRARY (SERIAL ACQUISITIONS)
        ATTN: DOCUMENT SUPPLY CENTRE

CENTRE DE RECHERCHES DU SERVICE DE SANTE DES
ARMEES
        ATTN: DIRECTOR

INHALATION TOXICOLOGY RESEARCH INSTITUTE
        ATTN: LIBRARY

INSTITUTE OF RADIOBIOLOGY
ARMED FORCES MEDICAL ACADEMY
        ATTN: DIRECTOR

KAMAN SCIENCES CORPORATION
        ATTN: DASIAC

NBC DEFENSE RESEARCH AND DEVELOPMENT CENTER OF
THE FEDERAL ARMED FORCES
        ATTN: WWDBW ABC-SCHUTZ

NCTR-ASSOCIATED UNIVERSITIES
        ATTN: EXECUTIVE DIRECTOR

RUTGERS UNIVERSITY
        ATTN: LIBRARY OF SCIENCE AND MEDICINE

UNIVERSITY OF CALIFORNIA
        ATTN: LABORATORY FOR ENERGY-RELATED
                HEALTH RESEARCH
        ATTN: LAWRENCE BERKELEY LABORATORY

UNIVERSITY OF CINCINNATI
        ATTN: UNIVERSITY HOSPITAL, RADIOISOTOPE
                LABORATORY